Filtration Mechanics Project

Annual Report --- 1964

(Phase I – Final)

Prepared for

George C. Marshall Space Flight Center

National Aeronautics and Space Administration

Huntsville, Alabama

Fluid Power Controls Laboratory

School of Mechanical Engineering

OKLAHOMA STATE UNIVERSITY

Stillwater, Oklahoma

Sept. 1965

TECHNICAL SUMMARY REPORT

Date: 30 November 1964

Contractor: Oklahoma State University, Stillwater, Oklahoma
Segment Generating Report: School of Mechanical Engineering
Fluid Power and Controls Laboratory

STUDY OF FILTRATION MECHANICS AND SAMPLING TECHNIQUES

CONTRACT: NAS 8 11009

Prepared for: George C. Marshall Space Flight Center, Huntsville, Alabama

Prepared by: Robert E. Reed, Project Leader
Roger H. Tucker, Project Associate
Kirby Stone, Graduate Assistant

H. C. Fitch, Project Director

FOREWORD

This Technical Summary Report was prepared by the Fluid Power and Controls Laboratory of the School of Mechanical Engineering, Oklahoma State University of Agriculture and Applied Science. The study was initiated by the George C. Marshall Space Flight Center, Huntsville, Alabama, and accomplished under Contract NAS 8 11009.

The contract with Oklahoma State University is titled "Study of Filtration Mechanics and Sampling Techniques." It is being accomplished under the technical monitorship and guidance of Mr. Victor Neiland, Chief, Engine Control Systems Section, R-P&VE-PAE, and Mr. Royce Church, Chief, Research Unit, R-P&VE-PAE. The work on the project at O.S.U. has been the duties of Dr. E. C. Fitch, Project Director; Mr. R. E. Reed, Project Leader; Mr. R. H. Tucker, Project Associate; and, Mr. K. L. Stone, Graduate Assistant.

This report covers work conducted from 1 September 1963 through 30 November 1964.

ABSTRACT

20970

This report delineates the activities and findings of the studies conducted under contract NAS8-11009, entitled "Study of Filtration Mechanics and Sampling Techniques," in its initial phase at Oklahoma State University. A basic theoretical and experimental approach has been initiated in filtration mechanics to determine the importance of physical parameters to filter performance. Methods of measuring the physical parameters of wire cloth media, which are contained in theoretical relationships between fluid flow through a medium and the corresponding pressure drop across the medium, have been investigated. Assumptions are made for using relationships for laminar flow through wire cloth media and it is shown that the assumptions are valid for the case.

The report also covers many of the important aspects of sampling the fluid of dynamic hydraulic systems of the high performance fluid power and control types. Practical considerations for extracting and analyzing a fluid sample for its particulate contamination content are described or otherwise defined. Theoretical considerations to establish a basis for sampling techniques are discussed. Comprehensive data from isokinetic sampling of a laminar flow test section are included. Also, it is shown how an isokinetic test section can be utilized in the evaluation of commercially available sample valves under specific conditions. A bibliography concerned with literature that applies to filtration mechanics and dynamic sampling is presented for reference purposes. In the interest of clarity, the materials pertaining to the two research areas are presented in separate divisions within the report.

TABLE OF CONTENTS

LIST OF TABLES

LIST OF FIGURES

CHAPTER I

INTRODUCTION TO FILTRATION MECHANICS

The two principal functions that a filter medium must discharge are diametrically opposite to each other. That is, a filter is required to block passage of contaminants of a given particulate size range while offering as little resistance as possible to fluid transmission. Under relaxed filtration and flow specifications, selection of a suitable filter medium may be a routine engineering task. But, when low-micron filtration is required with additional restrictions of filter unit size as well as stringent mechanical strength specifications, the problem of selecting a medium takes on new aspects of decided engineering interest. The main interest being to achieve a high degree of reliability in contaminant retention with a minimum loss in flow energy.

Accurate appraisals of filter media, whereby predictions can be made for the purposes of optimum design, are dependent upon the applicability of theories that have been proven experimentally for the individual case. That is, it must be possible to measure, in terms of a theory, the geometrical properties of the medium before any theories relating flow through the medium, or contamination removal by the medium can be verified for application. Considerable effort has been devoted in the referenced research toward the measurement of media parameters. The import of this work to current and future filtration studies should not be underestimated.

For the work reported herein, special care has been exercised in restricting the study to one type of media. Wire cloth media were selected for the study because of their relative simplicity and/or uniformity in construction, and the availability of media specimens. Furthermore, flat specimens were used in order to circumvent as many extraneous considerations as possible.

Although notable work has been accomplished by reputable filter manufacturers, which is demonstrated by their production of high quality merchandise, it is evidenced in the literature that the present knowledge of filtration is largely the result of empirically derived conclusions. Research toward a theoretical "breakthrough" in basic filtration laws will institute new concepts that should prove beneficial to manufacturers as well as system designers. The premise throughout this study has been that basic filtration laws can be determined which will lead to a well-founded science with significant practical contributions.

CHAPTER II

ANALYSIS OF FLOW PARAMETERS IN A FILTER MEDIUM

The description of the filtration process has been restricted primarily to empirical relationships which are applicable to various types of media. Grace (1), in an article published in 1956, presented the existing theory for various modes of filtration. He also included in his article an extensive list of references referring to the filtration process. Comer (2) in a survey report gives 753 references of articles pertinent to filtration. Although the quantity of material available in the literature is great, that which is applicable to filtration through modern filter media is limited. Therefore, it is of basic interest to this study to describe the media parameters important in the filtration process. The same physical parameters which are important to particulate removal by a medium are also directly related to fluid transmission. Since the relations of the latter are well founded, an analysis of the flow process through porous media has been conducted for the sake of parameter definition.

The French engineer, Henri Darcy, was one of the first persons to describe the flow of a fluid through a porous medium. He observed that the fluid velocity within a porous medium was proportional to the pressure drop per unit length and inversely proportional to the viscosity of the flowing fluid. His findings can be stated mathematically by the differential equation

$$V = - \frac{K}{\mu} \frac{dP}{dL} \qquad (2\text{-}1)$$

where:

V = Velocity of fluid in capillary

μ = Dynamic viscosity

dP/dL = Pressure gradient in medium

K = Proportionality constant, defined as permeability

The negative sign in the equation above results from the fact that the pressure gradient is a negative quantity.

In order to apply equation (2-1) in an ideal situation, consider a hypothetical model of a porous medium consisting of N straight capillaries of diameter D and length t. The pressure gradient then becomes $\Delta P/t$, and the pore velocity can be replaced by

$$V = \frac{q}{A_p} = \frac{q}{\pi D^2/4} \tag{2-2}$$

where:

q = Rate of Flow through an individual pore

A_p = Area of an individual pore

Recognizing that the total flow rate through the medium, Q, is equal to the product of the number of passages (N) and the flow through a single passage, equation (2-1) may be written in the form,

$$Q = \frac{KN\pi D^2 \Delta P}{4\mu t} \tag{2-3}$$

Defining the porosity of porous medium to be equal to the ratio of void volume to bulk volume, the porosity for the theoretical medium under consideration is

$$\Phi = \frac{N\pi D^2 t/4}{A_t t} = \frac{N\pi D^2}{4A_t} \tag{2-4}$$

where:

Φ = Porosity

A_t = Total Surface Area of Medium

Substituting this result into equation (2-3) yields,

$$Q = \frac{K\Phi A_t \Delta P}{\mu t} \qquad (2\text{-}5)$$

Dimensional examination of the equation above reveals that the dimensions of the media permeability, K, are those of area.

The permeability of a porous medium is a measure of the resistance offered by the medium to fluid transmission. A large permeability indicates that the medium has a high fluid conductance, i.e., a low flow resistance. Conversely, a material with a low permeability has a low conductance and consequently a greater pressure loss for a given flow rate. Therefore, if two media should exhibit identical filtration characteristics, the one with the higher permeability would be the most practical from the standpoint of pressure loss across the medium.

Another equation for flow through a porous medium can be obtained by performing a force balance on the fluid within the medium. (See Figure 1) For the porous model previously considered, the external force on the fluid inside of an individual capillary is given by,

$$F_e = A_p \Delta P = \frac{\pi D^2}{4} \Delta P \qquad (2\text{-}6)$$

The internal drag force on the interstitial fluid can be equated to the product of the internal surface area and the viscous shearing stress at the capillary wall in the following manner:

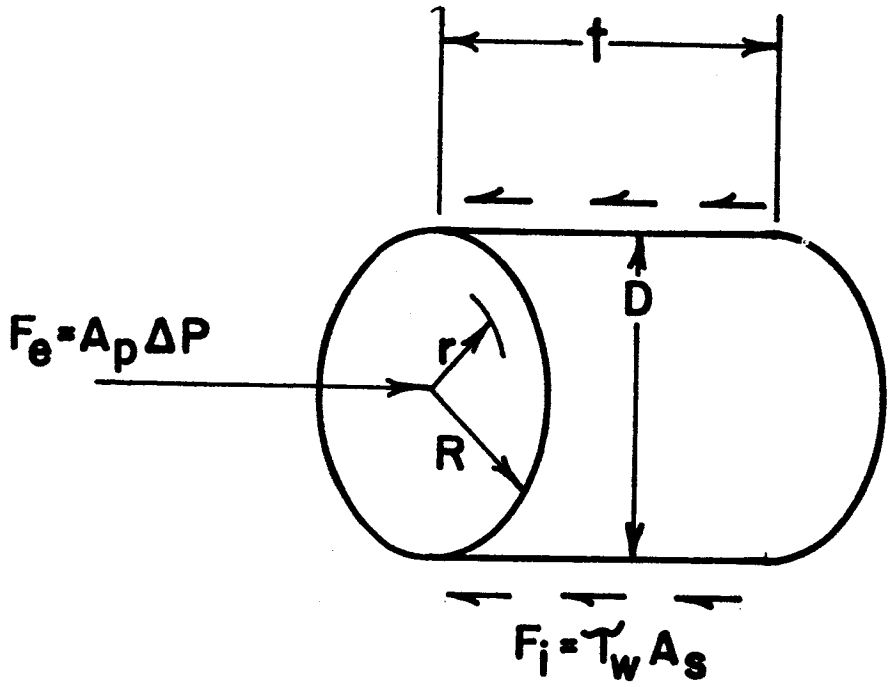

$$A_p = \frac{\pi D^2}{4} \qquad A_s = \pi D t$$

$$\tau_w = \mu \left(-\frac{dV}{dr} \right)_{r=R=\frac{D}{2}}$$

Fig. 1 Force Balance on Fluid in a Cylindrical Capillary

$$F_i = \tau_w A_s = \mu\pi Dt\left(-\frac{dV}{dr}\right)_{r=\frac{D}{2}} \qquad (2\text{-}7)$$

For laminar flow, the velocity distribution within the capillary is parabolic. Therefore, the velocity at any radial distance equals,

$$V = 2V_A\left(1 - \frac{r^2}{R^2}\right) \qquad (2\text{-}8)$$

where:

V_A = Average pore velocity

It follows that,

$$\left(\frac{dV}{dr}\right)_{r=\frac{D}{2}} = -\frac{8V_A}{D}$$

Substituting the results above into equation (2-7) yields,

$$F_i = \mu\pi Dt\left(\frac{8V_A}{D}\right) = 8\pi\mu tV_a = 8\pi\mu t\left(\frac{4q}{\pi D^2}\right) = \frac{32\mu tq}{D^2} \qquad (2\text{-}9)$$

Equating the internal and external forces gives the familiar form of the Hagen-Poiseville Law for flow through a single capillary.

$$q = \frac{\pi D^4 \Delta P}{128\mu t} \qquad (2\text{-}10)$$

Multiplying both sides of (2-10) by the total number of passages, N, forms an equation which is applicable to the entire medium,

$$Q = \frac{N\pi D^4 \Delta P}{128\mu t} \qquad (2\text{-}11)$$

Substituting the results of (2-4) leaves the equation in the form

$$Q = \left(\frac{D^2}{32}\right) \frac{\Phi A_t \Delta P}{\mu t} \qquad (2\text{-}12)$$

If equations (2-5) and (2-12) are compared it can be observed that they are identical for the theoretical porous model when

$$K = \frac{D^2}{32} \qquad (2\text{-}13)$$

This result points out the interrelationship between the filtration properties of a filter medium and its resistance to flow. As the pore diameter decreases the medium's flow capacitance also decreases. Although this effect is intuitively apparent, equation (2-13) describes the exact nature of this relationship in a simplified medium.

Extension of equation (2-12) to modern filter media, such as wire cloth and sintered metal media, requires the recognition that several of the assumptions which were valid for the ideal model are no longer adequate. Deviation from the theoretical case are as follows:

(1) The cross sectional areas of the capillaries are not constant through a medium. In the case of wire cloth media the capillary openings are considerably larger at the surface than within the media.

(2) The flow path through the medium is not straight, and consequently has a length greater than the thickness of the medium. This deviation is more pronounced in depth media since the fluid must follow a more tortuous path through the porous material.

Fitch (3) revised the Hagen-Poiseuille equation to account for the additional length in the flow path. This was accomplished by introducing the tortuosity of a medium as a parameter. The tortuosity, τ, of a medium is defined as the ratio of the actual length of the flow path to the minimum theoretical flow path. Thus a medium with a thickness, t, would have a tortuosity,

$$\tau = \frac{L}{t} \tag{2-14}$$

where:

L = Actual flow path length

Since the actual capillary length is τt equation (2-11) becomes

$$Q = \frac{N\pi D^4 \Delta P}{128 \mu \tau t} \tag{2-15}$$

The porosity of the medium is also influenced by its tortuosity, the porosity in this case being,

$$\Phi = \frac{N\pi D^2 L/4}{A_t t} = \frac{N\pi D^2 \tau}{4A_t} \tag{2-16}$$

Substituting this result, equation (2-15) may be written

$$Q = \left(\frac{D^2}{32\tau^2}\right) \frac{\Phi A_t}{\mu t} \Delta P \tag{2-17}$$

As indicated above, media permeability is not only a function of pore diameter but also a function of tortuosity. The difficulty in directly applying equation (2-17) to an actual media is due to the fact that the determination of the tortuosity of a porous material is still a nebulous task. In a wire cloth medium the tortuosity can be calculated approximately

from an analysis of the geometry of the material. However, in a depth type media there is, as yet, no effective means of making this measurement.

The utilization of any of the flow equations discussed above depends upon the accuracy with which media parameters, such as pore diameter and porosity, can be determined. The test methods involved in measuring the various parameters and the correlation between the experimental and theoretical results are included in the following chapters.

CHAPTER III

EXPERIMENTAL DETERMINATION OF FILTER MEDIA PARAMETERS

The analysis of a porous medium with respect to either its filtration capabilities or flow resistance depends upon the ability to obtain accurately the parameters of the medium which influence its performance. In this regard several experimental methods have been applied or developed to obtain such properties as media pore size and distribution, media efficiency, porosity, and permeability.

A. Pore Diameter

The most important property of a filter medium is its pore size, since this governs its effectiveness as a filtration material. Consequently, considerable effort has been expended in developing methods which yield an accurate value for the pore size of a medium. The three tests which have been used to obtain this parameter are the mercury intrusion porosimeter test, the boiling pressure test, and the filtration efficiency test.

The first two tests for pore size rely on a static balance of forces within a pore. Consider the case where a liquid is being forced into a capillary. At an equilibrium condition, the external force is balanced by an internal force resulting from the surface tension of the liquid at the perimeter of the opening. (See Figure 2) This equilibrium condition can be stated mathematically as,

$$F = PA_p = \sigma L_p \cos \theta \qquad (3\text{-}1)$$

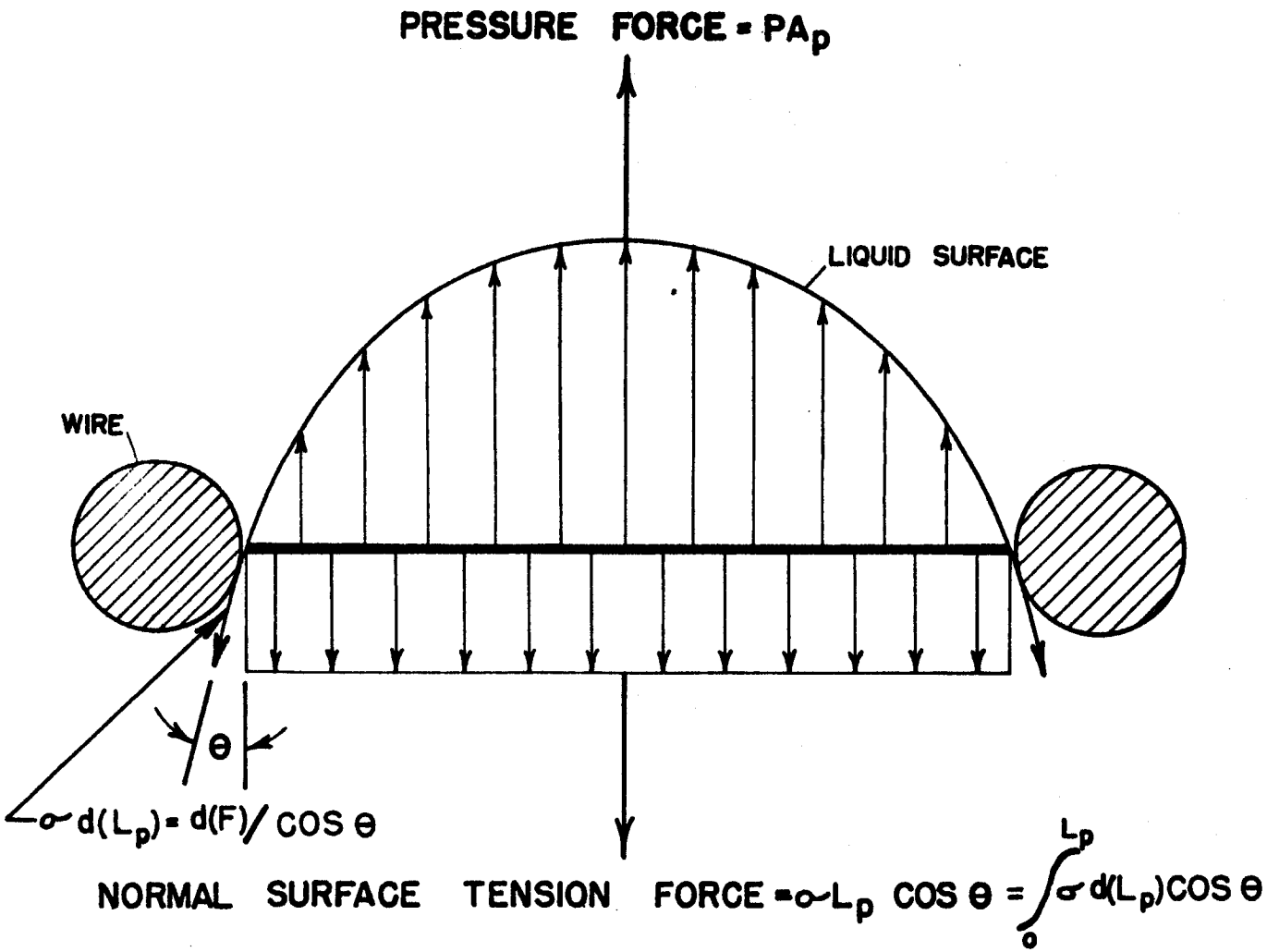

Fig. 2 Force Balance on Fluid Surface at Pore Opening in Medium

where:

F = Force required

P = Absolute pressure

A_p = Cross sectional pore area

L_p = Length of wetted perimeter of pore

σ = Surface tension of liquid

θ = Wetting angle of liquid on solid

if equation (3-1) is applied to a pore of circular cross section, the values for A_p and L_p become

$$A_p = \frac{\pi D^2}{4}$$

and

$$L_p = \pi D$$

Thus, the force equation readily reduces to

$$D = \frac{4\sigma \cos \theta}{P} \qquad (3\text{-}2)$$

The equation above has been thought to be restricted to circular pores; however, re-examination of the theory shows that it is a much more powerful tool in the determination of media pore sizes. Consider the force balance within a triangular pore of sides a, b, and c. The cross sectional area is given by the expression,

$$A_p = \sqrt{S\ (S-a)\ (S-b)\ (S-c)}$$

where:

$$S = \tfrac{1}{2}\ (a + b + c)$$

Also,

$$L_p = a + b + c = 2S$$

Substitution into equation (3-1) yields as a result,

$$D = \frac{2\sqrt{S\,(S-a)\,(S-b)\,(S-c)}}{S} = \frac{4\sigma \cos\theta}{P} \qquad (3\text{-}3)$$

The diameter D, given in (3-3), is the diameter of the circle which can be inscribed in the triangle. It should be noted that this is also equal to the hydraulic diameter, D_h, defined for a non-circular flow passage as,

$$D_h = \frac{4A_p}{L_p} \qquad (3\text{-}4)$$

The fact that equation (3-3) gives the diameter of the inscribed circle is important, since this is also the diameter of the largest spherical particle which will pass through such a pore. The validity of the theory for triangular pore openings is also noteworthy because many common wire cloth configurations have triangular pores as their primary barrier.

An analysis of the forces within a rectangular pore also has important applications since media with a square weave have pores of this type. Considering a rectangle with a width D and a length C, the pore area and wetted perimeter are given by,

$$A_p = CD$$

and,

$$L_p = 2\,(C + D)$$

Substitution into equation (3-1) yields,

$$D_h = \frac{2\,CD}{C + D} = \frac{4\sigma \cos\theta}{P} \qquad (3\text{-}5)$$

Representing C by some multiple of D, KD, and recognizing that D is the diameter of the largest sphere which will pass through the pore, equation (3-5) may be written,

$$D = \left(\frac{1 + K}{2K}\right) \frac{4\sigma \cos \theta}{P} \qquad (3\text{-}6)$$

It can be observed from equation (3-6) that for a square pore, where K equals 1, the equation reduces to the same form as equations (3-2) and (3-3)

The principles above are utilized in determining media pore sizes by means of the intrusion of mercury into the pores of a medium. The instrument used in this test, a mercury intrusion porosimeter manufactured by the American Instrument Company, is designed to give pore size distribution information on porous media whose diameters may range from 0.035 to 100 microns (Figure 3 & 4). In performing the test, a filter sample is placed in a small chamber to which a graduated stem is attached. After evacuating the sample, mercury is added to the chamber. The pressure on the mercury is increased incrementally, and the volume change is noted in the graduated stem. As the pressure is increased, the mercury passes into pores of decreasing diameter until the void volume is completely filled with mercury. In this manner a plot of pressure versus volume injected can be prepared (Figure 5).

Considering the porous medium being analyzed, let the incremental pore volume between diameters D + dD and D be represented by,

$$dV_p = - F(D)\, dD \qquad (3\text{-}7)$$

where:

V_p = Pore volume

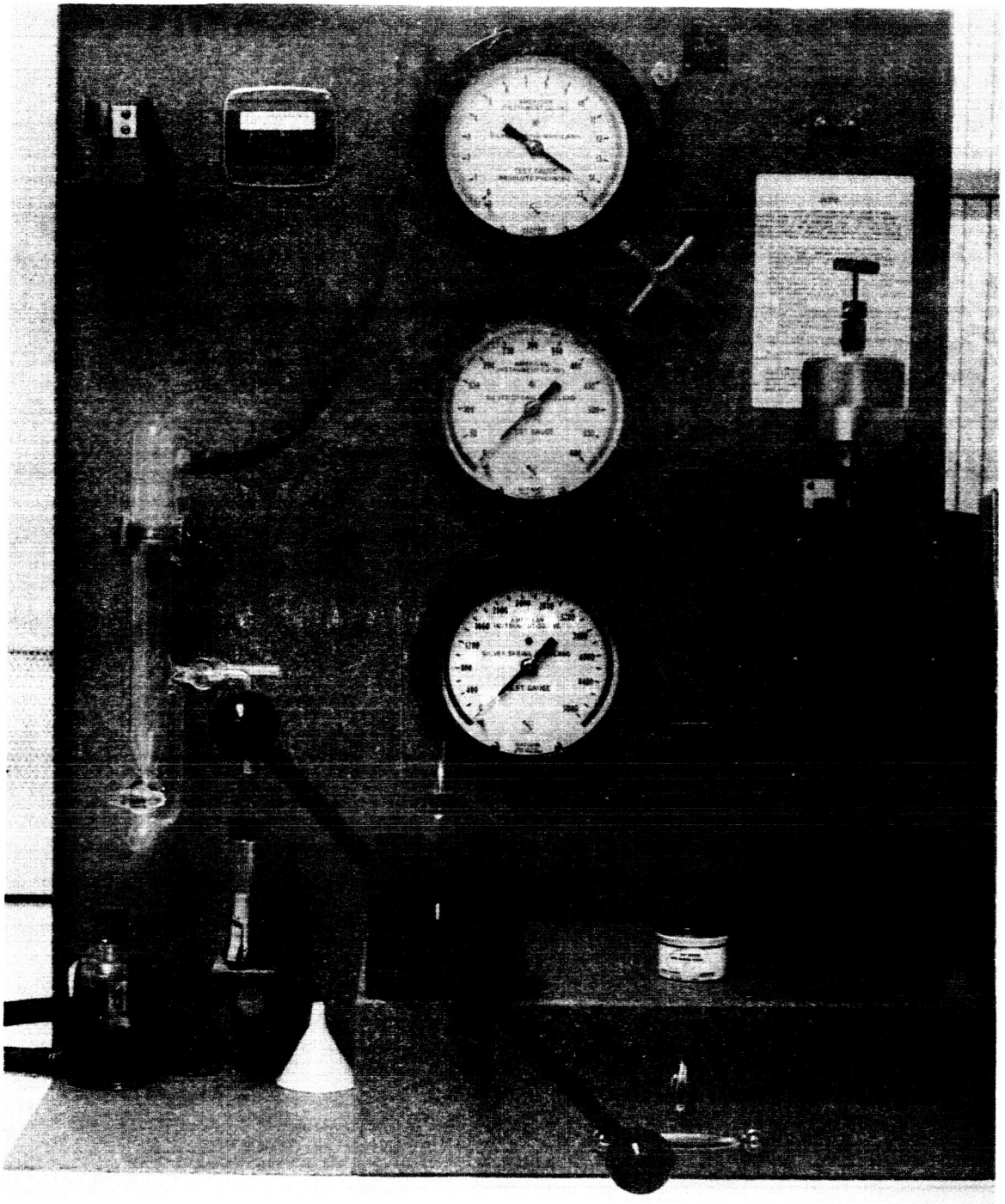

Fig. 3 Mercury Intrusion Porosimeter

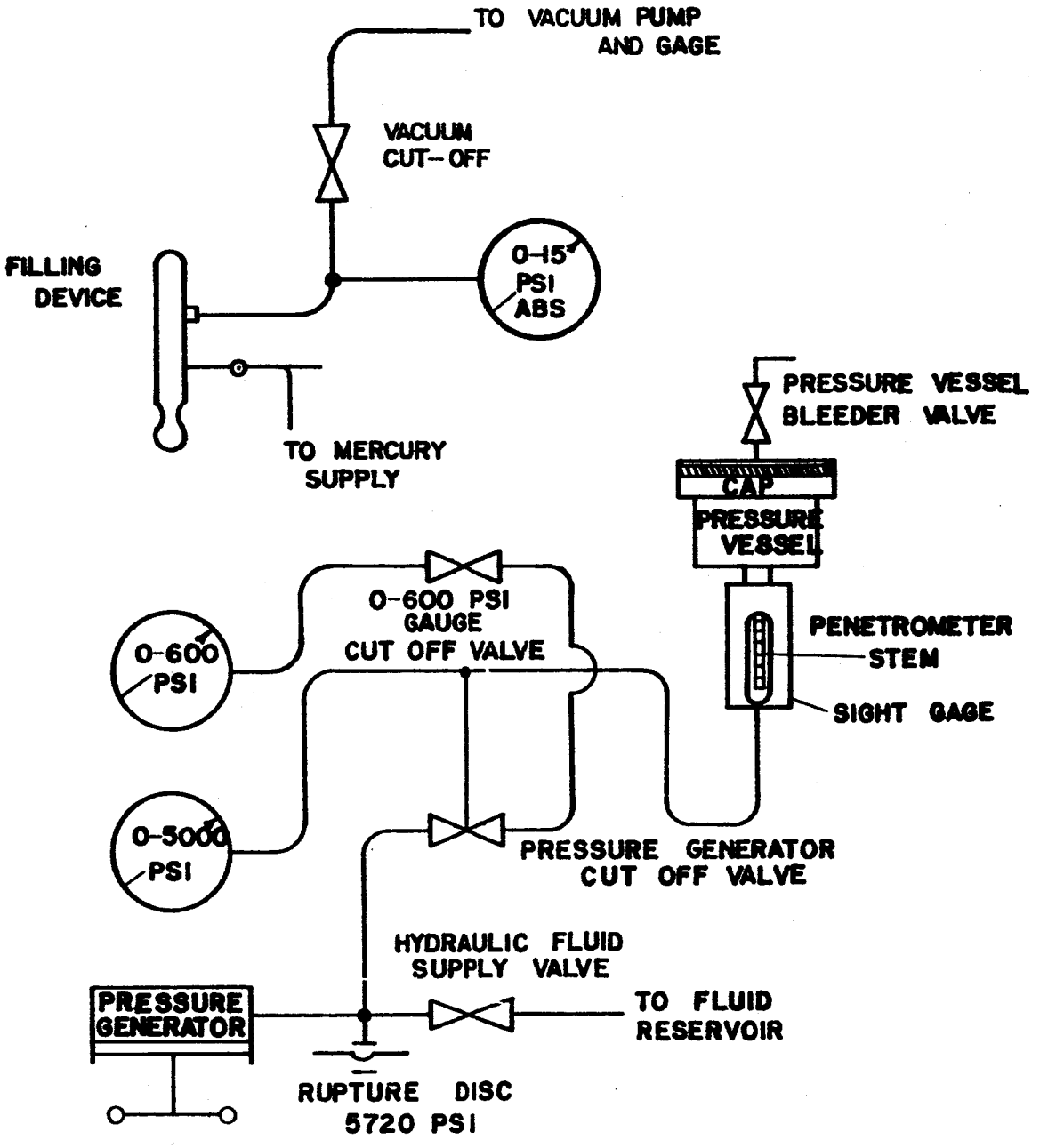

Fig. 4 Schematic Diagram of Mercury Intrusion Porosimeter

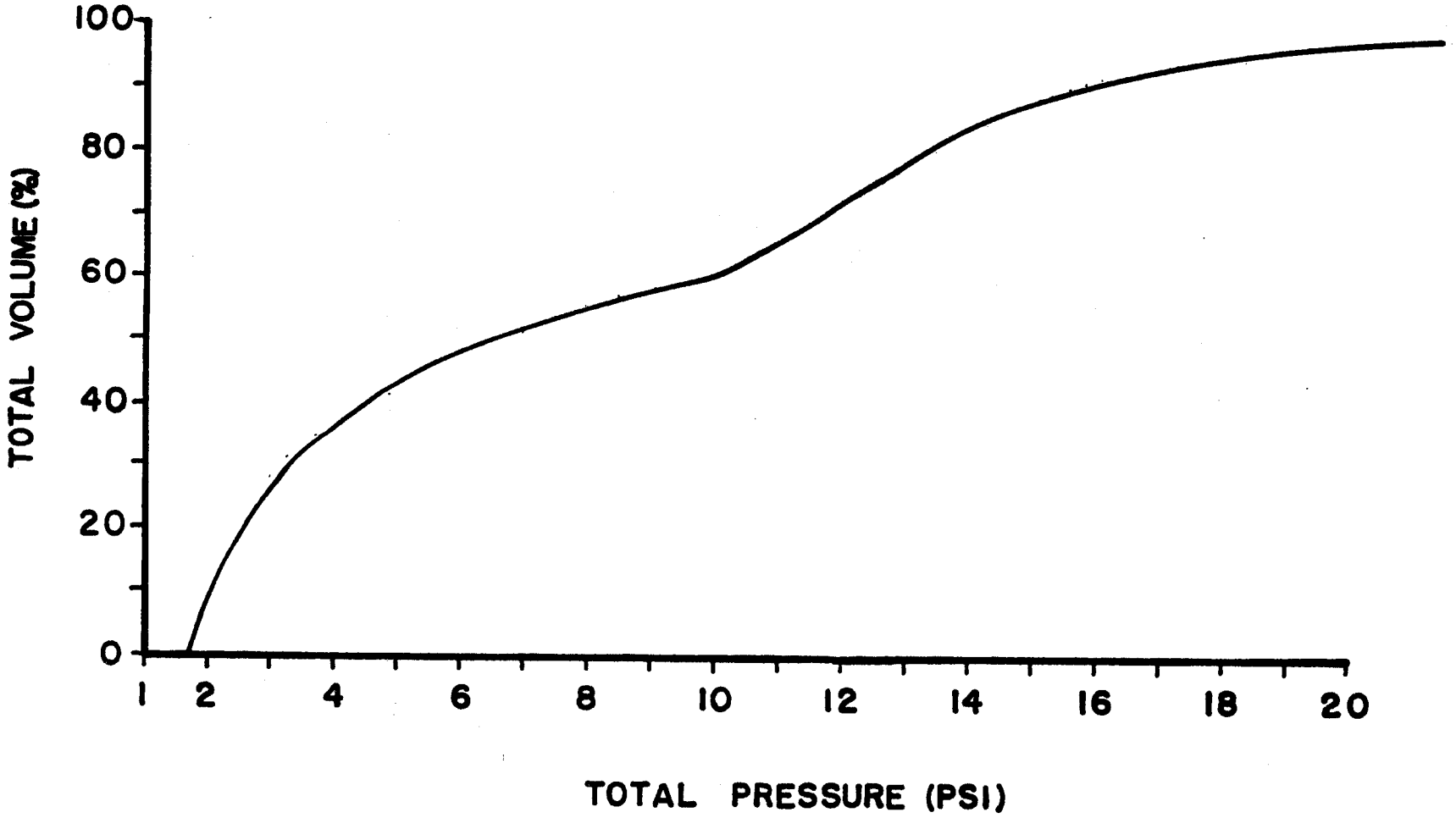

Fig. 5 Mercury Intrusion Curve

F(D) = Pore Size Distribution Function

For mercury on stainless steel equation (3-2) reduces to

$$D(\text{Microns}) = \frac{175}{P(\text{PSIA})} \tag{3-8}$$

Differentiation of (3-8) yields

$$PdD + DdP = 0 \tag{3-9}$$

Solving for dD and substituting into (3-7) gives an expression for the distribution function,

$$F(D) = \frac{P}{D} \frac{dV_p}{dP} \tag{3-10}$$

The pore size distribution function may be determined for various pore diameters using equation (3-8) and the slope of the V_p versus P curve. Figure (6) shows a plot of F(D) versus D for a medium with a dutch twill weave. The highest point which F(D) obtains occurs at the average pore size of a medium. This point appears as an inflection point on the V_p versus P curve.

The value of this method lies in the fact that it is applicable to both surface and depth type filter media. The test can be performed on a two square inch sample of material in less than one hour.

The second technique used to determine the average pore size of a medium is similar to the "Bubble Point Test" which has been widely accepted as a means to determine the maximum pore size of a medium. As in the "Bubble Test," the medium is submerged in a fluid and air is introduced underneath the material. The pressure is then increased until the first air bubble breaks through the upper surface of the medium. The pressure at which this

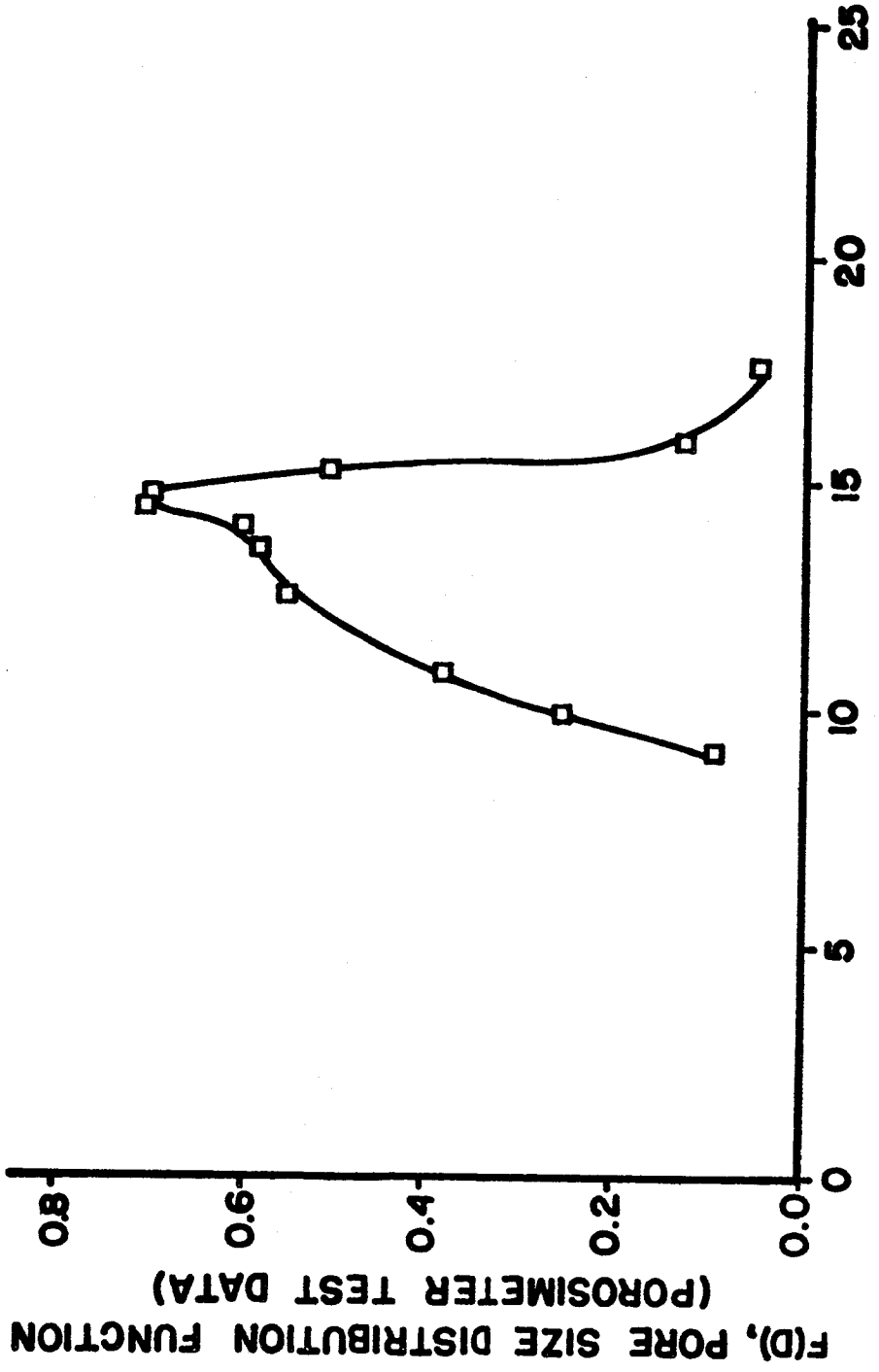

Fig. 6 Pore Size Distribution Function, F(D)

occurs is the "Bubble Point Pressure" which is substituted into an equation of the form of (3-2) in order to solve for the pore diameter. The numerator of the equation is usually determined experimentally for a given type of medium by determining the bubble pressure for a series of samples and then observing the largest particle which can pass through them. Pall (4) reported that, when denatured ethyl alcohol is used as the fluid medium, the equation takes the form,

$$D(\text{Microns}) = \frac{238}{P(\text{In. of } H_2O)} \qquad (3\text{-}11)$$

According to Ludvig (5) when Solox 190 is used as the test fluid the equation changes to,

$$D(\text{Microns}) = \frac{356}{P(\text{In. of } H_2O)} \qquad (3\text{-}12)$$

For the "Boiling Pressure Test" the air pressure is increased above the bubble point pressure until a uniform "boiling" occurs on the surface of the medium. A typical curve of flow rate versus pressure (Figure 7) shows that the pressure increases with increased flow rate up to a point at which there is no appreciable increase in pressure for an increase in flow rate. At this pressure, the boiling pressure, the air is passing through a representative number of pores, and therefore an "average" pore diameter can be obtained from an equation of the form

$$D = \frac{C}{P} \qquad (3\text{-}13)$$

In this case C is an empirically determined constant. At pressures above the boiling pressure a layer of air forms above the sample and the pressure is primarily due to frictional losses from the flow of air through the medium.

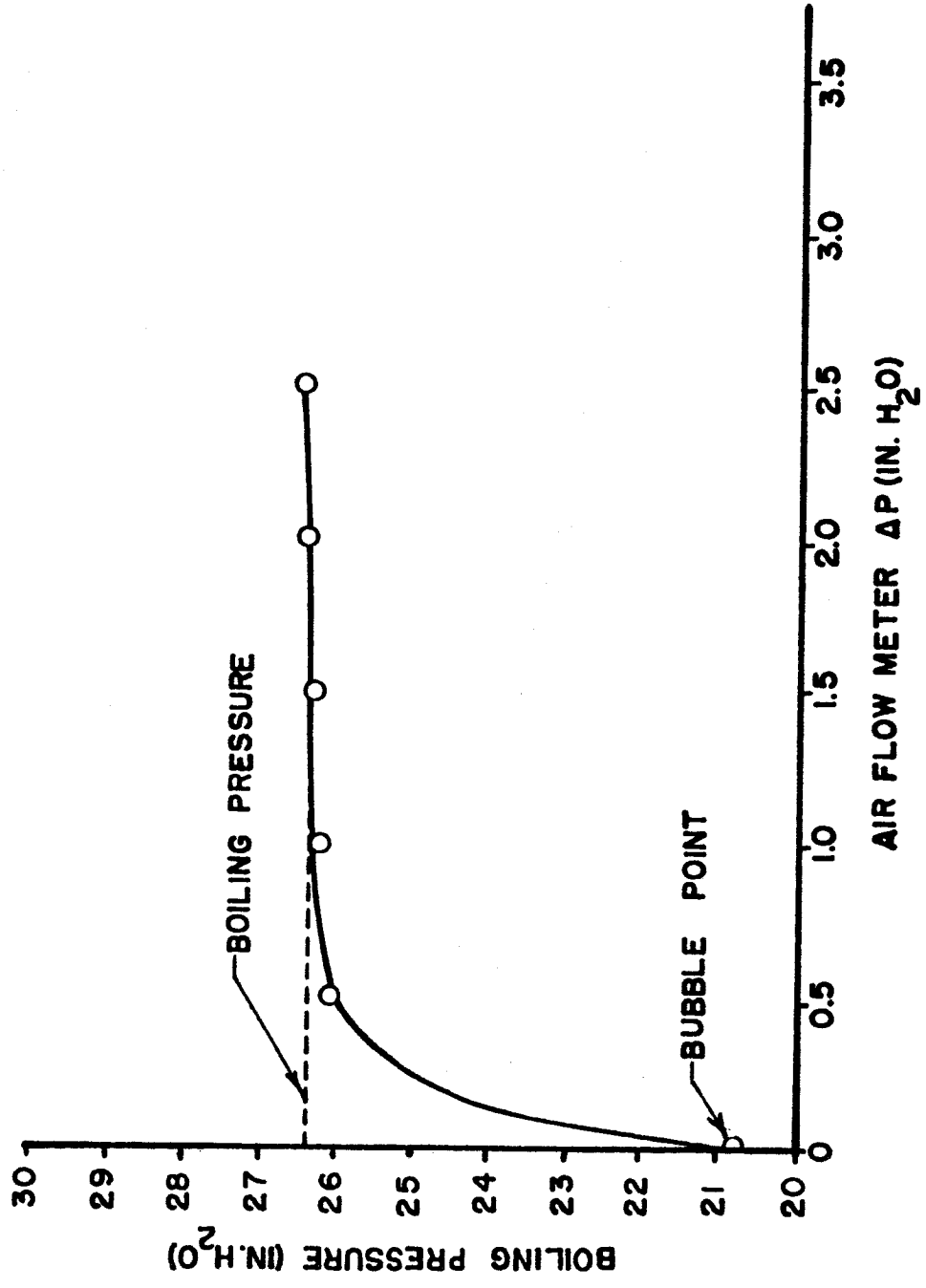

Fig. 7 Typical "Boiling Pressure Test" Curve

The boiling test apparatus (See Figures 8 & 9) consists of an instrument panel containing necessary flow and pressure measurement equipment and a plexiglass test vessel. The sample being tested is clamped and sealed between two plexiglass flanges as shown in Figure 10, and the media sample holder is then placed into the test vessel. Introducing air pressure into the alcohol reservoir forces the alcohol up into the test container. After the fluid reaches a height of one-half inch above the medium, the flow of fluid is stopped. Air is then admitted under the sample and the boiling pressure test is performed.

The value of the boiling pressure method of pore diameter determination lies in the fact that it is a simple, non-destructive test which can be applied to many commercial filter elements. The results, which are contained in the following section, are excellent for wire cloth media. However, for some depth media the frictional flow losses through the material negate the forces due to surface tension, and therefore the application of the theory becomes invalid.

The validity of either of the test procedures outlined above depends upon how well their results compare with the actual filtration capabilities of a given media. Insuring that the tests are valid includes:

(1) Comparing the average diameter obtained from the porosimeter with the actual average diameter of the medium.

(2) Determining the empirical constant in equation (3-13) by correlating boiling pressures with actual average diameters.

The actual average diameter of a medium, which is called for in both instances above, can be obtained experimentally by filtration efficiency tests on the medium.

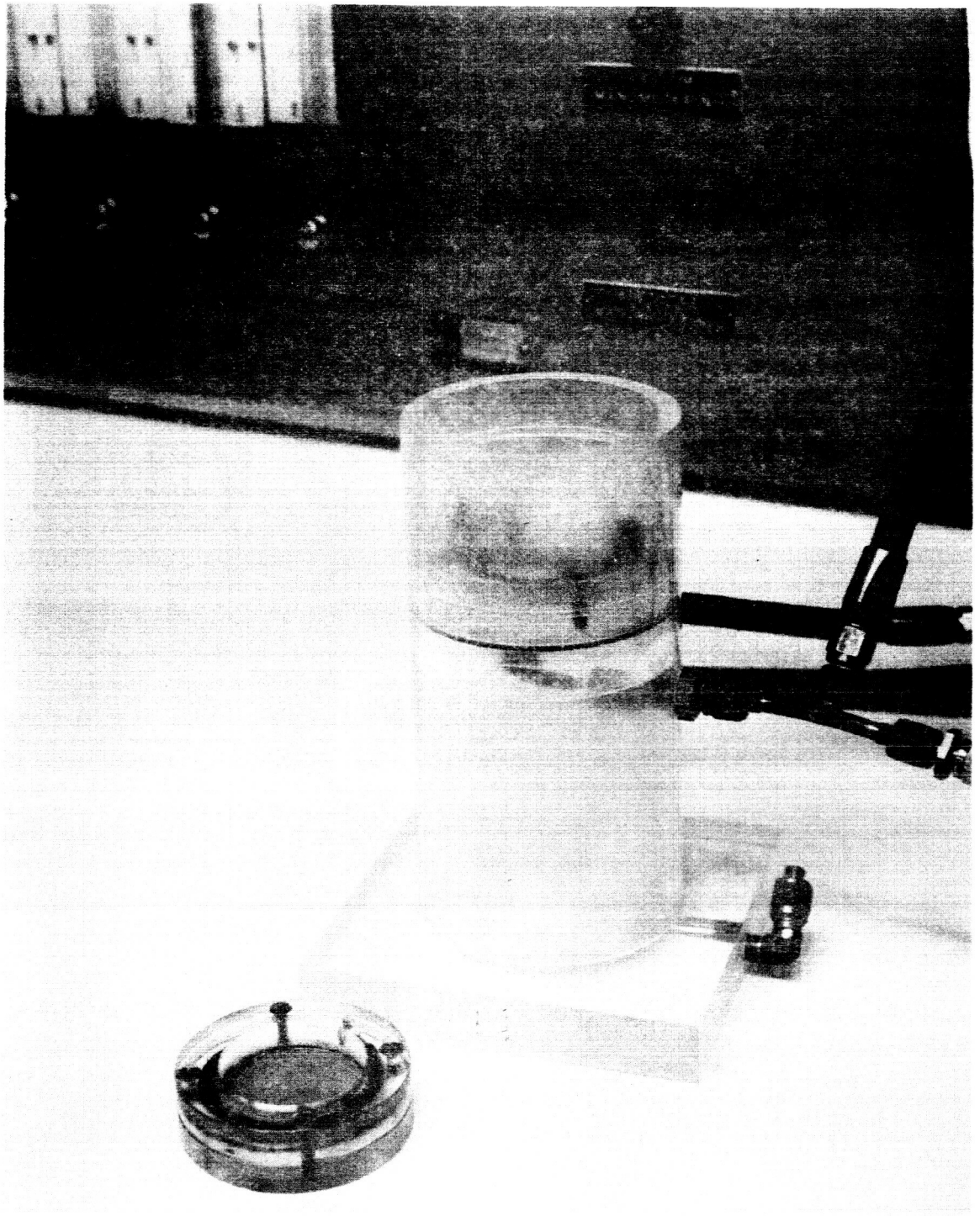

Fig. 8 "Boiling Pressure Test" apparatus

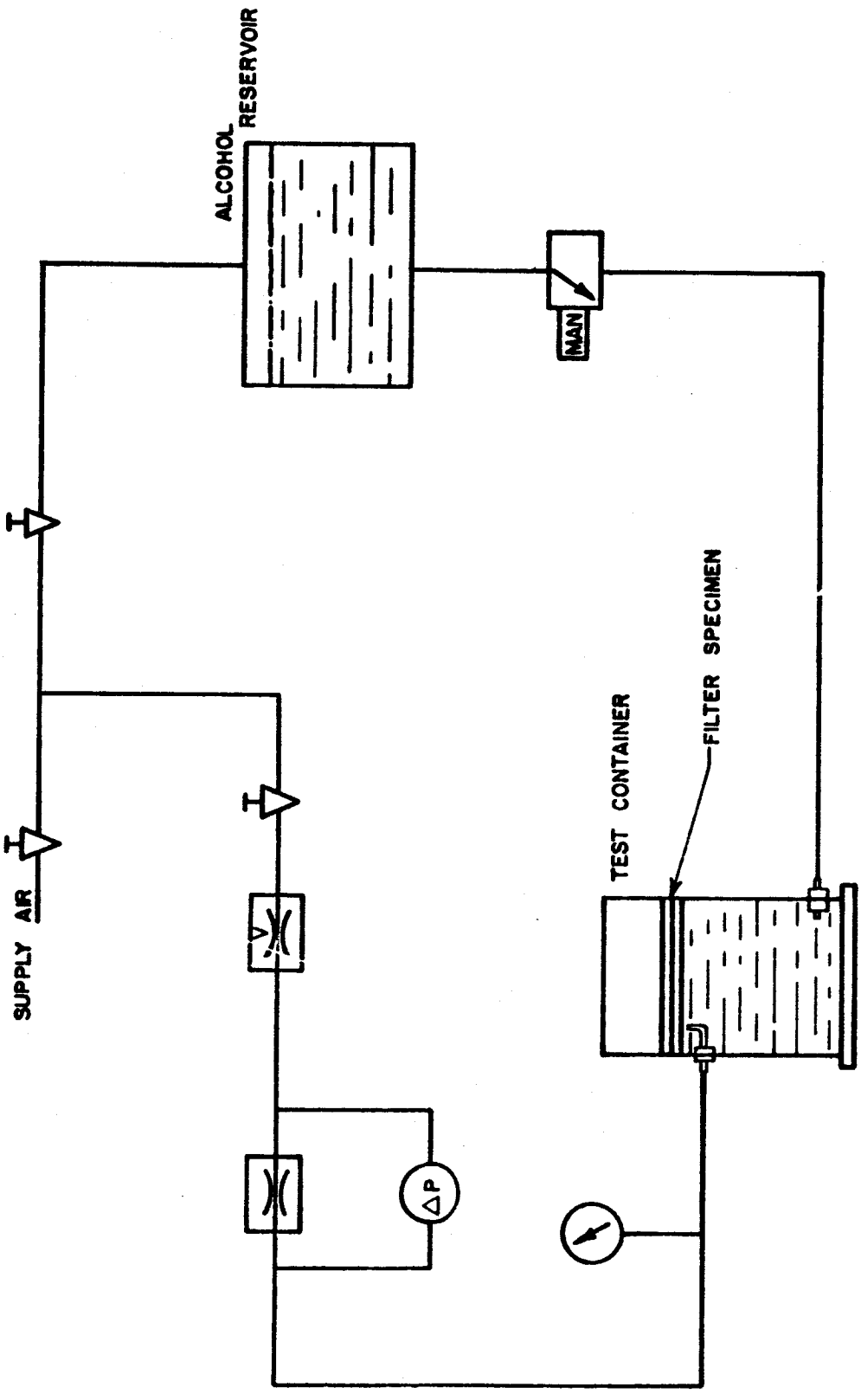

Fig. 9 Schematic of Boiling Pressure Apparatus

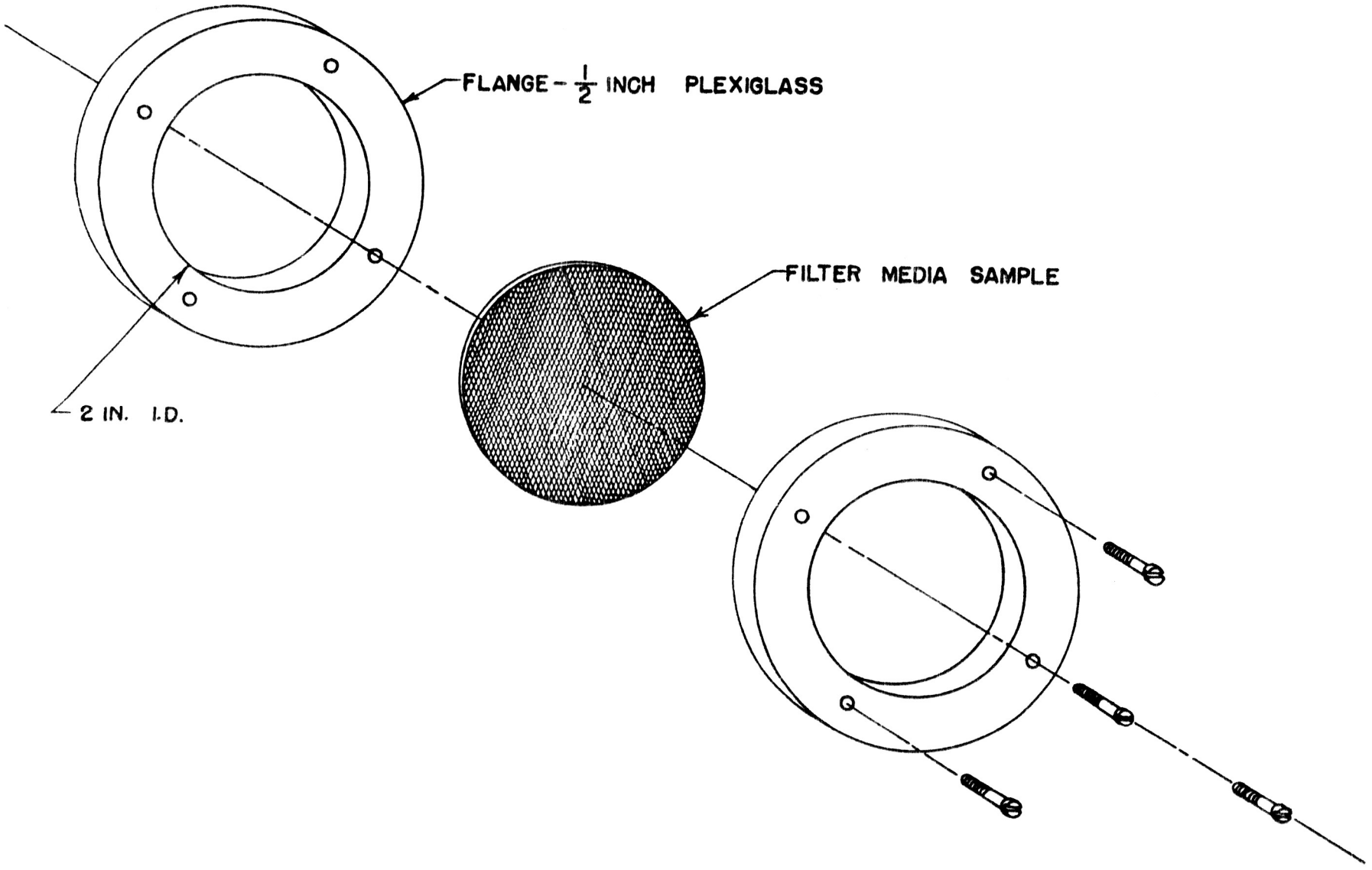

Fig. 10 Filter media sample holder

Filter efficiency tests are performed in the clean room using the apparatus shown in Figure 11. Filter specimens to be tested are mounted in the holder shown in Figure 10. In conducting an efficiency test, 50 ml. of a 100 ml. premixed slurry of glass beads in triple-filtered MIL-F-5606 hydraulic fluid is forced through the filter specimen being tested into the precleaned filtration flask. This filtrate is then refiltered through a 0.45 μ membrane thereby removing that part of the original glass beads which had passed through the filter specimen. The quantity and size distribution of the glass beads in the filtrate is obtained by optical analysis of the beads retained on the membrane. The remaining 50 ml. of contaminated fluid is filtered directly through a 0.45 μ membrane. Optical analysis of this membrane gives the size and distribution of the contaminant in the slurry prior to its passage through the filter medium being tested.

An efficiency curve for the filter medium is prepared from the results of the analysis of the contaminant in the feed and filtrate. The efficiency at a given diameter can be determined from the relationship,

$$\text{Efficiency (@ Dia. X)} = 100 \left(1 - \frac{\text{No. of particles of Dia. X in Filtrate}}{\text{No. of particles of Dia. X in Feed}}\right) \qquad (3\text{-}14)$$

The efficiency curve, generated through calculations in the above manner, is the cumulative pore size distribution curve for the filter sample. Figure 12 shows a typical cumulative pore size distribution curve. Assuming that the pore sizes follow a Gaussian or normal distribution, the average pore size for the filter medium occurs at the diameter for which the filtration efficiency is 50 percent. Correlation between the efficiency test results and the other two methods of determining pore

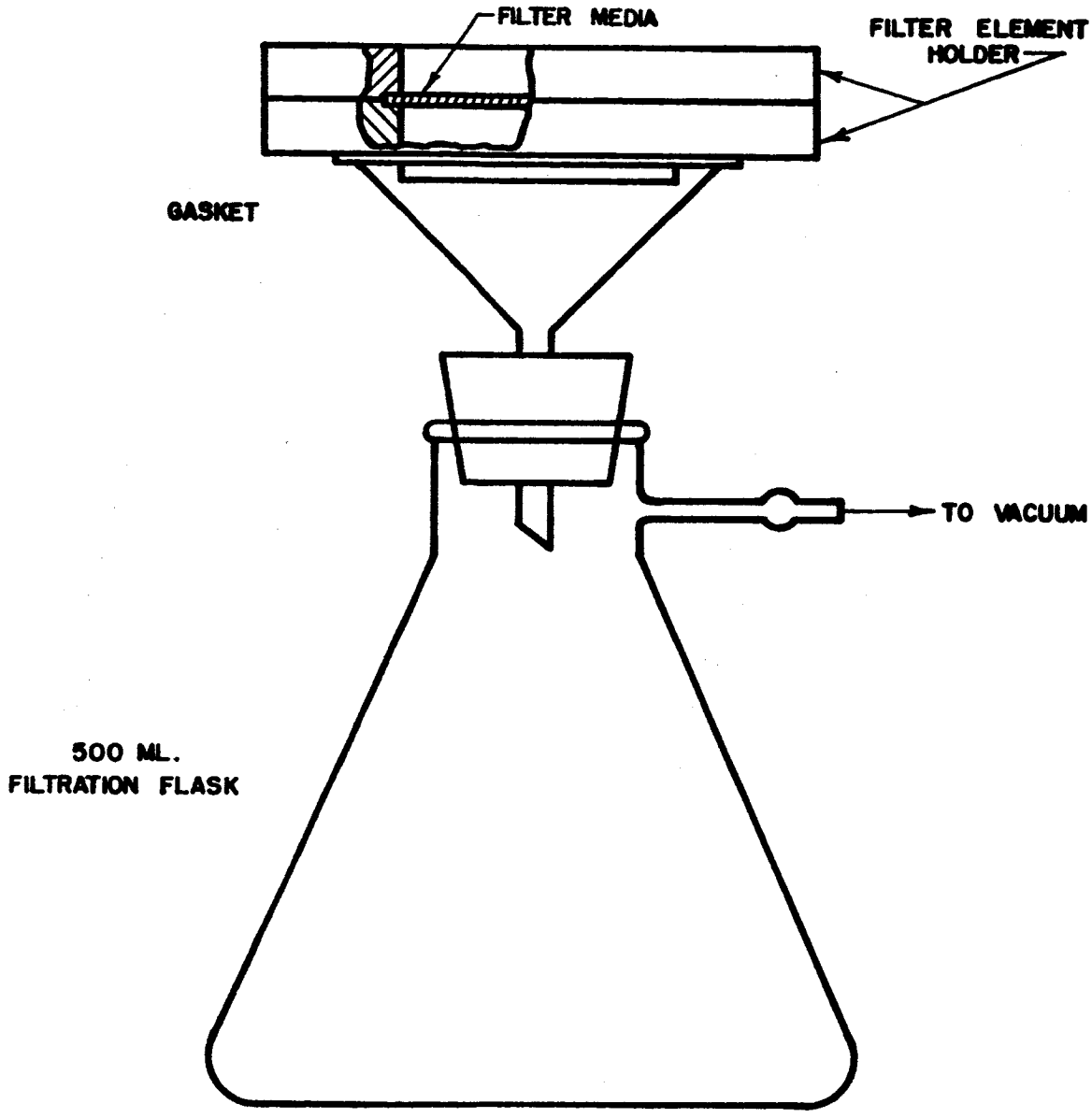

Fig. 11 Filter efficiency test apparatus

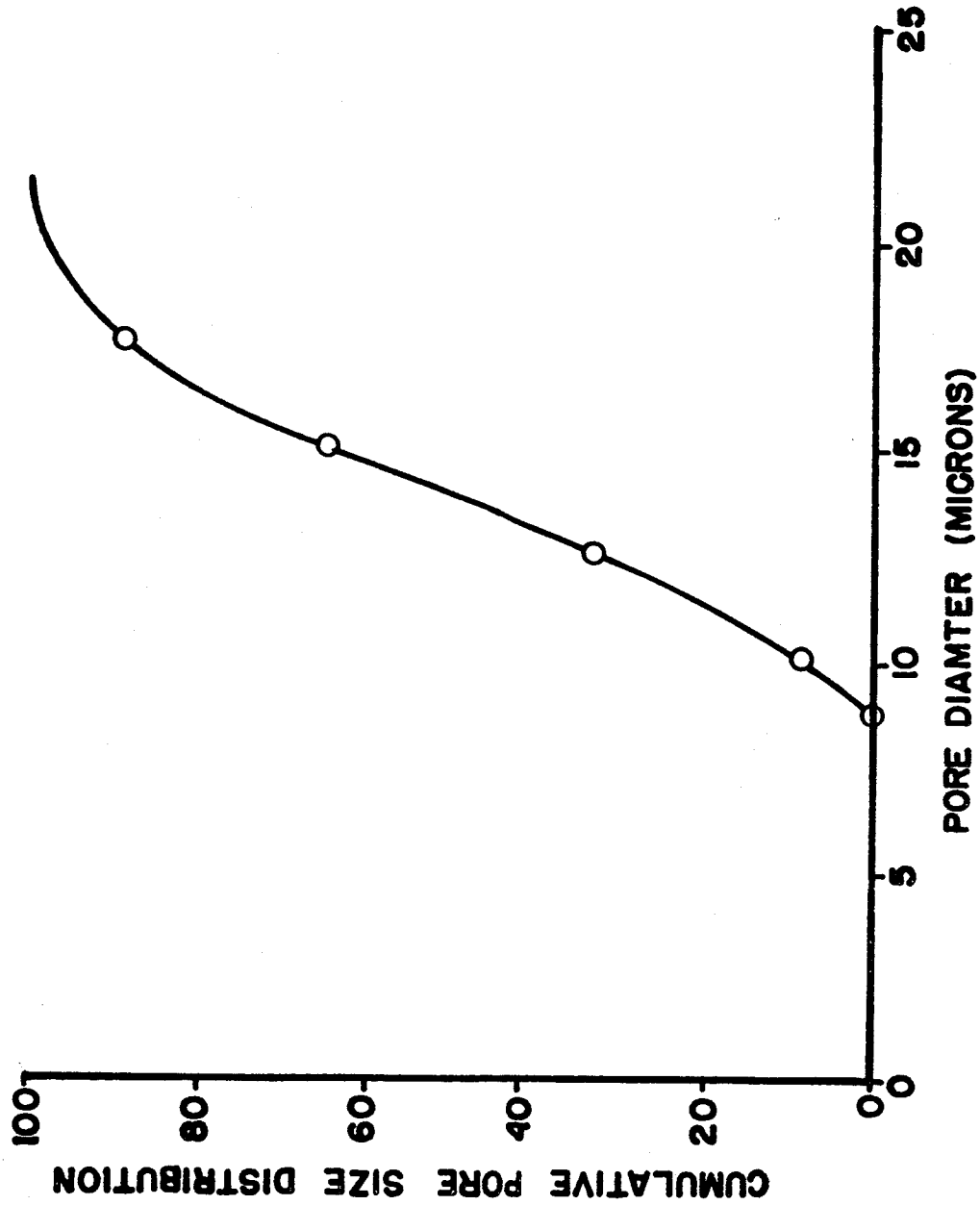

Fig. 12 Cumulative Pore Size Distribution Curve

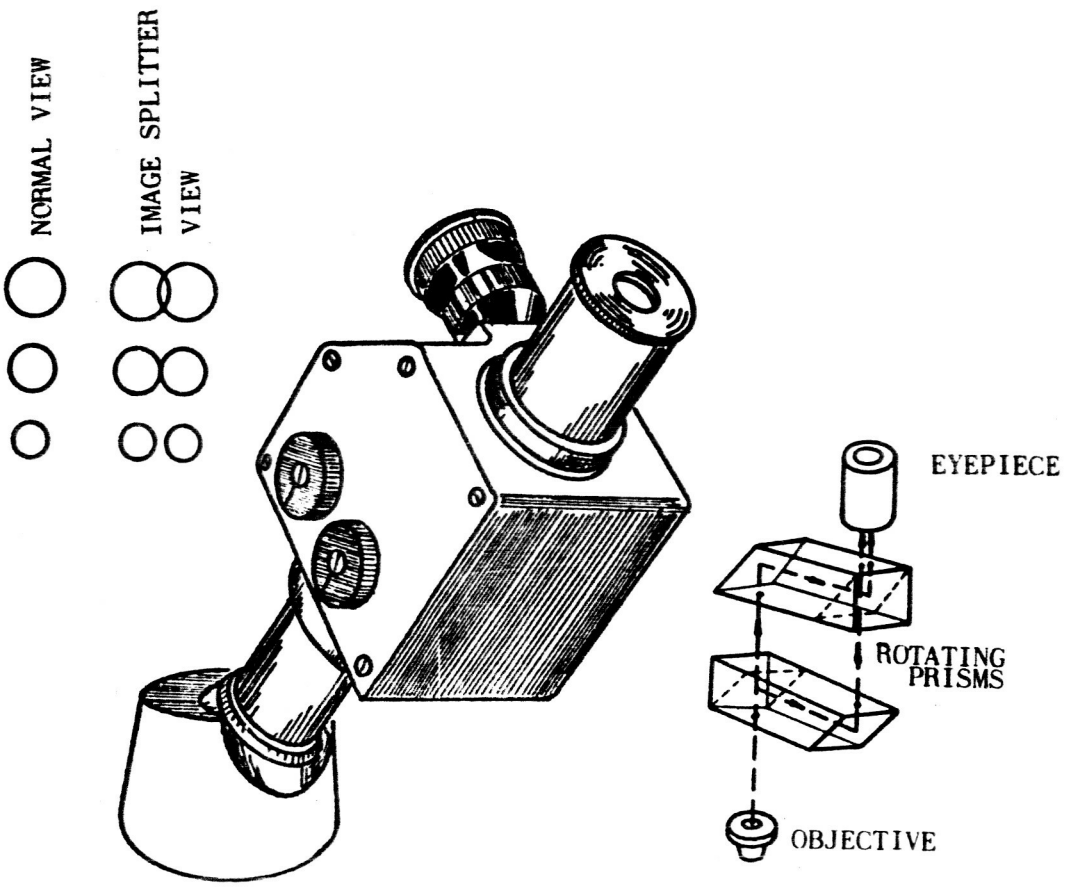

Fig. 13 Cooke-A.E.I. Image-splitting Eyepiece

size will be presented and discussed in the following chapter.

The microscope counts for the efficiency tests were carried out with the aid of a Cooke-A.E.I. Image-Splitting Microscope Eyepiece, manufactured by Cooke, Troughton, & Simms, Inc. (Figure 13). The Image Splitting Eyepiece consists essentially of a special prism assembly mounted in a conventional compound microscope system. Prisms are linked to a micrometer screw by means of which their angular relation to each other can be varied. When the prism faces are parallel to each other, two images of the object, exactly superimposed and appearing as one, will be visible in the eyepiece. As the micrometer screw is turned the images move (or shear) across each other. If the images of the object are overlapping, the amount of shear is less than the object dimension; if they are just touching, the amount of shear is equal to the object dimension; and, if the images are separated, the amount of shear is greater than the object dimension. The absolute value of the object's dimensions can be read from the micrometer drum once it has been calibrated for the microscope objective being used. Since all objects in the microscope field are sheared by an equal amount, the entire field can be counted for particles above or below any specified size by dialing the desired dimension on the micrometer. The advantage of this instrument is that the reference measure is no longer a calibrated scale located somewhere in the field of view; rather the direct relationships between individual particle images serve as the standards of measure. This is a distinct improvement over the conventional filar micrometer where the traveling fiduciary line has to be imposed optically upon each object from above. With the Image Splitter, parallax problems are eliminated since the images are in the same plane.

B. Porosity

Several methods exist to determine the fraction of void space or the porosity of a porous medium. Three methods were investigated during the study in order to find one which provides the most accurate value for the porosity of filter media. Of the techniques used the density method proved to be the most reliable provided the density of the filter material is known. The total volume of a filter medium is given by the sum of the pore volume and the volume of the solid material,

$$V_t = V_p + V_s = \Phi V_t + V_s \qquad (3\text{-}15)$$

If the material is dry and is weighed in air, its volume can be found equal to

$$V_s = \frac{W}{\rho_s} \qquad (3\text{-}16)$$

where:

W = Weight of Media

ρ_s = Specific Weight of Filter Material

Substituting for V_s in (3-15) and solving for Φ yields,

$$\Phi = 1 - \frac{W}{\rho_s V_t} \qquad (3\text{-}17)$$

The dependence of this method upon an accurate knowledge of a medium's density is the primary source of error in the results. However, all of the media tested thus far are of stainless steel construction and therefore the media density is essentially constant. The weight of a medium sample is determined with a Satorious Semi-micro Balance which has a readability of 10^{-5} gram.

The mercury intrusion porosimeter can also be used as an aid to find the porosity of a medium. The pore volume is obtained directly as the volume of mercury which is injected into a specimen. Thus the porosity

can be calculated from

$$\Phi = \frac{V_p}{V_t}$$

The method is satisfactory for fine media with small pore sizes, but an error is introduced when applied to coarse media with larger pores. The error is due to the capabilities of the porosimeter, since all pores larger than 100 microns are already filled before any volume change is recorded.

The volumetric method of porosity determination is similar to the density technique in that the volume of the solid material in a medium is measured. This volume is found by measuring the volume of liquid displaced in submerging a sample of filter material. The porosity can then be solved for from,

$$\Phi = \frac{V_p}{V_t} = \frac{V_t - V_s}{V_t} = 1 - \frac{V_s}{V_t} \qquad (3\text{-}18)$$

In order to insure accuracy with this technique the liquid must completely fill the void spaces of the medium. Complete filling is accomplished by applying a vacuum pump to evacuate entrained air from the medium. Withdrawing all of the air from very dense media is sometimes difficult and this is the limitation on the method.

C. Permeability

The permeability of porous media was defined in preceeding chapter as being equal to

$$K = - \frac{\mu V}{dP/dL}$$

From equation (2-5) the permeability can be found in terms of the medium parameters as

$$K = \frac{\mu t}{\Phi A_t} \frac{Q}{\Delta P}$$

Using conventional units the equation above becomes,

$$K(\text{Microns}^2) = 360 \frac{\mu(\text{CP.})\ t(\text{In.})\ Q(\text{gpm})}{\Phi A_t(\text{In}^2)\ \Delta P\ (\text{PSI})} \qquad (3\text{-}19)$$

A medium's permeability can be calculated by measuring the geometrical, fluid, and flow parameters, on the right hand side of equation (3-19). The geometrical parameters can be determined with the techniques previously discussed. The viscosity of the fluid was measured with a Brookfield Synchro-Lectric Viscometer.

The inter-related flow parameters Q and ΔP are obtained from flow versus pressure drop tests conducted using the filter media performance stand (Figures 14 & 15). For the tests, the medium sample is installed in the sample holder and placed in the test housing (Figure 16); the housing is then located in the test section of the hydraulic test stand. Flow through the filter medium is varied from 1 to 20 GPM in increments of 1 GPM. At each of the flow rates the differential pressure across the test section and filter sample is measured and recorded. After subtracting the test section pressure loss, the pressure drop across the medium is graphed as a function of flow rate (Figure 17).

Extremely accurate instrumentation is used in order to insure the reliability of the flow resistance test results. The flow rate is measured with a Fisher & Porter Turbine meter which is accurate to within 0.1%. The pressure differential measurements are taken with a Fisher & Porter "Press-i-cell", a differential pressure instrument with a readability of 0.05 psid and a repeatability to within 0.066 psid. In order to maintain a constant fluid viscosity, the test temperature is maintained within 0.5° F. using a Minneapolis-Honeywell temperature controller.

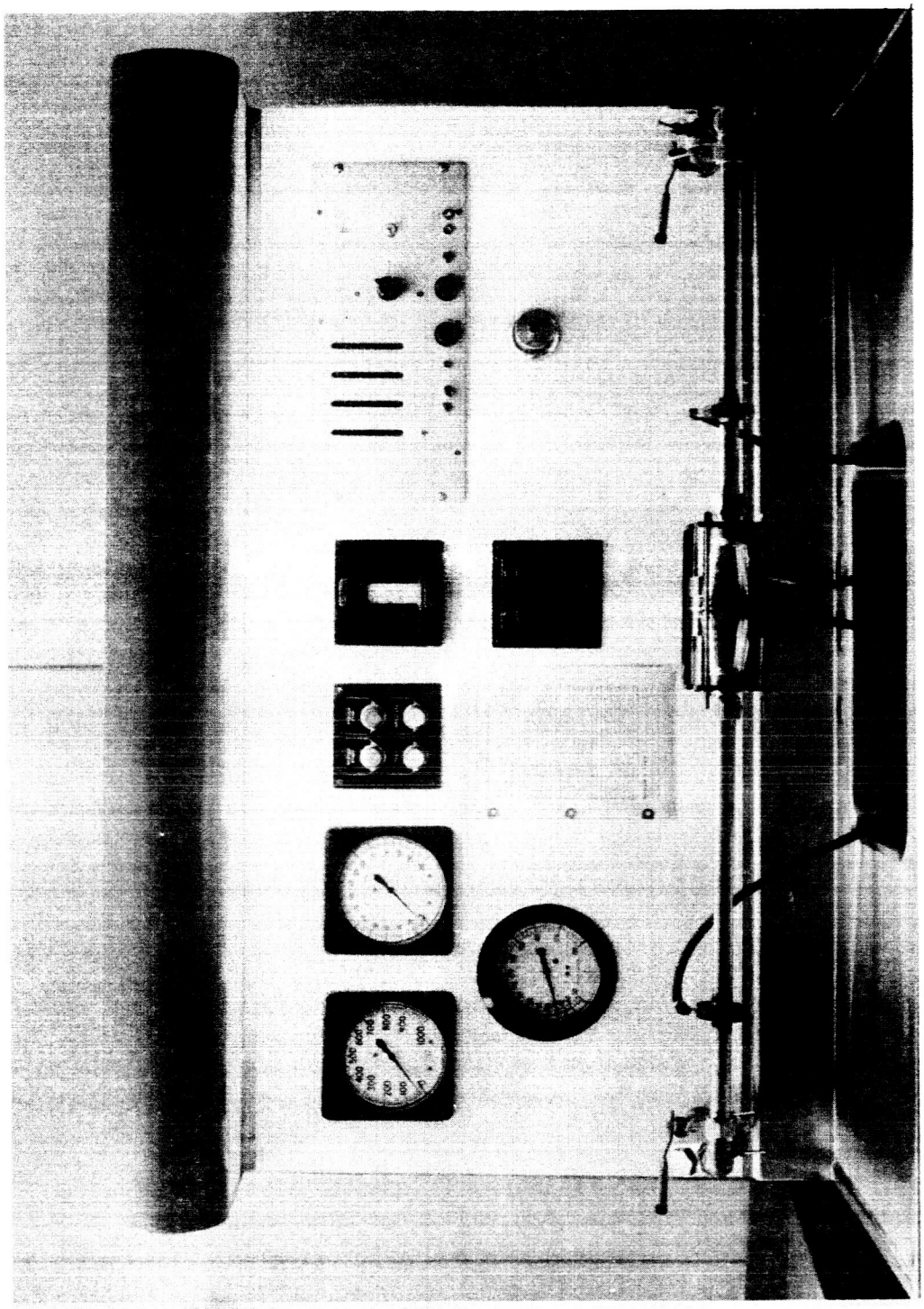

Fig. 14 Filter Media Performance Stand

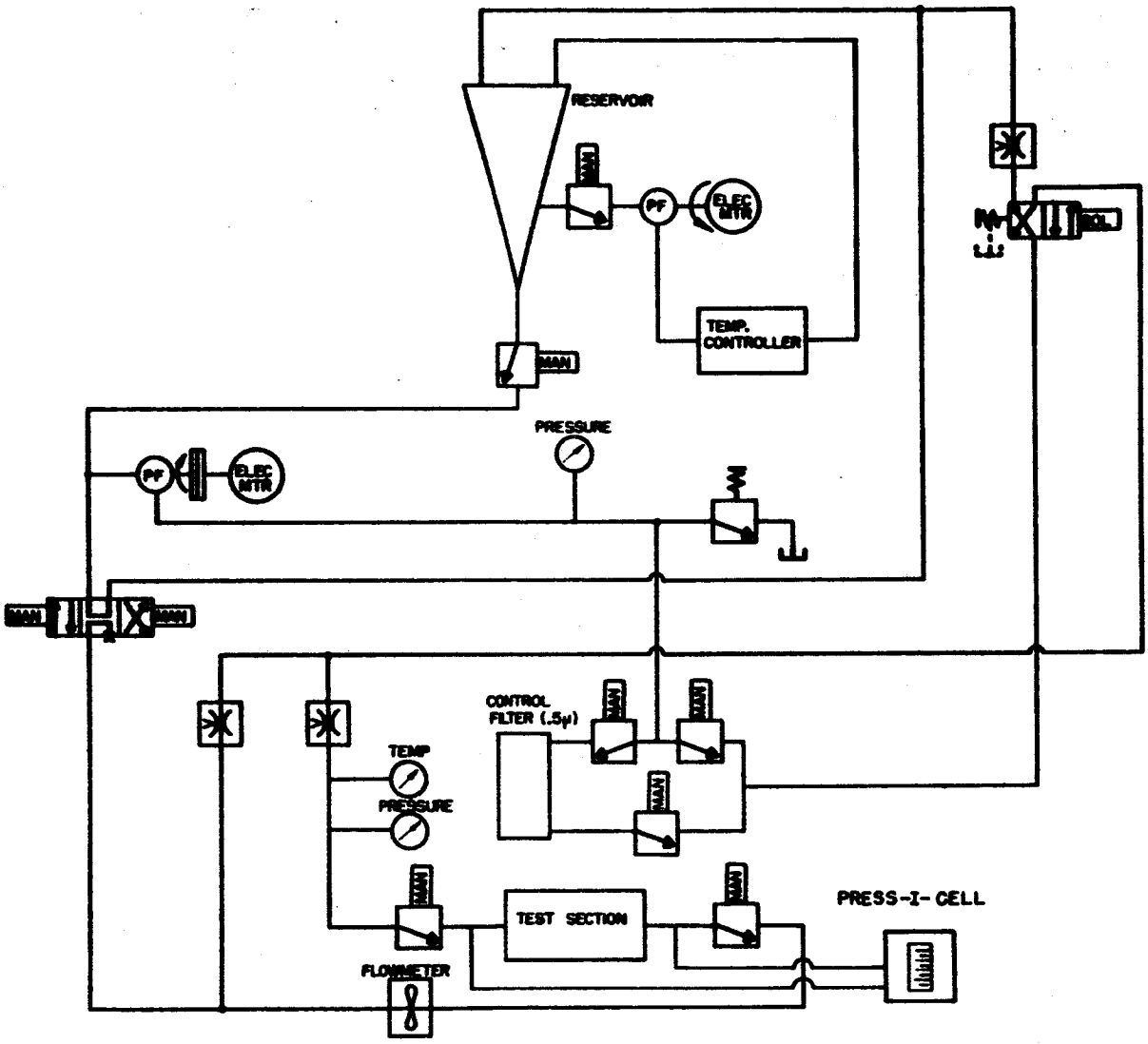

Fig. 15 Schematic of filter media performance stand

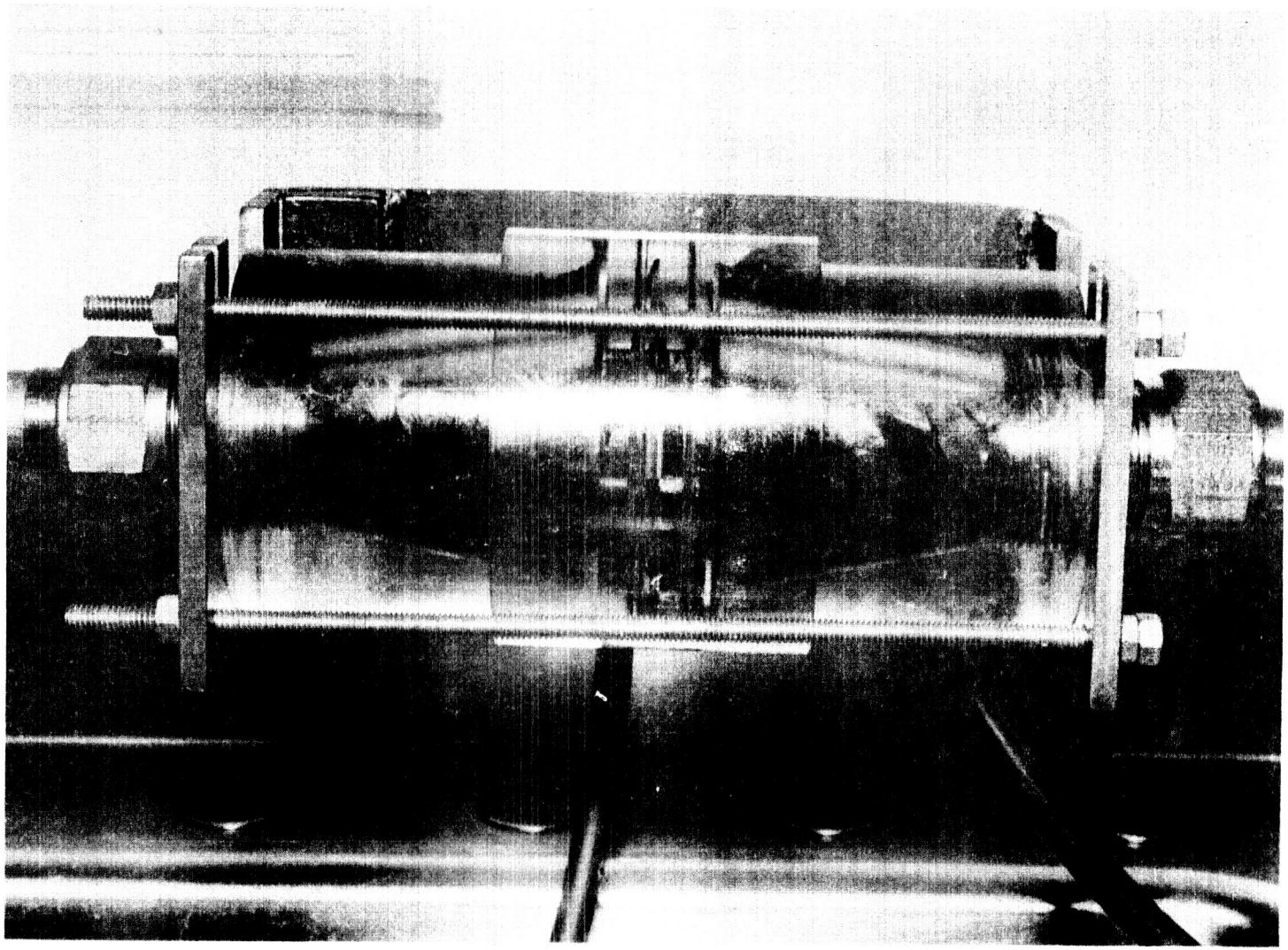

Fig. 16 Filter Media Test Housing

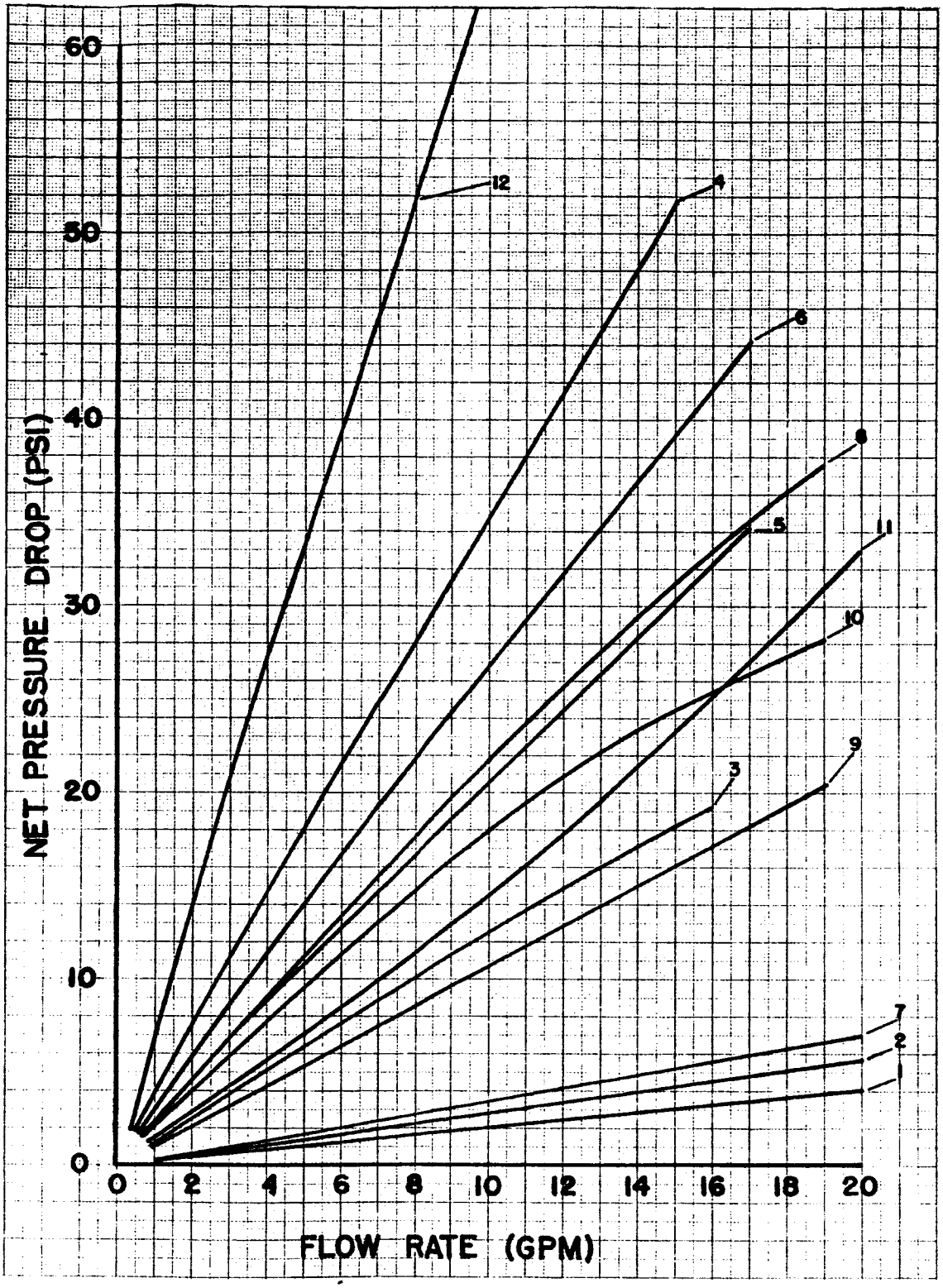

Fig. 17 Flow resistance curves

The techniques discussed in this chapter represent a composite of the methods used to determine filter media parameters. The information gained from these tests yields significant insight into the structure and properties of filter media. The tests have been successfully performed on a wide variety of media as the data in the following chapter will show.

CHAPTER IV

ANALYSIS AND CORRELATION OF EXPERIMENTAL DATA

The test methods described in Chapter III were applied to twelve different specimens of filter media in order to determine the properties of the media. The twelve specimens of media included: Six single-layer unsintered wire cloth samples, four single-layer sintered wire cloth samples, one two-ply sintered wire cloth sample (Figure 18), and one metal fiber depth medium (Figure 19). The wire cloth media that were tested included seven with a dutch twill weave (Figure 20), and three with a modified dutch twill weave (Figure 21). A partial list of the media properties is shown in Table 1.

The validity of the average media diameter as obtained from the porosimeter was determined by comparing this diameter with the average diameter resulting from filtration efficiency test. Table 2 is a listing of the porosimeter diameters for all of the media tested and the efficiency diameters for a selected group of samples. The results show excellent agreement with the exception of sample No. 11. For this sample the porosimeter test showed an average diameter of 48.0 microns, while the efficiency test yielded a diameter of 30.5 microns. This deviation is to be expected, since this medium is made up of two layers of wire cloth. The filtration efficiency of multi-layered media at any diameter is equal to one minus the product of the efficiencies of the individual layers at the given diameter. Therefore, a multi-layered medium will have an average

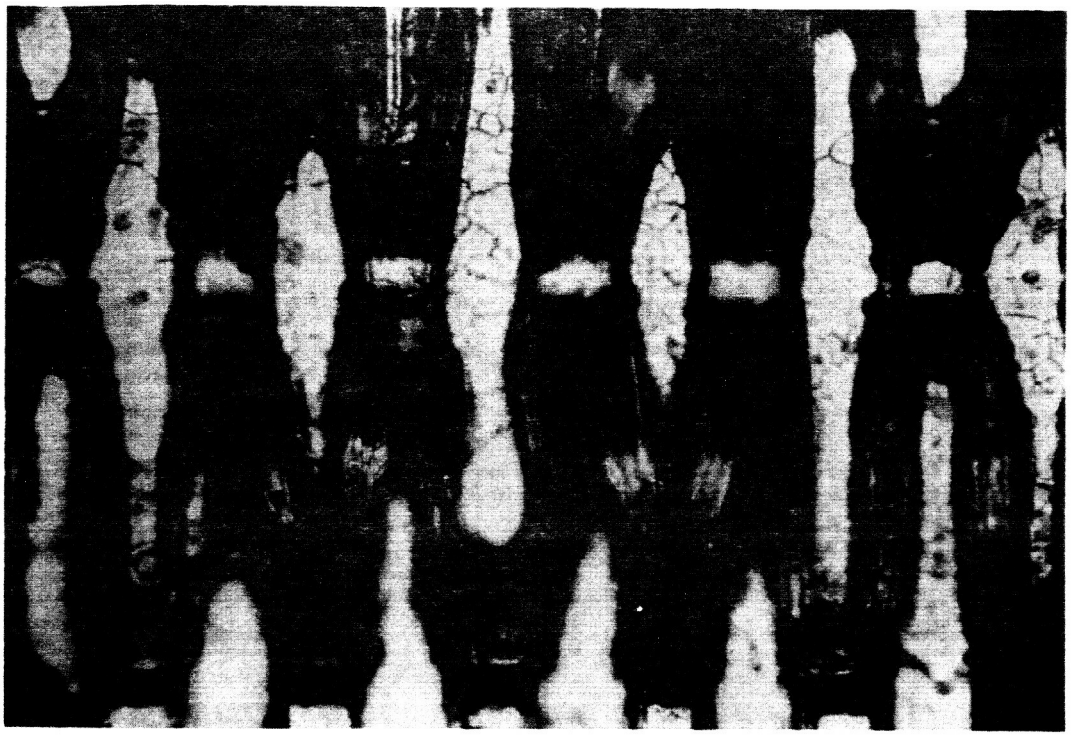

Fig. 18 Two ply wire cloth filter sample

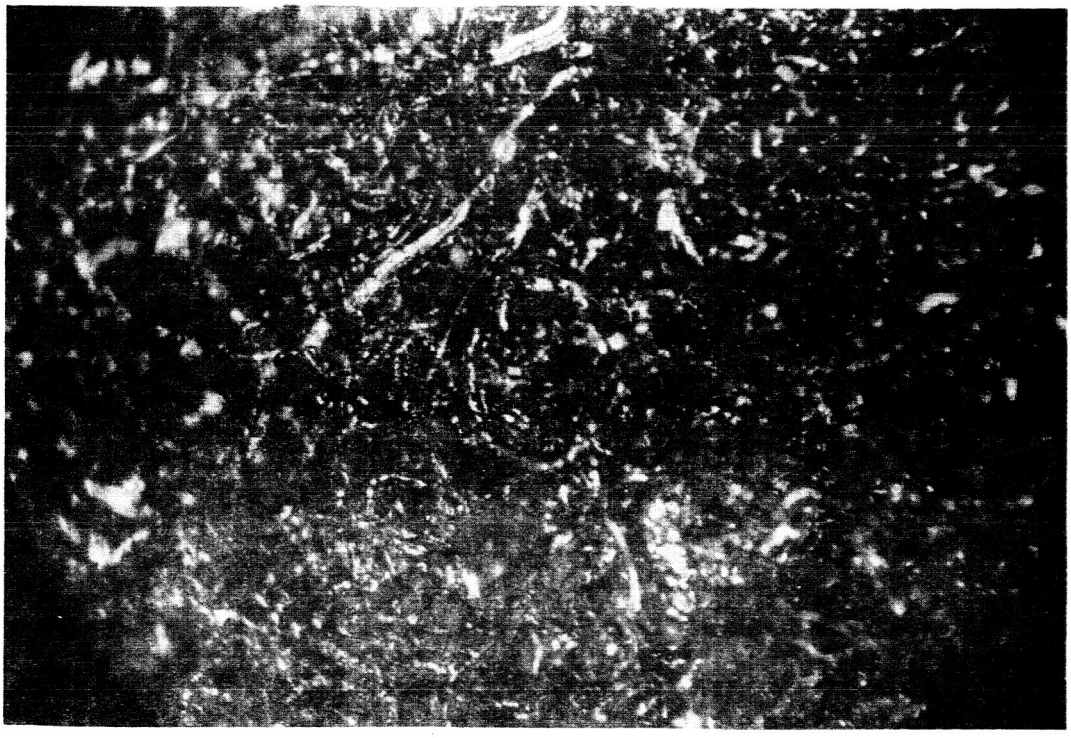

Fig. 19 Metal fiber depth filter medium

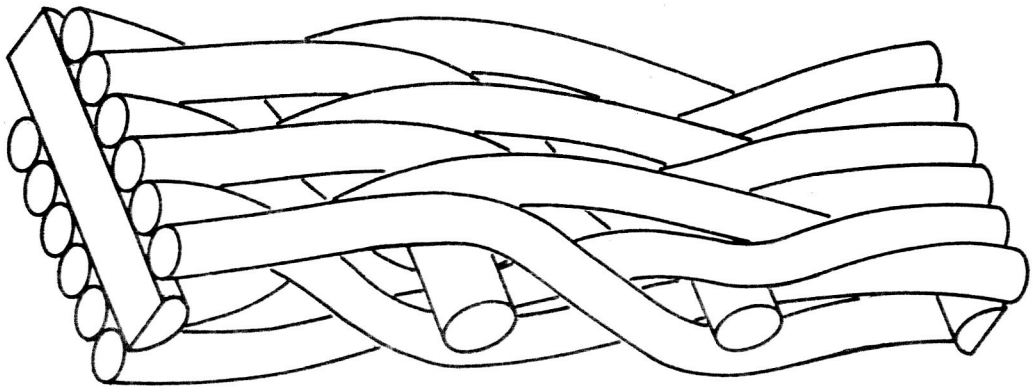

Fig. 20 Wire cloth medium (Dutch Twill Weave)

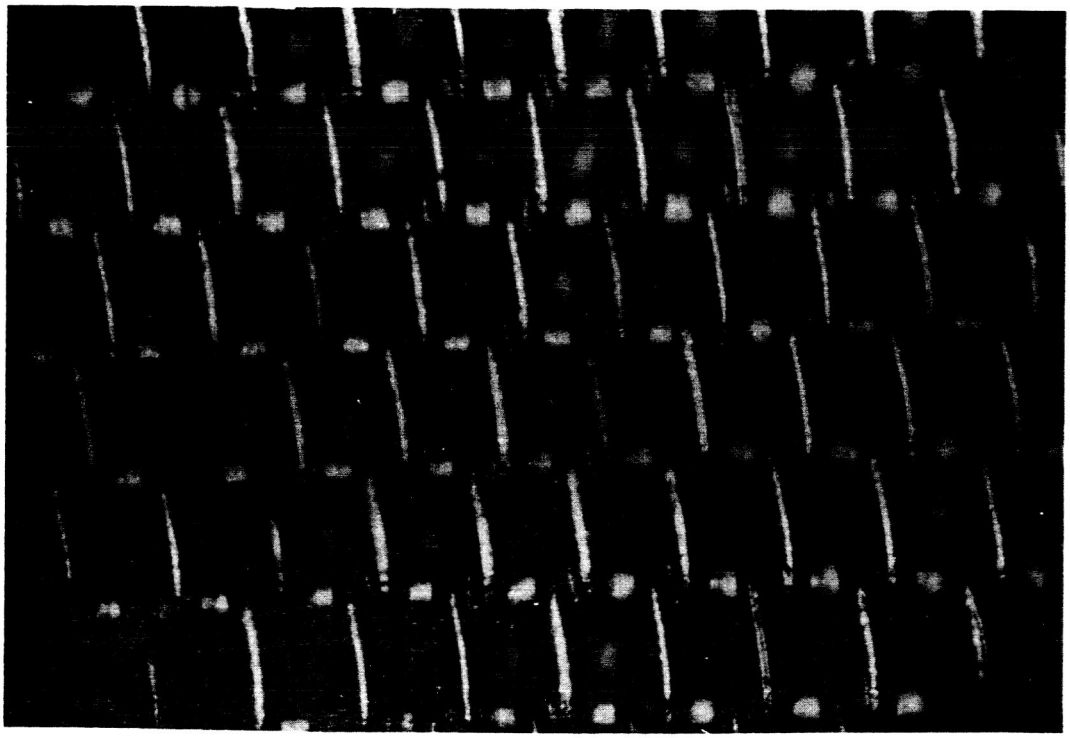

Fig. 21 Wire cloth medium (Modified Dutch Twill Weave)

TABLE 1

MEDIA PROPERTIES

SAMPLE NUMBER	MESH TYPE	MEASURED WEAVE	THICKNESS	POROSITY*
1	Modified Twill	107 x 544	.0087 In.	53.1 %
2	Modified Twill	180 x 532	.0055	60.5
3.	Dutch Twill	150 x 1200	.0057	38.4
4	Dutch Twill	297 x 1850	.0038	36.7
5	Dutch Twill	180 x 1200	.0060	37.8
6	Dutch Twill	296 x 2030	.0034	37.8
7	Modified Twill**	145 x 728	.0066	52.5
8	Dutch Twill**	183 x 1240	.0057	37.9
9	Dutch Twill**	148 x 1210	.0058	42.2
10	Dutch Twill**	291 x 1750	.0035	42.3
11	Square (2 ply)**	45 x 219	.0132	32.2
12	Depth (Metal Fiber)		.029	67.0

* Porosity determined by Density Method

** Sintered Wire Cloth Specimens

TABLE 2

PORE SIZE TEST RESULTS

SAMPLE NUMBER	AVERAGE DIAMETER (μ) (POROSIMETER TEST)	AVERAGE DIAMETER (μ) (EFFICIENCY TEST)	BOILING PRESSURE (IN. OF H_2O)
1	51.0	46.0	5.90
2	35.0		9.10
3	23.5		12.60
4	12.0		27.80
5	19.5		18.70
6	13.0	12.8	28.45
7	32.0	33.5	8.65
8	16.5	16.5	19.15
9	23.5		13.05
10	14.5	14.5	25.60
11	48.0	30.5	5.90
12	19.0		13.15

filtration diameter which is smaller than the average diameter of any of the layers.

The curves in Figure 22 illustrate a typical comparison of data for average pore diameter determination by the porosimeter and the filtration efficiency techniques. Note that the average diameter determined by the peak of the porosimeter curve, f(D), corresponds with the 50% point on the efficiency curve. Fifty percent filtration is achieved on particles with diameters equal to the average pore size of the medium if the pore size distribution is normal. Figure 23 shows that the porosimeter diameter on the single layered wire cloth media tested are virtually the same as the average diameter corresponding to a 50% filtration efficiency.

The results obtained through comparison and correlation of porosimeter and filtration efficiency test data exemplifies the utility of the porosimeter as a means to analyze simple media with respect to pore diameter. The porosimeter technique is a significant simplification over the tedious particle counting procedures required in the efficiency technique. Also, the porosimeter test is not operator sensitive and provides extremely repeatable results.

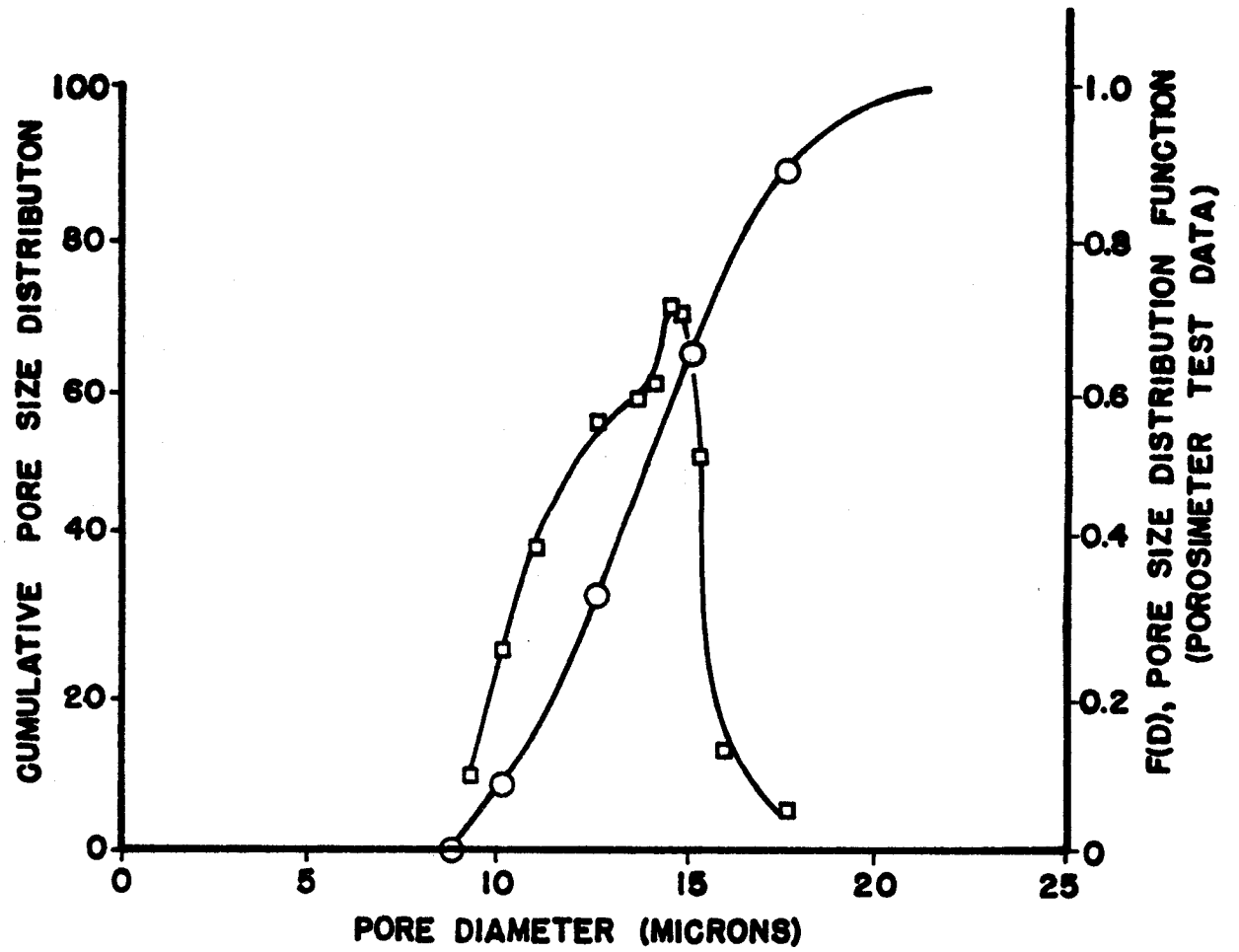

Fig. 22 Comparison of Date From Porosimeter and Filtration Tests

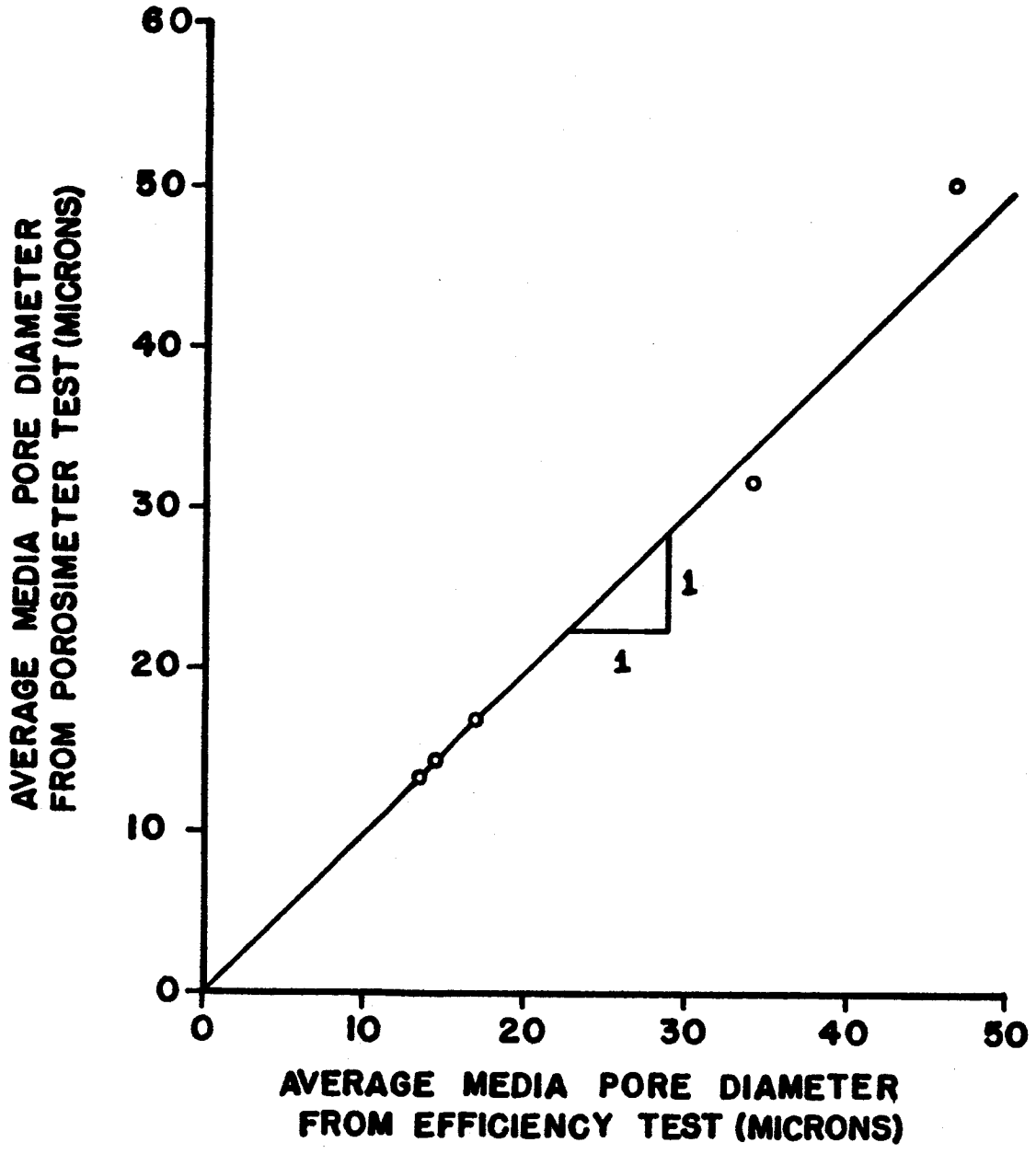

Fig. 23 Porosimeter Vs Efficiency Diameter

The close agreement between the porosimeter and efficiency diameters allows their use as a standard for correlating the boiling test results. A graph of boiling pressure versus average media diameter is shown in Figure 24. A hyperbolic curve, PD = constant, is also shown on the same graph. The value of the constant was determined to be 320 by averaging the boiling pressure-diameter products for all of the test points. The boiling pressure test, like the porosimeter test, offers a simple means of determining the average diameter of media. While not as accurate as the porosimeter test, the boiling pressure test offers the advantage of being applicable to assembled filter elements.

The permeability constants for the media samples were obtained by solving equation (3-19) using the media parameters and the flow-pressure drop results (Figure 17). The value of K in Table 3 was evaluated at a flow rate of 10 GPM and a viscosity of 12 cp. It may be recalled from equation (2-13) that the permeability of the hypothetical medium was equal to $D^2/32$. Figure 25 shows the relationship between the experimental and theoretical values for permeability.

The empirical and theoretical values are equal for media whose permeabilities are less than $20\mu^2$. Therefore, the results are valid for media having average diameters smaller than 25 microns. In the range above 25 microns the empirical and theoretical values deviate. A portion of this deviation can be explained by the fact that any errors in diameter measurements are also subject to flow pattern effects in this range since the pressure loss across the media is of the same order of magnitude as the housing tare. The accuracy of the results in the lower micron range is significant since this is the principle area of concern in filters for high performance hydraulic systems.

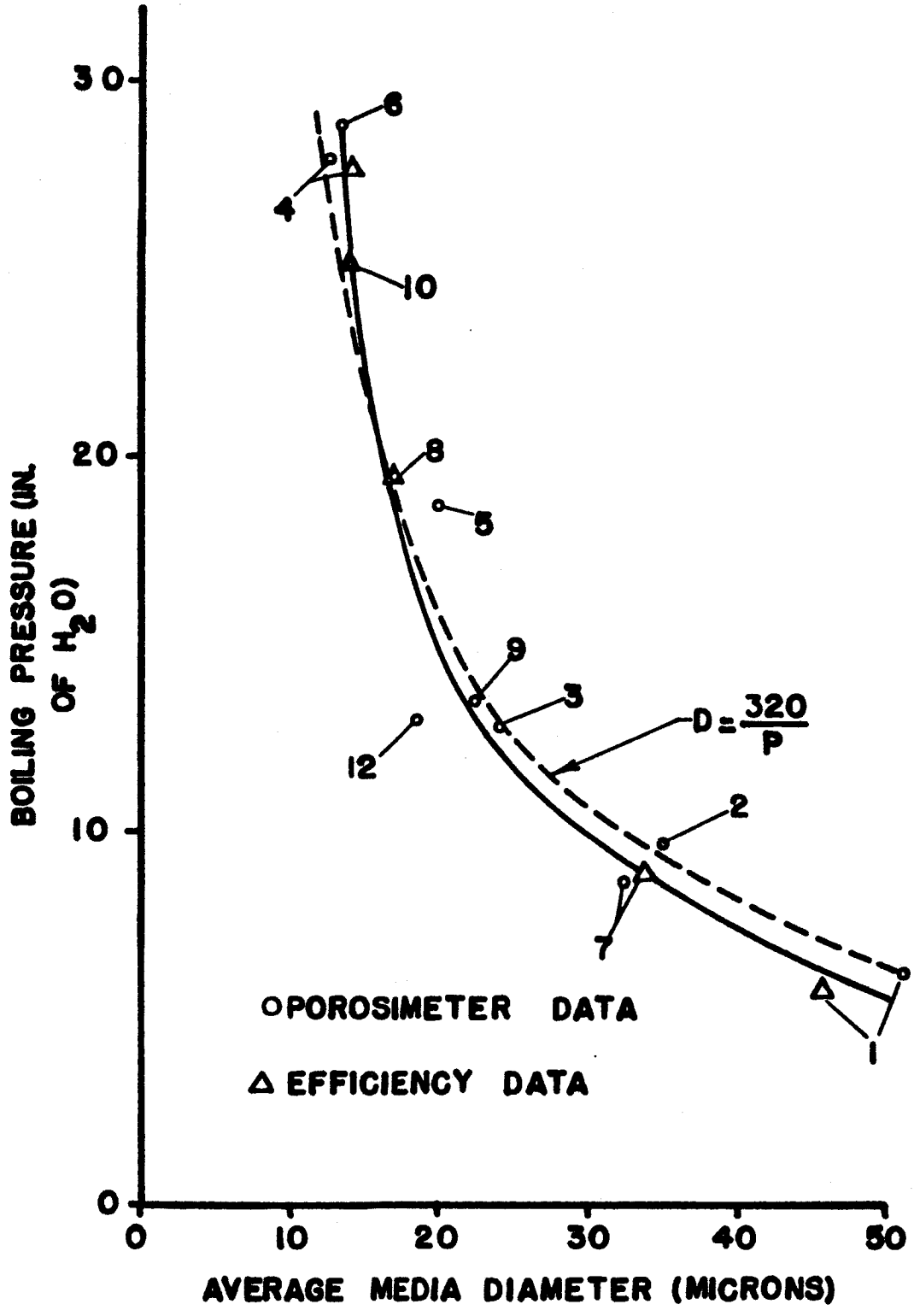

Fig. 24 Correlation of Boiling Pressure Data

TABLE 3

EXPERIMENTAL AND THEORETICAL VALUES OF PERMEABILITY

SAMPLE NUMBER	Measured $K(\mu^2)$	Calculated $D^2/32\ (\mu^2)$
1	98.0	81.0
2	42.4	38.2
3	16.3	17.3
4	4.1	4.5
5	9.9	11.9
6	4.6	5.3
7	46.8	32.0
8	9.5	8.5
9	16.7	17.3
10	6.3	6.6
11	--	--
12	9.3	11.3

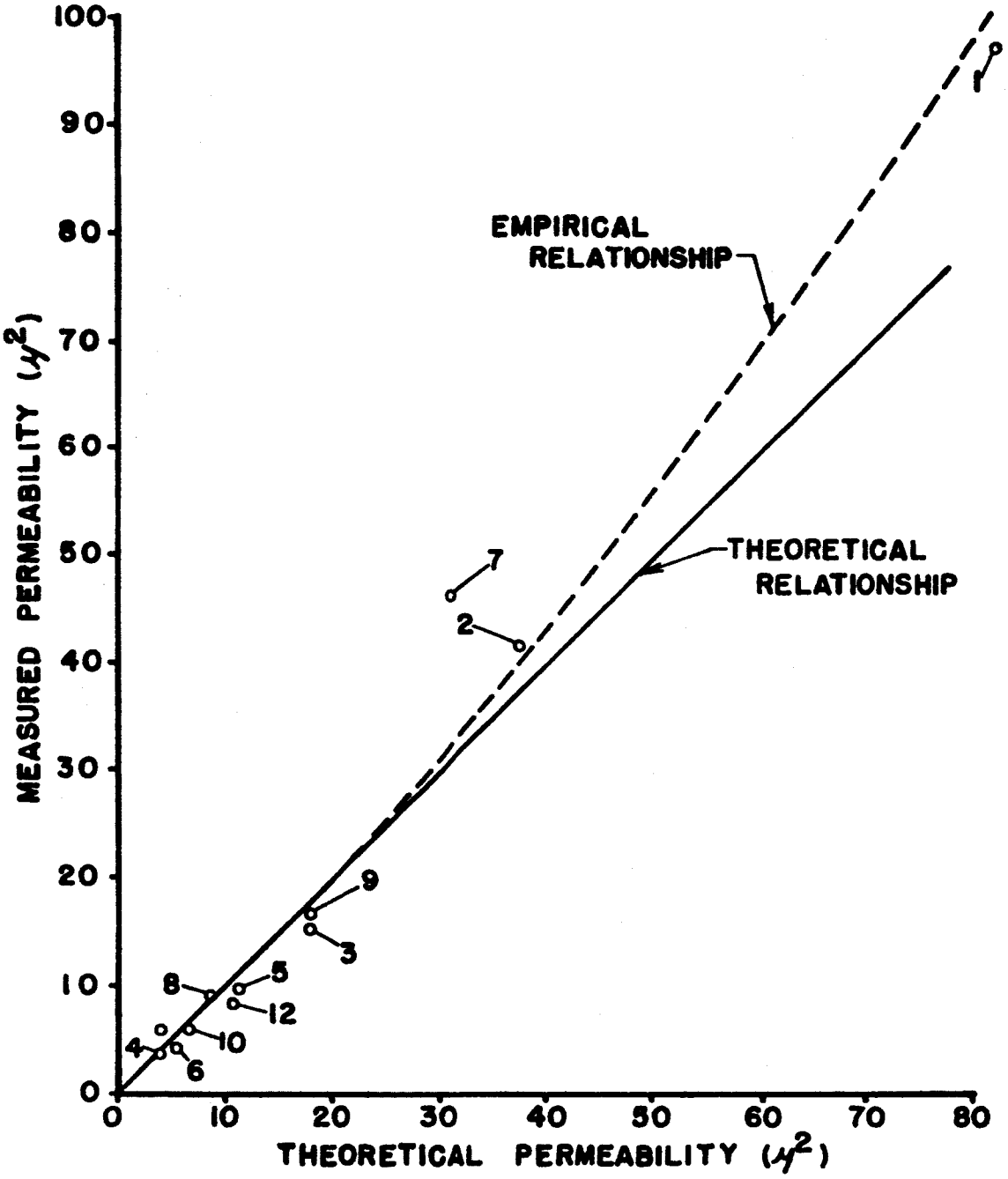

Fig. 25 Correlation of Experimental and Theoretical Values of Permeability

For media with pore diameters of 25 microns or smaller, the flow equation for simple wire cloth media can be represented by,

$$Q(gpm) = 0.87 \times 10^{-4} \frac{\phi\, D^2(Micron^2)\, A_t(In^2)\, \Delta P(PSI)}{\mu(cp.)\, t(In.)} \qquad (4\text{-}1)$$

The equation above offers a means of determining analytically the performance of a medium on the basis of its properties. The result does not represent the ultimate defining equation for filter media; however, it does reflect the distinctive trend in the results of tests performed on a representative sample of media. Although future testing will be necessary to generalize the results for depth media and multi-layered wire cloth media, the background obtained in this study will facilitate the extension of the theory.

CHAPTER V

CONCLUSIONS AND RECOMMENDATIONS FOR FILTRATION MECHANICS

The important parameters of filtration are interrelated with the parameters involved in fluid transmission. Experimental results have shown close agreement with the theoretical analysis of the filtration flow process through wire cloth media with average pore sizes less than 25 microns.

Media properties such as porosity, average pore size, and permeability of simple wire cloth media can be measured readily in the laboratory, but care must be exercised to assure that a given measuring technique is valid for the case in question. The mercury intrusion porosimeter is very effective for obtaining average pore sizes of single-layered wire cloth media of the types tested. The "average" diameters determined by filter efficiency tests, boiling pressure techniques, and by mercury intrusion can be correlated with each other for wire cloth media. Mercury intrusion shows definite promises as a media quality check technique. "Boiling Pressure Testing" has a distinct advantage of being non-destructive when used for checking the average diameters of wire cloth media in manufactured filter element configurations..

The results obtained thus far support the expectations that further studies will reveal valid analysis criteria for more exotic filter materials. Also, it is anticipated that the contaminant holding capacity of wire cloth media can be directly related to their physical parameters.

CHAPTER VI

INTRODUCTION TO DYNAMIC SAMPLING

Samples of fluid, taken from dynamic fluid systems, must accurately and consistently reflect the distribution or level of particulate contamination within the sampled systems. It is readily understood that the contaminant generation rates within fluid systems are not constant and the systems require continuous maintenance and checking. Unfortunately, when the literature concerned with fluid sampling is assayed, it becomes categorically evident that the state of the art is improficient when applied to modern fluid power systems of high performance requirements. Full knowledge of the direct and indirect parameters involved in fluid sampling, which is prerequisite to accurate measurement and specification of the contamination found in hydraulic systems, has not been achieved to date.

More specifically, there is a need for dynamic sampling techniques which can be utilized in relatively clean systems. Systems which tolerate the higher concentrations of contamination, such as found in general use in industry, are not considered to be difficult to sample. However, in "clean" fluid systems, where the contamination has been rarefied by high-quality filtration devices, the difficulties incurred in achieving a fluid specimen which accurately reflects the condition of the subject system are magnified several times. As a system approaches the more

elegant states of cleanliness, the effects of velocity and pressure gradients with a system and with the sampling device itself, become increasingly significant to resulting samples of the system. Also, contamination originating extraneously to the system becomes highly critical to sample analysis when the sampled system is relatively clean initially. Ultraistic care is a must when fluid samples are taken from high-quality systems of low-contaminant level classification.

Actually the taking of a sample of fluid from a dynamic sampling device is only one of the important steps in a given sampling technique. Every action that involves handling or manipulating the fluid sample throughout its useful tenure must incorporate extremely rigorous measures if the results of the analysis are to be considered valid.

The scope of the research conducted on fluid sampling techniques in the OSU Fluid Power Laboratory thus far has been to devise a complete sampling and analysis operation whereby the individual steps which may be incorporated in sampling techniques can be examined comprehensively. This has included:

1. Fabricating a test stand that would facilitate accurate temperature and flow rate control of the test fluid (MIL-F-5606).
2. Fabricating and calibrating a laminar flow isokinetic sampling probe section.
3. Refinement of procedures for the analysis of fluid samples by HIAC automatic particle counter.
4. Defining cleaning procedures for the sample bottles used in the tests.

5. Application of the developed technique details to evaluate commercial sampling devices.

The research in the areas mentioned has been conducted with systematic scrupulousness in order that the efforts would result in comprehensive conclusions and support recommendations for further study.

CHAPTER VII

SAMPLE ANALYSIS

The applicability of a method of extracting fluid samples from dynamic fluid systems is evaluated from analyses made on samples of fluid taken by the extraction method under investigation. Obviously, the procedures incorporated in the analyses are of primary importance to the ultimate judgment of the method. This poses a serious problem because any technique of sample analysis for particulate contamination involves factors which can affect the accuracy of the end results. Moreover, the research of this project has shown that to achieve measurements which can be reliably compared, precise control of the critical factors must be practiced from the time of withdrawing a volume of fluid from the subject system until measurements of the contamination in the sample can be accomplished. Any inconsistency in the analysis operation results in erratic deviations in the data that may be inadvertently charged to the extraction method. Such deviations, in many instances, have a greater effect on the contamination level indications of the analysis than the deviations that can be legitimately charged to the sample removal technique.

The procedures that have been followed on this project for achieving contamination measurement data from bottled samples using the HIAC automatic particle counter are described in the following paragraphs. The details that are presented are supported by a substantial amount of experimental work.

All samples of fluid were collected in 100 milliliter glass bottles. In preparing the bottles for sampling, they were initially cleaned with a soap solution in an ultrasonic cleaner and rinsed with filtered (.45 micron) isopropyl alcohol. After drying the bottles in an oven, they were rinsed with filtered (.45 micron) low-boiling petroleum ether and covered. Subsequent cleaning of the sample bottles was accomplished by using only a filtered petroleum ether rinse as described in the remaining procedure. Prior to taking samples, a plastic covered magnetic stirring rod was added to each bottle, and they were rinsed again with filtered petroleum ether using a specially designed bottle rinser. The bottles that were used in the sampling study were used exclusively in the program. That is, no new bottles were introduced after the sampling program was begun. Also, the bottles used for sampling were not used for any other purpose. It appears that repeatability is gained in the counting operation by using the same bottles in subsequent samplings.

The rinser was constructed to facilitate large volume rinsing of the sample bottles. The rinser is designed to direct a continuous jet of petroleum ether vertically out of a nozzle into an inverted sample bottle (See Figure 26). The ether is re-cycled in the rinser system, being filtered through a 0.45 micron Millipore filter unit which is located immediately upstream of the nozzle. By rinsing in this manner, the bottom and sides of the sample bottle and the magnetic stirrer are showered with a voluminous amount of clean petroleum ether which removes contaminant particles as it drains out of the inverted bottle. After the rinse, the bottle openings are covered immediately with a patch of polyethylene film and the cap screwed on. The polyethylene film insures against infiltration of contaminant particles from the cap and the air.

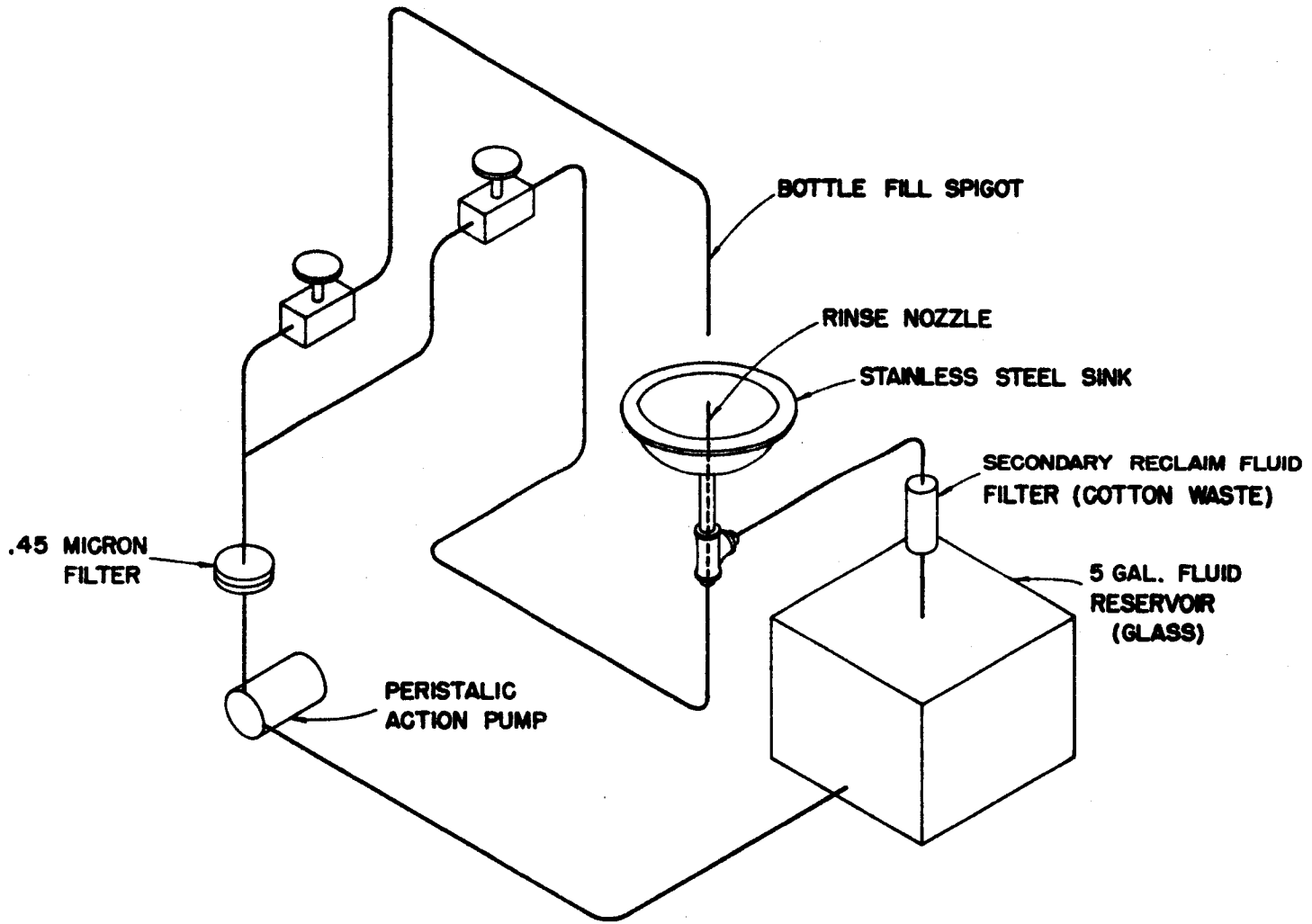

Fig. 26 Sample Bottle Rinser

Hypodermic type adapters (See Figure 27) were used in conjunction with the sampling valves used in this study. The adapters being designed to puncture the polyethylene patch as the sample bottles were screwed into place for receiving the sample. The fluid passages of the sampling apparatus and the adapter were flushed out before each sample was collected. At least 200 milliliters of fluid was released during the flushing of the assembly.

The samples were counted on a High Accuracy Products Corporation, Model PC-202 automatic particle counter. The HIAC counter was calibrated for simultaneous counting of four different particle sizes, whereby all particles equal to and larger than the calibrated size are counted. The particle sizes counted in all tests of this study were: 6, 10, 15, and 20 microns. In order to minimize drift in the counter's calibration, throughout the counting of samples, it was necessary to have the HIAC at a steady-state operating temperature. This was accomplished by allowing the device to remain on for at least 12 hours before calibration. The samples from a related series of tests were counted as a complete set in order to reduce any error due to a drift in the calibration of the HIAC. It was found that any recalibration made after counting part of a series of samples, caused difficulty in comparing the counts of the remaining samples with those counted before the recalibration.

The sample bottle was pressurized with an external air supply in order to force the fluid from the sample bottle through the standpipe pickup tube and the microcell assembly of the particle counter. A Millipore filter (.45 microns) was used to clean the air that displaced the fluid in the sample bottle. The flow rate of the fluid through the micro-

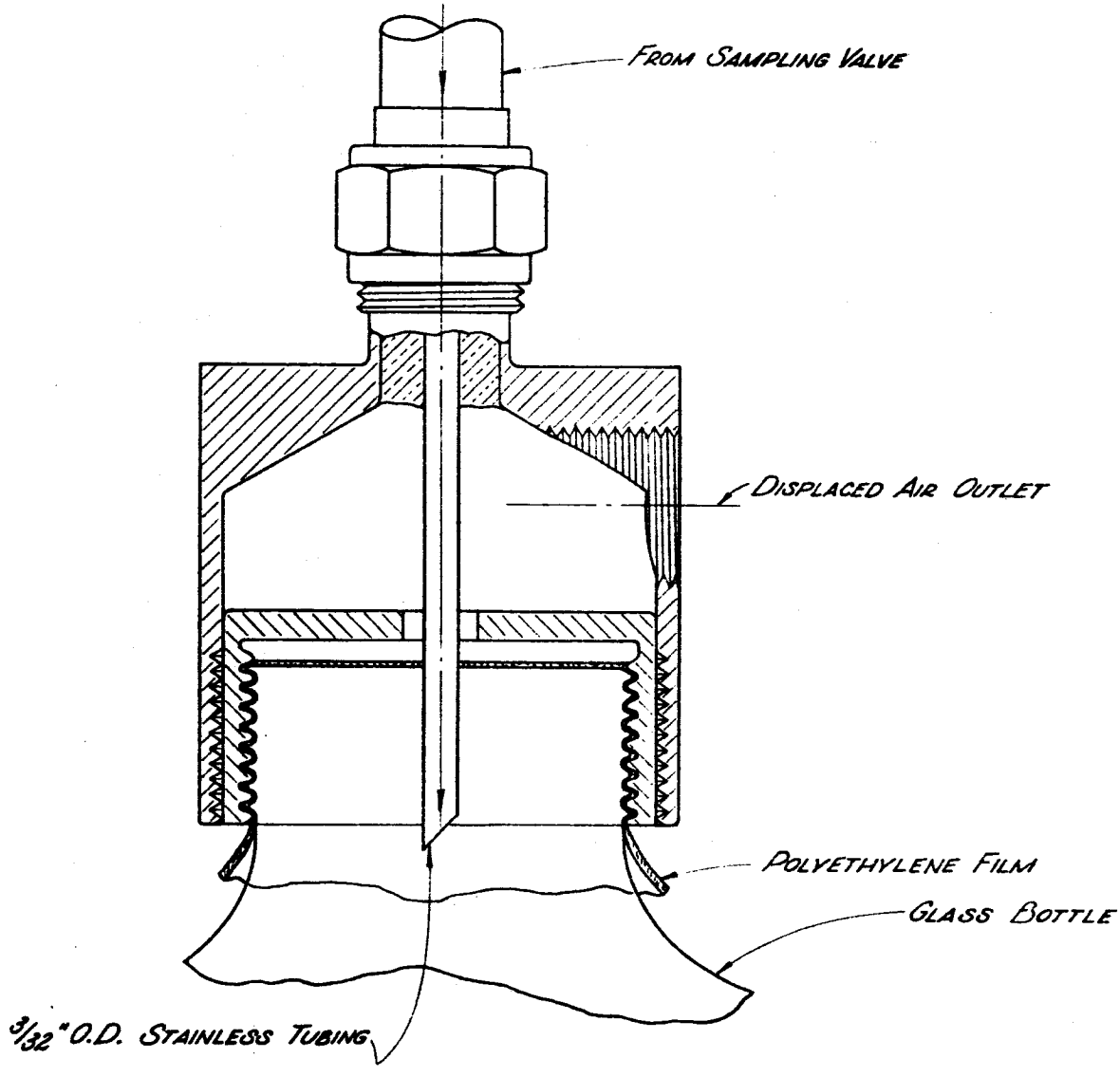

Fig. 27 Hypodermic Adapter

cell was regulated at 60 drops per minute (0.8 milliliters per min.). Deviations in the flow rate are accompanied by inverse variations in the resulting particle count. That is, an increase in the flow rate results in a decrease in count and vice versa. For critical work, it is recommended that flow rates through the counter be held within close limits to set point. On all tests conducted on this project, the flow rate setting was maintained within $\pm$ 2 per cent. Particle counts were for 5 milliliter increments of fluid passing through the counter; and a minimum of 2 counts were used to obtain a value representing the number of particles of specified size in each sample. The reported values were obtained by calculating an average of the counts that were made on a given specimen of fluid.

Before the samples were processed through the HIAC particle counters, they were prestirred for approximately 10 minutes with a bench-type magnetic stirrer to remix contaminant particles which might have settled in the bottles. The stirring was continued during counting with the regular magnetic stirrer mounted on the particle counter.

Stirring the fluid sample to maintain the suspension is desirable; and magnetic stirring devices are adequate for the job when the contaminants in the fluid are nonmagnetic. However, it was discovered during this study that the magnetic stirring bars in the fluid sample can be a source of significant error to the particle count. Tests have shown that the plastic covering of the bars experiences mechanical failure and generates particles in the sampled fluid if the bars are allowed to "tip" the sides of the sample bottles as they whirl about in the fluid. Figure 28 shows points plotted on coordinates of increasing particle counts versus

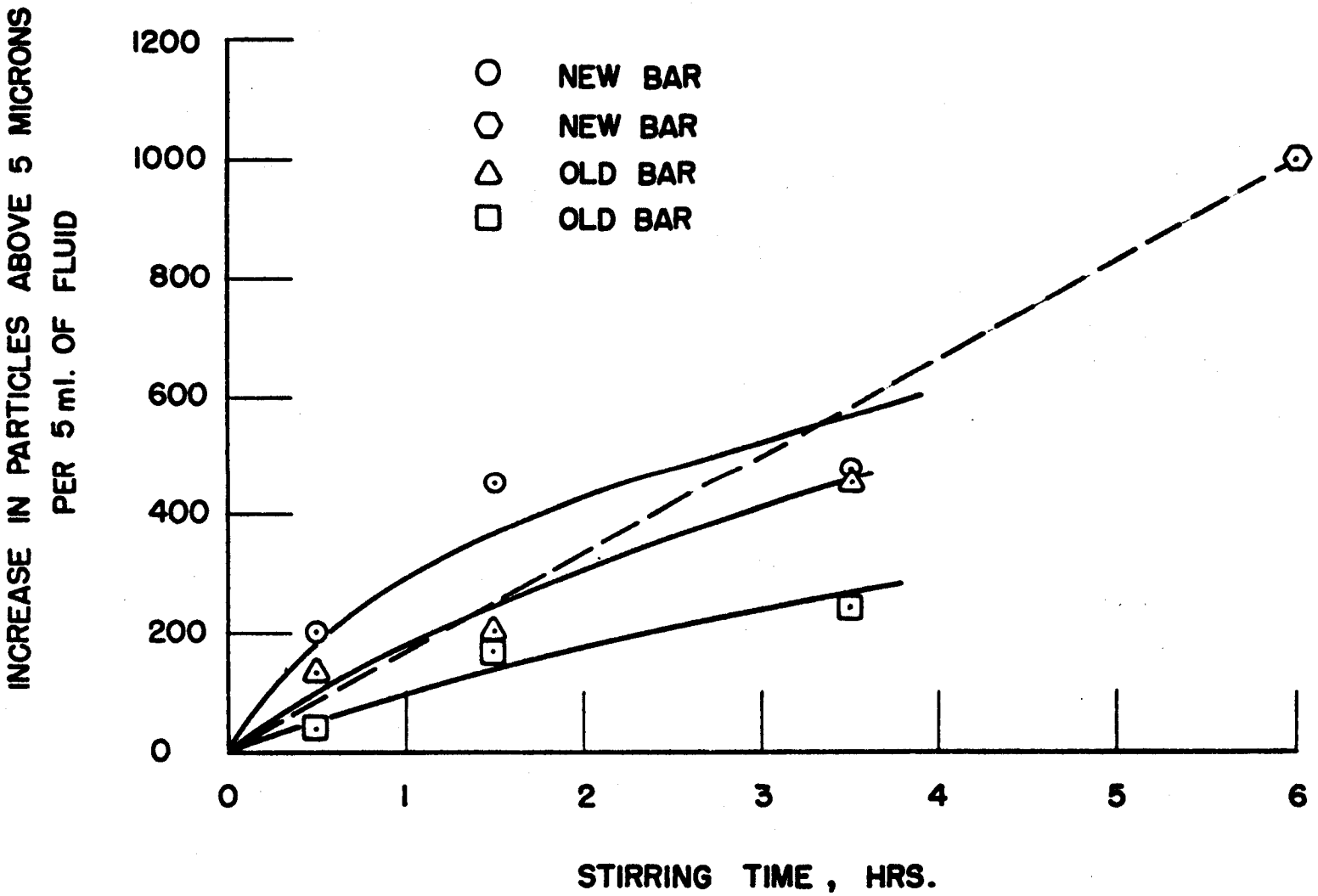

Fig. 28 Graph of Particle Counts Vs. Time

stirring time for a fluid specimen. The curves show that the stirring rods continue to generate particles as the testing time increases. The problem is serious, but it is easily circumvented. Careful alignment of the stirring motor, along the center line of the sample bottle, where the stirring bar can rotate without contacting the sides of the container, effectively eliminates the condition which creates the trouble.

CHAPTER VIII

CONSIDERATIONS FOR ISOKINETIC SAMPLING

Sampling of "nonsettling" solid particle-liquid mixtures has been the major subject area of this study. According to Govier (7), such mixtures behave as pseudo-homogeneous fluids when settling velocities are below 0.002-0.005 ft/sec., and the concentration of solid particles in the mixture is low. The assumption of such a mixture is basic to sampling dynamic fluid power systems with most sampling devices. Considering the capabilities of the low-micron filtration devices available to hydraulic systems today, this assumption is certainly realistic to the case.

Using the usual settling relationship for spherical particles by applying Stoke's law, it is seen that 136 micron particles for AC test dust in MIL-F-5606 hydraulic fluid will satisfy the upper settling velocity limit. Seventy micron metal particles in the same fluid are also considered to be "nonsettling" in the dynamic system.

For hydraulic systems with rarefied particle concentrations, a reasonable estimate of the diameter of nonsettling particles is given by the relationship:

$$d = \left[\frac{5.43 \times 10^3 \mu}{\gamma - \rho} \right]^{\frac{1}{2}} \quad \text{(micron)}$$

where μ = dynamic viscosity of fluid (centipoise)

γ = mass density of particle (slugs/ft^3)

ρ = mass density of fluid (slugs/ft^3)

Turbulence in the pseudo-homogeneous fluid will increase the limiting diameter given by the preceding equation.

Isokinetic flow sampling is generally accredited to be highly accurate when used on systems containing pseudo-homogeneous fluids under carefully controlled laboratory conditions. The initial direction of the activities concerned with sampling on this project was to set up a system whereby conditions could be controlled in the interest of calibrating equipment, working out the details of a sample evaluation technique, and observing the general disposition of AC Fine Test Dust dispersed in a nonsettling mixture with MIL-F-5606 hydraulic fluid in the dynamic state. A regular pitot tube-type isokinetic sampler was constructed and installed in a laminar flow section (see Figures 29 and 30) for the isokinetic sampling study. The testing section was installed so as to become an integral part of a fluid power system in which the fluid temperature, flow rate, and contamination level could be regulated (see Figure 31). The temperature of the fluid was maintained by automatic control at 100° F. $\pm$ 0.5° for all tests. The flow rate was measured with a Fischer-Porter turbine meter and could be regulated manually over a range of 0 to 25 gpm. The contamination level of the dynamic system was increased to discrete levels by adding contaminant with a hypodermic injector or decreased by circulating the fluid through a control filter.

A complete collection of arguments for isokinetic sampling over anisokinetic sampling is not attempted here since the method is quite

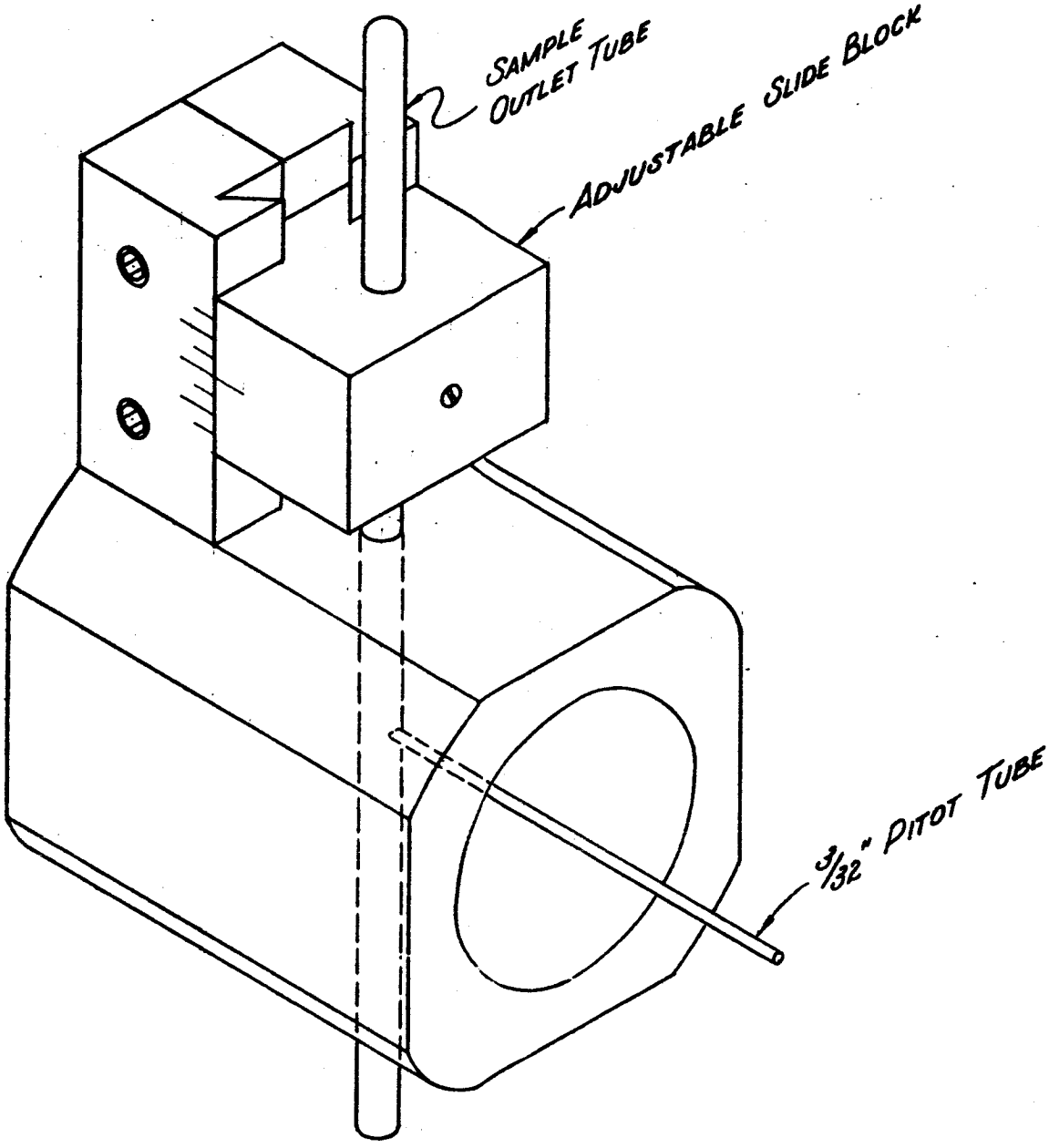

Fig. 29 Assembled Isokinetic Sampler

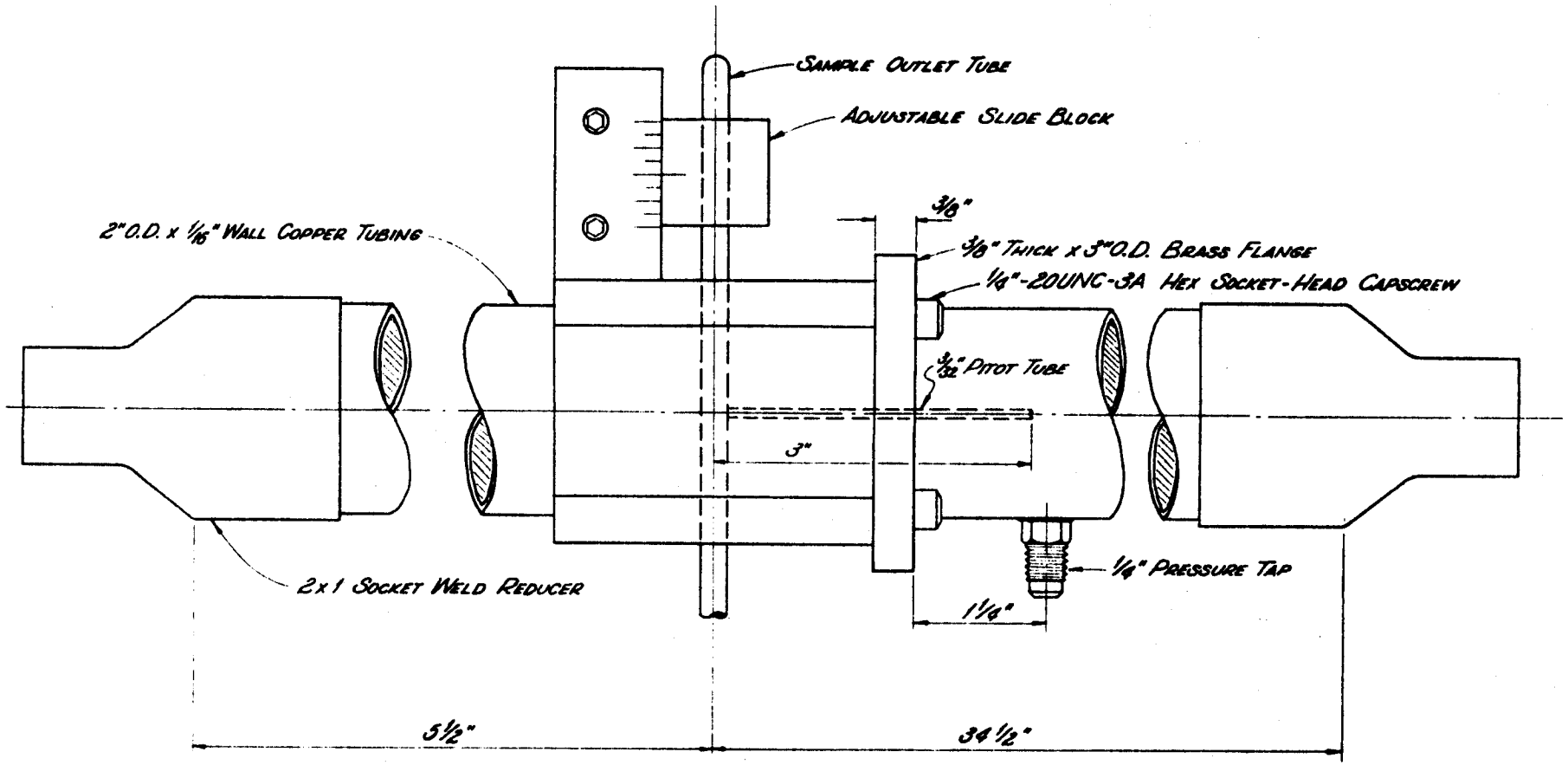

Fig. 30 Details of Isokinetic Sampler

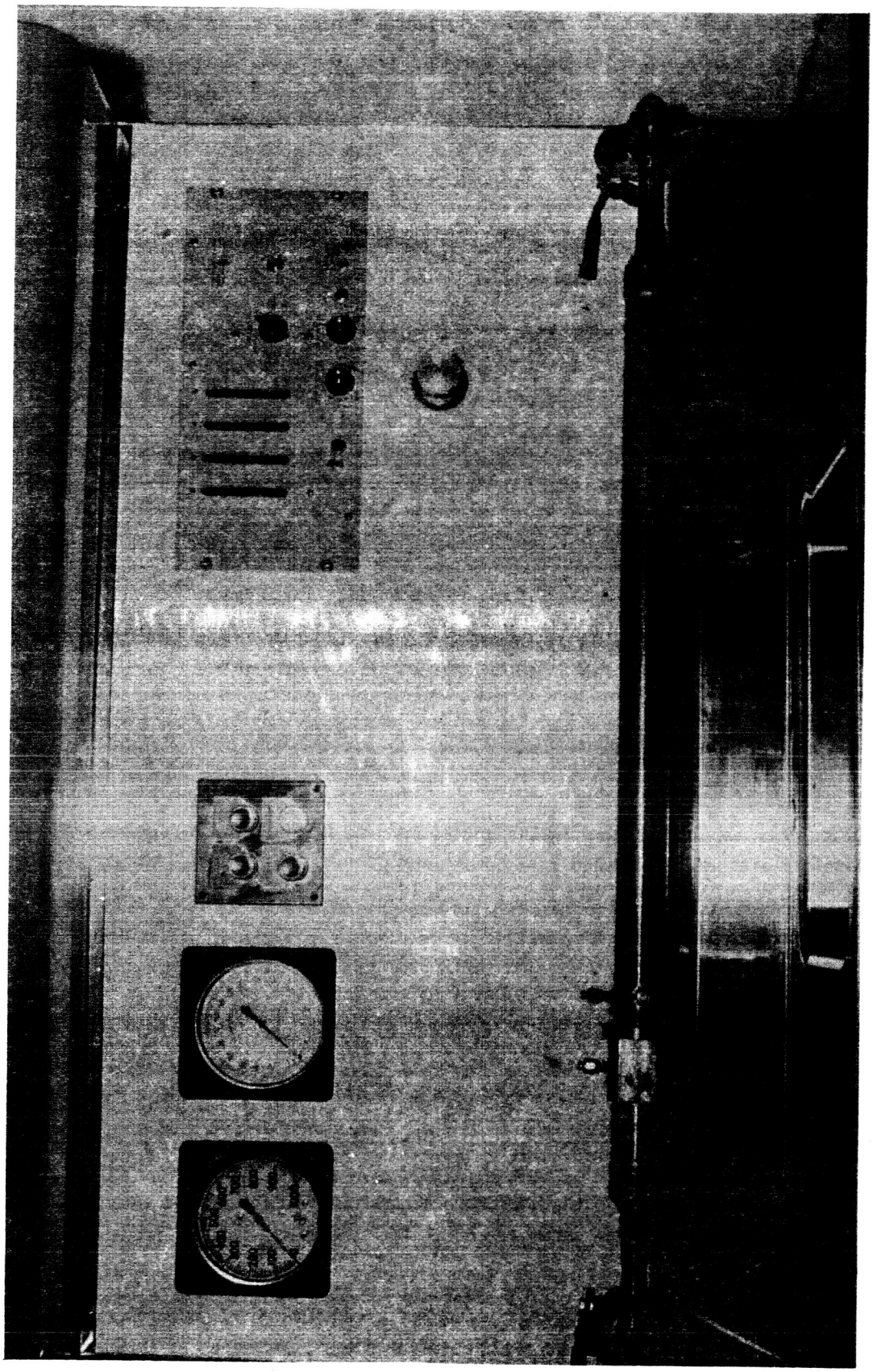

Fig. 31 Fluid Power Test Stand

generously discussed in the literature. Briefly, the establishment of isokinetic flow conditions circumvents the development of pressure gradients between the oncoming fluid stream and the sampler opening. The elimination of pressure gradients permits the selective extraction of a pseudo-homogeneous fluid as it may exist in the streamlines which are included in the sample, but developed upstream of the device in laminar flow. Colinear with the stream flow, the sampled fluid area is equal to the projected area of the sampler opening, i.e., there is no converging or diverging of streamlines to predispose contaminant separation by inertia forces. Figure 32 illustrates the two distinct anisokinetic flow condition characteristics, and the isokinetic condition as well. It is readily seen that the acceleration due to the change in direction of the streamlines in the anisokinetic cases would create definite problems to collecting a representative sample of the fluid. A concentration of larger particles is created by diverging streamlines, and a concentration of smaller particles is created in the converging case. Obviously, laminar flow conditions are prerequisite to using an isokinetic sampler.

The laminar flow section and the isokinetic samples of this study were calibrated by determining the velocity profile established in the section at specific system flow rates, then setting the pitot tube sampling rate according to the streamline veloctiy associated with the radial position of the probe. The sampler is designed to accommodate a radial traverse of the two inch diameter laminar flow section. Figure 33 shows that full laminar flow was established in the sampling section for the tests.

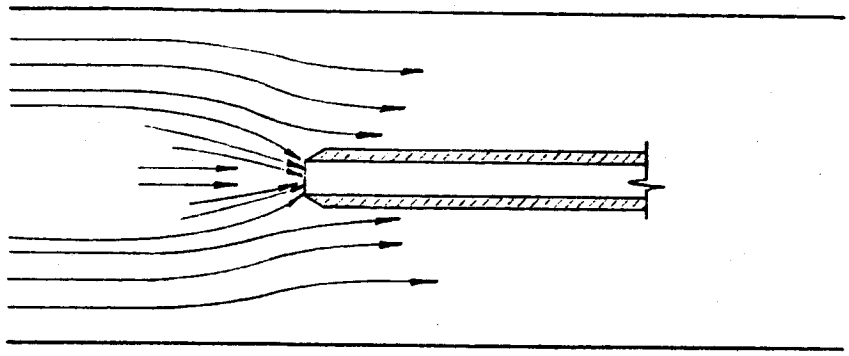

Anisokinetic Sampling Condition
Streamline Velocity < Velocity in Probe

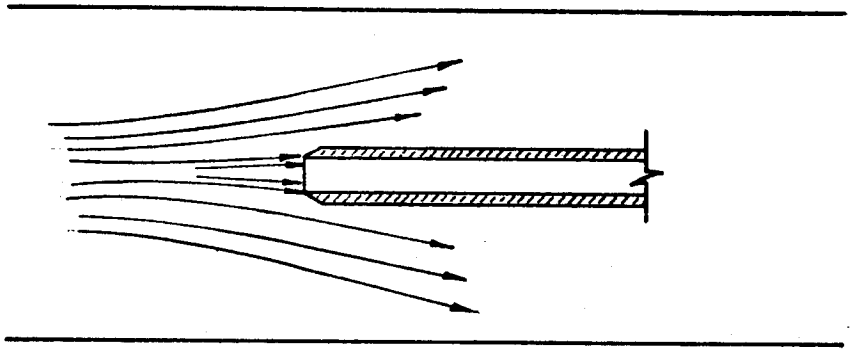

Anisokinetic Sampling Condition
Streamline Velocity > Velocity in Probe

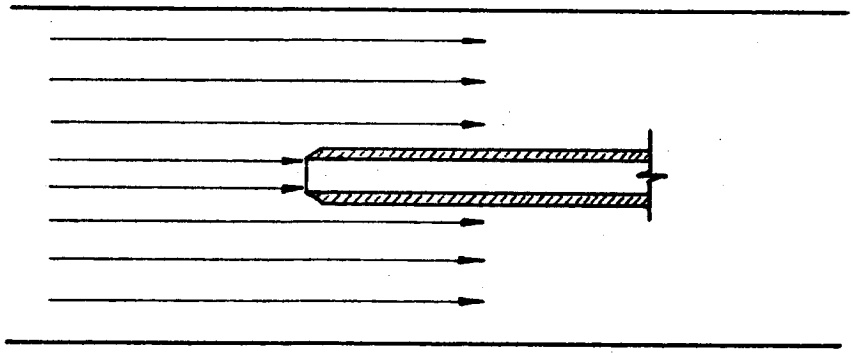

Isokinetic Sampling Condition
Streamline Velocity = Velocity in Probe

Fig. 32 Typical Sampling Conditions in Laminar Flow Section

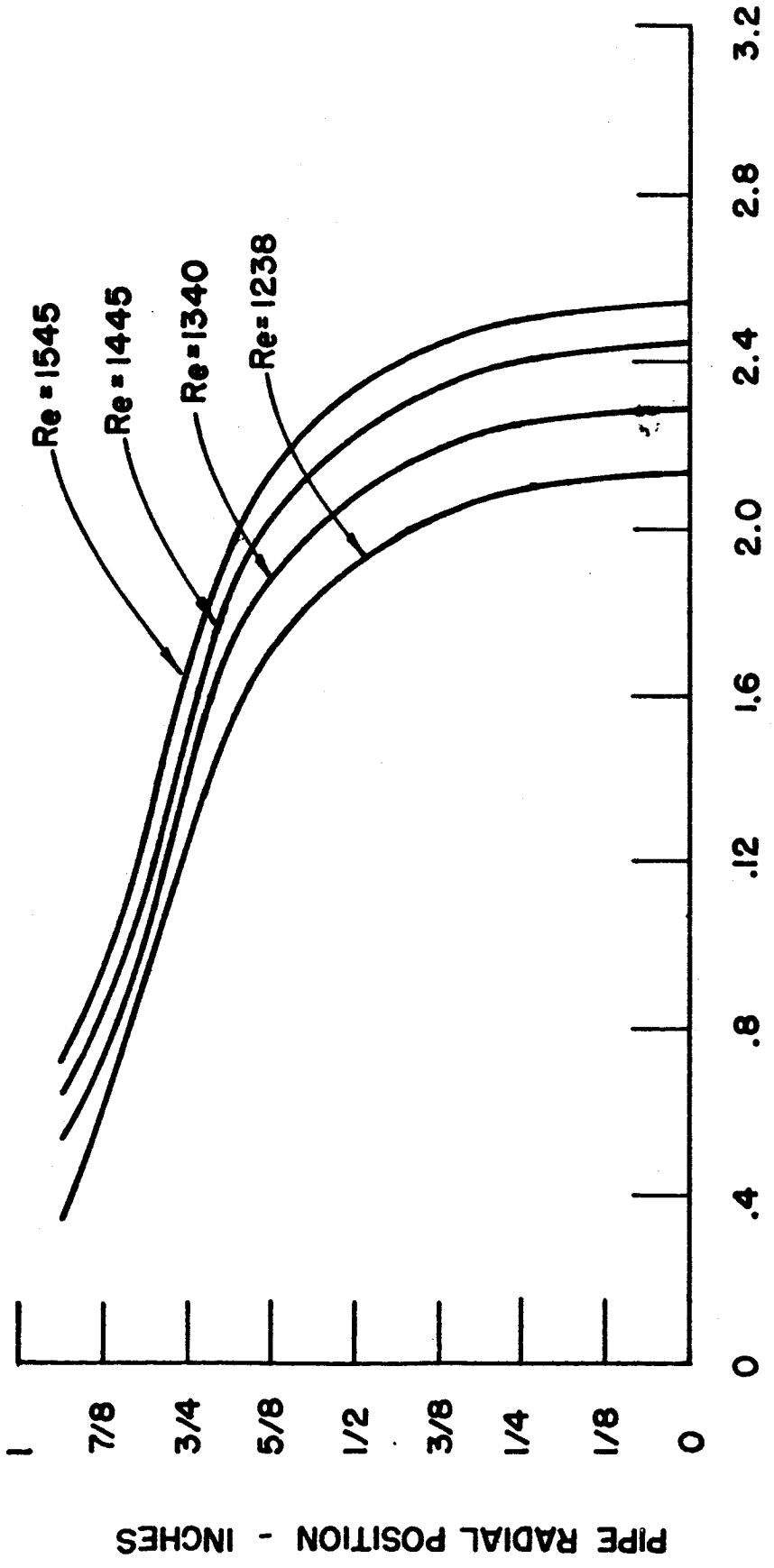

Fig. 33 Velocity Profiles in Laminar Flow Section

CHAPTER IX

ISOKINETIC SAMPLING RESULTS

Several series of extensive tests were conducted before the isokinetic sampling device was accepted as yielding an accurate sample from a dynamic liquid system. These tests were designed to indicate the possible limitations of the method and, in addition, to determine the behavior of contaminant within the dynamic test section.

The first series of tests consisted of analyzing samples taken isokinetically at nine calibrated probe positions for each of the five flow rates used in the test program. The purposes of these tests were twofold, namely:

(1) To determine if repeatable results could be obtained using the isokinetic device

(2) To determine the variation of the contaminant distribution in the laminar flow section in a plane normal to the flow.

In addition to these purposes, the initial tests provided a means of developing accurate sample analysis techniques.

In order to insure that a stabilized contaminant distribution existed in the system, all filtration devices were removed from the circuit and the fluid was circulated for a considerable time prior to the test. The quantity of contaminant (AC Fine Test Dust) was also varied between tests to add generality to the results.

The results of these tests (Figures 34 through 38 and Tables 4 through 11 show that no significant change in contaminant distribution existed across the plane of the probe's traverse. This can be explained by the fact that a turbulent flow section immediately preceded the laminar flow section containing the isokinetic probe. The entrained contaminant, which is uniformly mixed in the turbulent section, enters the laminar flow region in an evenly distributed state and is carried along the fluid streamlines. Thus, the uniform distribution which exists in the turbulent section is maintained across the streamlines in the laminar test section. This experimental observation is substantiated by the work of Starkey (8). According to Starkey, it is possible that a contaminant concentration will tend to develop in the central streamlines of a laminar flow section if sufficient length in the laminar flow path is present. Normally, such a condition will not be encountered in practical applications.

It may be noted that the deviation from the average contaminant count for each test remained generally within $\pm$ 5 per cent of the average for the total number of particles having diameters equal to or larger than 6 microns. The fact that the contaminant distribution is uniform over the cross section is significant, since this permits representative samples to be drawn off at any radial point in the tube as long as isokinetic flow exists within the sampling tube.

The effects of system flow rate upon the quality of the sample obtained were determined by sampling a uniformly contaminated system at each of the five flow rates. This was accomplished by circulating the test fluid at 19.3 gpm until the contaminant distribution at the probe reached a steady state value. A sample was then withdrawn isokinetically with the probe

TABLE 4

ISOKINETIC SAMPLING, TEST NO. 1 (13.0 GPM)

	PARTICLE DIAMETER (MICRONS)			
AVERAGE NUMBER OF PARTICLES WITH DIAMETERS GREATER THAN OR EQUAL TO THE SPECIFIED	6	10	15	20
	10,499	1,009	181	32
RADIAL PROBE POSITION (IN.)	PERCENT DEVIATION FROM AVERAGE			
0.000	2.0	3.9	3.3	7.3
0.125	0.2	0.1	9.4	4.9
0.250	-1.3	1.8	8.3	14.6
0.375	-0.8	-1.3	1.7	2.4
0.500	-1.8	-6.3	-9.9	-4.9
0.625	0.7	-2.5	-0.6	2.4
0.750	6.7	10.2	2.8	9.8
0.875	-2.0	0.4	-11.0	-34.1
0.938	-3.8	-6.4	-2.8	2.4

TABLE 5

ISOKINETIC SAMPLING, TEST NO. 7 (13.0 GPM)

	PARTICLE DIAMETER (MICRONS)			
AVERAGE NUMBER OF PARTICLES WITH DIAMETERS GREATER THAN OR EQUAL TO THE SPECIFIED	6	10	15	20
	10,225	477	165	17
RADIAL PROBE POSITION (IN.)	PERCENT DEVIATION FROM AVERAGE			
0.000	2.6	-8.8	-20.9	-17.6
0.125	-1.9	0.4	11.6	58.8
0.250	0.5	-6.3	-7.0	5.9
0.375	1.7	6.9	-4.7	0.0
0.500	-0.4	6.9	18.6	11.8
0.625	-1.5	-0.8	0.0	-17.6
0.750	0.7	8.6	15.1	0.0
0.875	1.8	-5.7	-7.0	-23.5
0.938	-3.5	-2.1	-5.8	-23.5

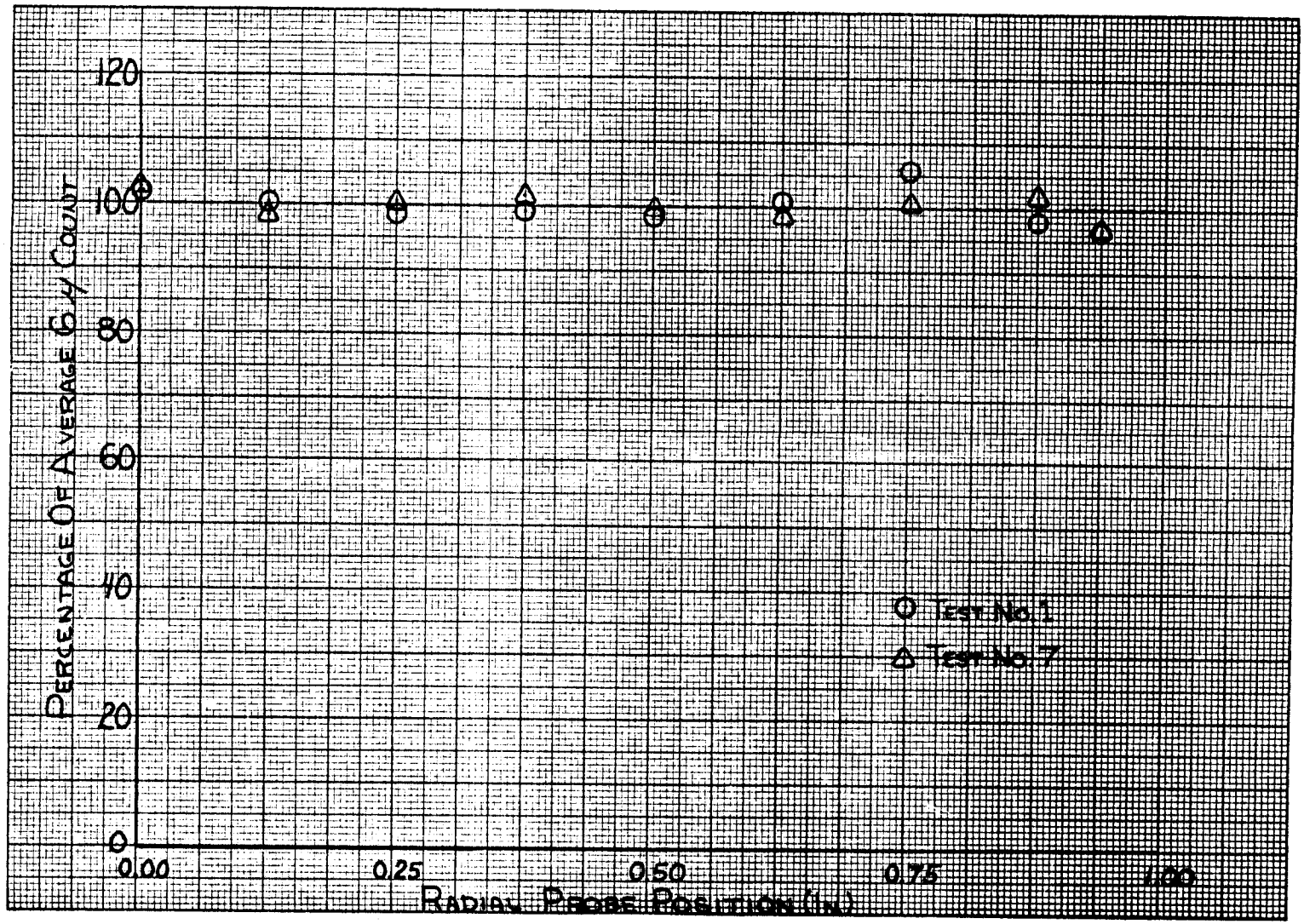

Fig. 34 Graph of Particle Count Percentages Vs Probe Position at 13.0 gpm Flow Rate (Tests 1 and 7)

TABLE 6

ISOKINETIC SAMPLING, TEST NO. 3 (15.6 GPM)

	PARTICLE DIAMETER (MICRONS)			
AVERAGE NUMBER OF PARTICLES WITH DIAMETERS GREATER THAN OR EQUAL TO THE SPECIFIED	6 4,697	10 609	15 165	20 32
RADIAL PROBE POSITION (IN.)	PERCENT DEVIATION FROM AVERAGE			
0.000	-5.5	1.0	4.8	15.6
0.125	-3.4	0.5	7.9	0.0
0.250	1.0	-5.9	-6.7	-3.1
0.375	2.9	1.1	1.8	-3.1
0.500	-2.2	0.8	0.0	-3.1
0.625	11.6	10.5	13.9	18.8
0.750	-2.9	-6.9	-9.7	-9.4
0.875	-2.8	0.0	-10.3	-18.7

TABLE 7

ISOKINETIC SAMPLING, TEST NO. 4 (15.6 GPM)

	PARTICLE DIAMETER (MICRONS)			
AVERAGE NUMBER OF PARTICLES WITH DIAMETERS GREATER THAN OR EQUAL TO THE SPECIFIED	6	10	15	20
	45,095	5,878	1,387	279
RADIAL PROBE POSITION (IN.)	PERCENT DEVIATION FROM AVERAGE			
0.000	1.5	6.5	10.5	14.7
0.125	0.5	6.8	7.9	20.8
0.250	3.0	-7.6	-5.7	-16.1
0.375	0.3	5.2	6.8	5.7
0.500	-4.3	-9.2	-7.7	-6.8
0.625	-4.4	-7.7	-2.9	-3.9
0.750	0.7	2.9	-0.6	-1.1
0.875	2.2	1.7	-5.3	-3.2
0.938	0.5	1.5	-3.0	-9.3

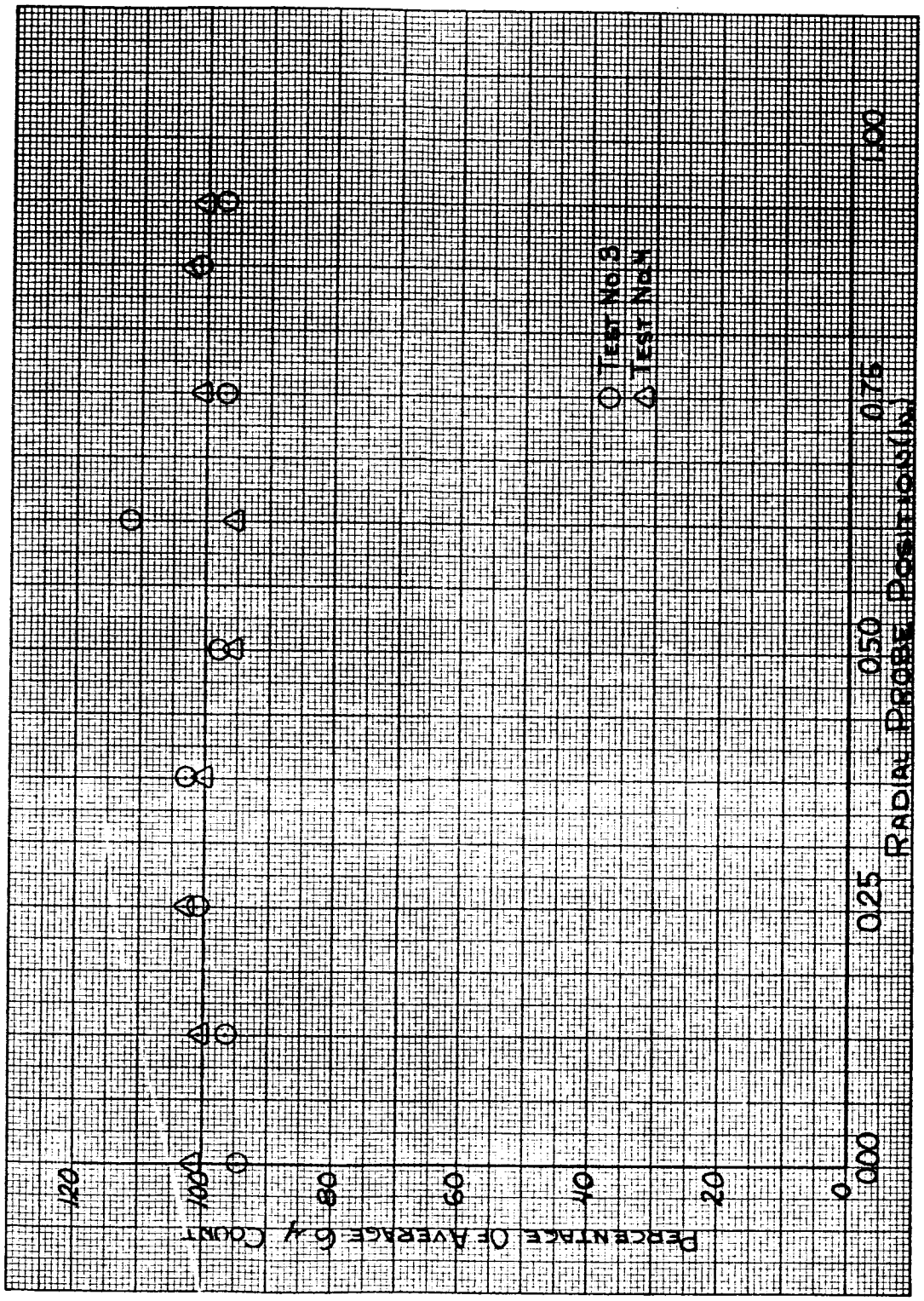

Fig. 35 Graph of Particle Count Percentages Vs Probe Position at 15.6 gpm Flow Rate (Tests 3 and 4)

TABLE 8

ISOKINETIC SAMPLING, TEST NO. 5 (16.85 GPM)

	PARTICLE DIAMETER (MICRONS)			
AVERAGE NUMBER OF PARTICLES WITH DIAMETERS GREATER THAN OR EQUAL TO THE SPECIFIED	6	10	15	20
	15,490	693	190	51
RADIAL PROBE POSITION (IN.)	PERCENT DEVIATION FROM AVERAGE			
0.000	2.3	12.8	43.7	86.3
0.125	-2.5	-11.8	-8.9	0.0
0.250	-3.6	-41.0	-65.3	-80.4
0.375	4.4	5.3	-6.8	-17.6
0.500	1.0	3.3	-11.6	-7.8
0.625	-5.7	-17.5	-16.8	-9.8
0.750	2.9	36.1	44.7	15.7
0.875	0.1	2.2	4.7	-3.9
0.938	1.2	10.7	14.2	15.7

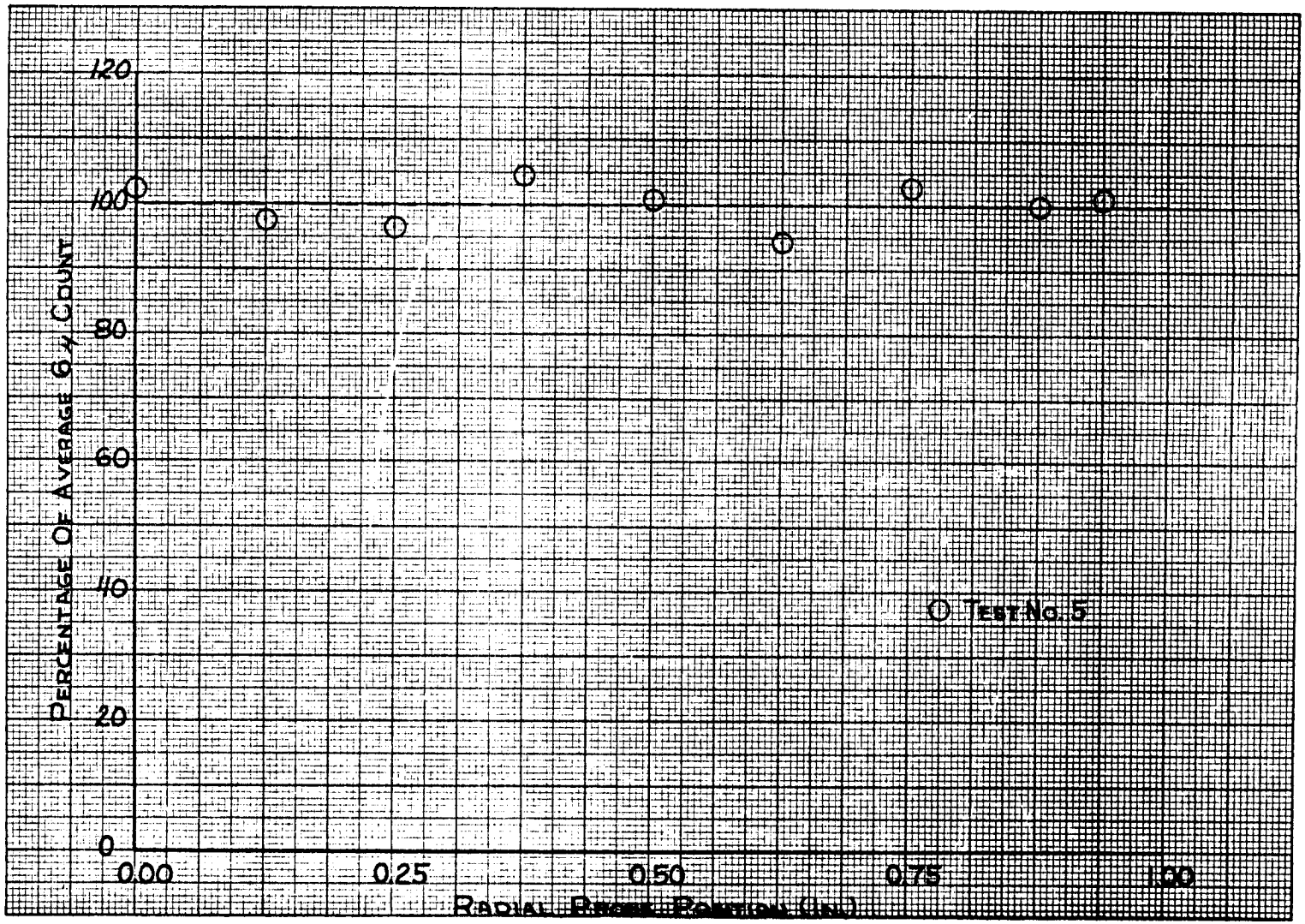

Fig. 36 Graph of Particle Count Percentages Vs. Probe Position at 16.85 gpm Flow Rate (Test 5)

TABLE 9

ISOKINETIC SAMPLING, TEST NO. 2 (18.15 GPM)

	PARTICLE DIAMETER (MICRONS)			
AVERAGE NUMBER OF PARTICLES WITH DIAMETERS GREATER THAN OR EQUAL TO THE SPECIFIED	6	10	15	20
	9,562	1,766	488	139
RADIAL PROBE POSITION (IN.)	PERCENT DEVIATION FROM AVERAGE			
0.000	-7.1	-2.7	-0.8	0.0
0.125	-3.1	0.4	-1.6	-2.2
0.250	0.6	-5.0	-9.0	-13.7
0.375	0.9	-2.9	-5.5	-9.4
0.500	1.9	4.1	7.8	15.8
0.675	3.5	0.1	0.6	-2.2
0.750	0.0	0.1	-1.6	2.2
0.875	5.3	3.4	2.5	2.9
0.938	-2.0	2.3	8.0	7.9

TABLE 10

ISOKINETIC SAMPLING, TEST NO. 6 (18.15 GPM)

	PARTICLE DIAMETER (MICRONS)			
	6	10	15	20
AVERAGE NUMBER OF PARTICLES WITH DIAMETERS GREATER THAN OR EQUAL TO THE SPECIFIED	17,047	477	91	21
RADIAL PROBE POSITION (IN.)	PERCENT DEVIATION FROM AVERAGE			
0.000	0.3	-2.1	1.1	-9.5
0.125	-0.2	0.2	5.5	-14.3
0.250	0.1	13.4	7.7	28.6
0.375	-0.1	-4.4	-1.1	-14.3
0.500	-2.5	-6.5	-13.2	-9.5
0.625	0.7	-7.5	-13.2	4.8
0.750	1.4	5.7	12.1	19.0
0.875	2.7	2.9	2.2	-28.6
0.938	-2.4	-2.3	-1.1	9.5

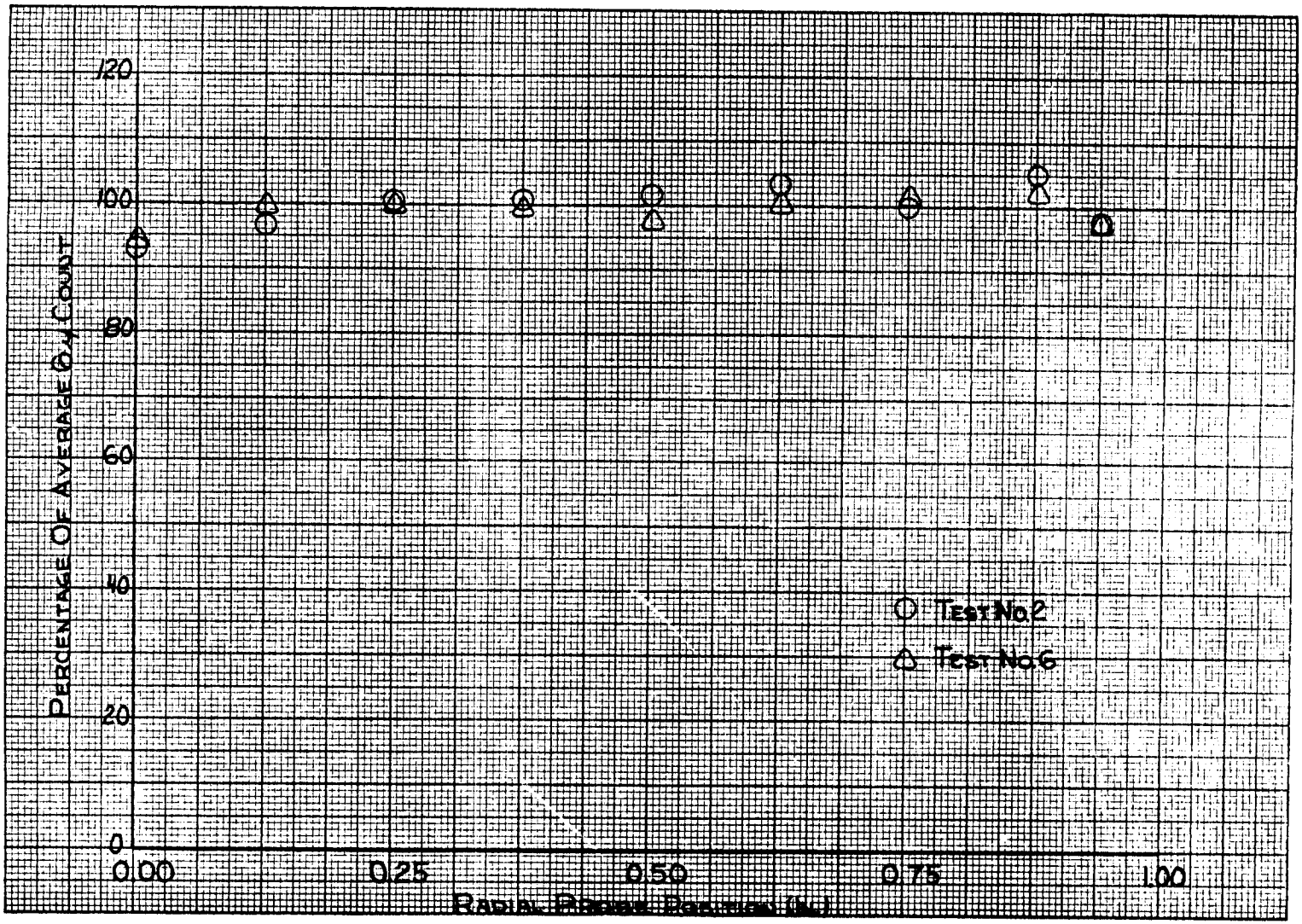

Fig. 37 Graph of Particle Count Percentages Vs Probe Position at 18.15 gpm Flow Rate (Tests 2 and 6)

TABLE 11

ISOKINETIC SAMPLING, TEST NO. 8 (19.3 GPM)

	PARTICLE DIAMETER (MICRONS)			
AVERAGE NUMBER OF PARTICLES WITH DIAMETERS GREATER THAN OR EQUAL TO THE SPECIFIED	6	10	15	20
	12,698	851	203	42
RADIAL PROBE POSITION (IN.)	PERCENT DEVIATION FROM AVERAGE			
0.000	-1.7	-1.3	-5.4	-28.6
0.125	1.3	4.6	9.4	26.2
0.250	0.2	3.9	13.3	26.2
0.375	-1.2	10.6	16.3	52.4
0.500	-0.3	1.1	6.4	2.4
0.675	1.0	-3.4	-0.5	0.0
0.750	-2.3	-2.8	-9.4	-21.4
0.875	2.3	-4.9	-18.7	-31.0
0.938	0.7	-8.6	-12.8	-21.4

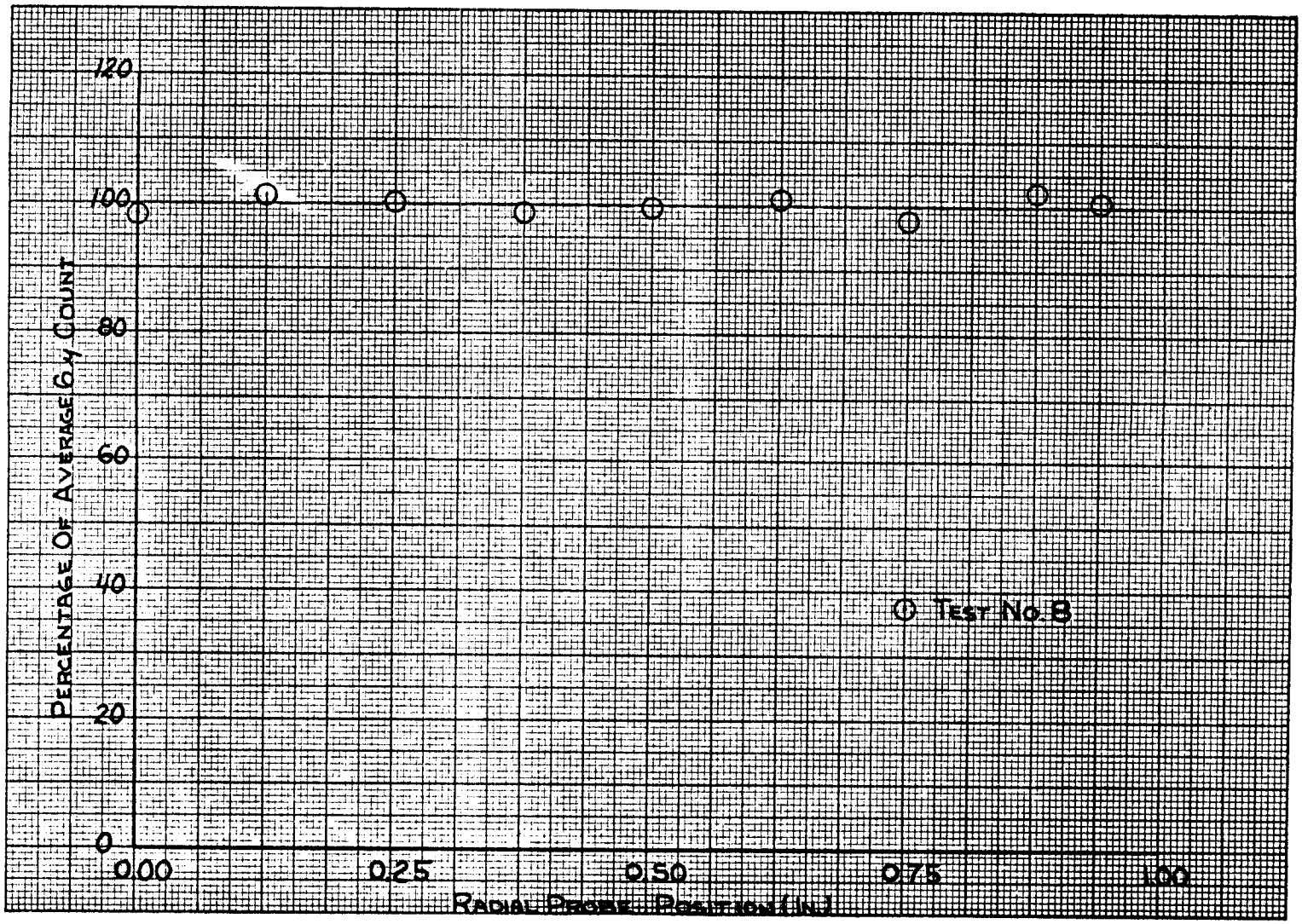

Fig. 38 Graph of Particle Count Percentages Vs Probe Position at 19.3 gpm Flow Rate (Test 8)

located at the 0.375 inch position. The flow was then reduced by bypassing a portion of the fluid around the test section. After sampling at the new flow, the flow was again reduced and the process repeated until a sample has been obtained for each flow rate. The results (Figure 39 and Table 12) again are within approximately $\pm$ 5 per cent of the average count. These results indicate that no significant error is incurred in the quality of sample by varying the system flow rate so long as laminar flow is maintained and the sample is withdrawn isokinetically.

The magnitude of error to be expected from a sample taken other than isokinetically was found by sampling at flow rates above and below the isokinetic value for a given probe position. The results (Table 13) for flow rates less than the isokinetic flow rate, although not appreciably different from the isokinetic count, are consistently lower than the isokinetic count. This shows that some of the particulate contaminat bypassed the probe, resulting in a preferential sample. At flow rates greater than the isokinetic rate, the opposite trend was noticed. In this case, the anisokinetic samples contained a slightly greater number of particles than the isokinetic sample.

The fact that anisokinetic conditions cause only a slight error can be attributed to the close relative densities of the liquid and the contaminant and also the high fluid viscosity. In a gaseous system where the fluid viscosity is negligible, the adverse effects of anisokinetic sampling can be expected to increase considerably.

The consistency and accuracy of the results obtained using the isokinetic probe provides a means by which the effectiveness of various sampling devices can be evaluated. If a sampling valve which is installed

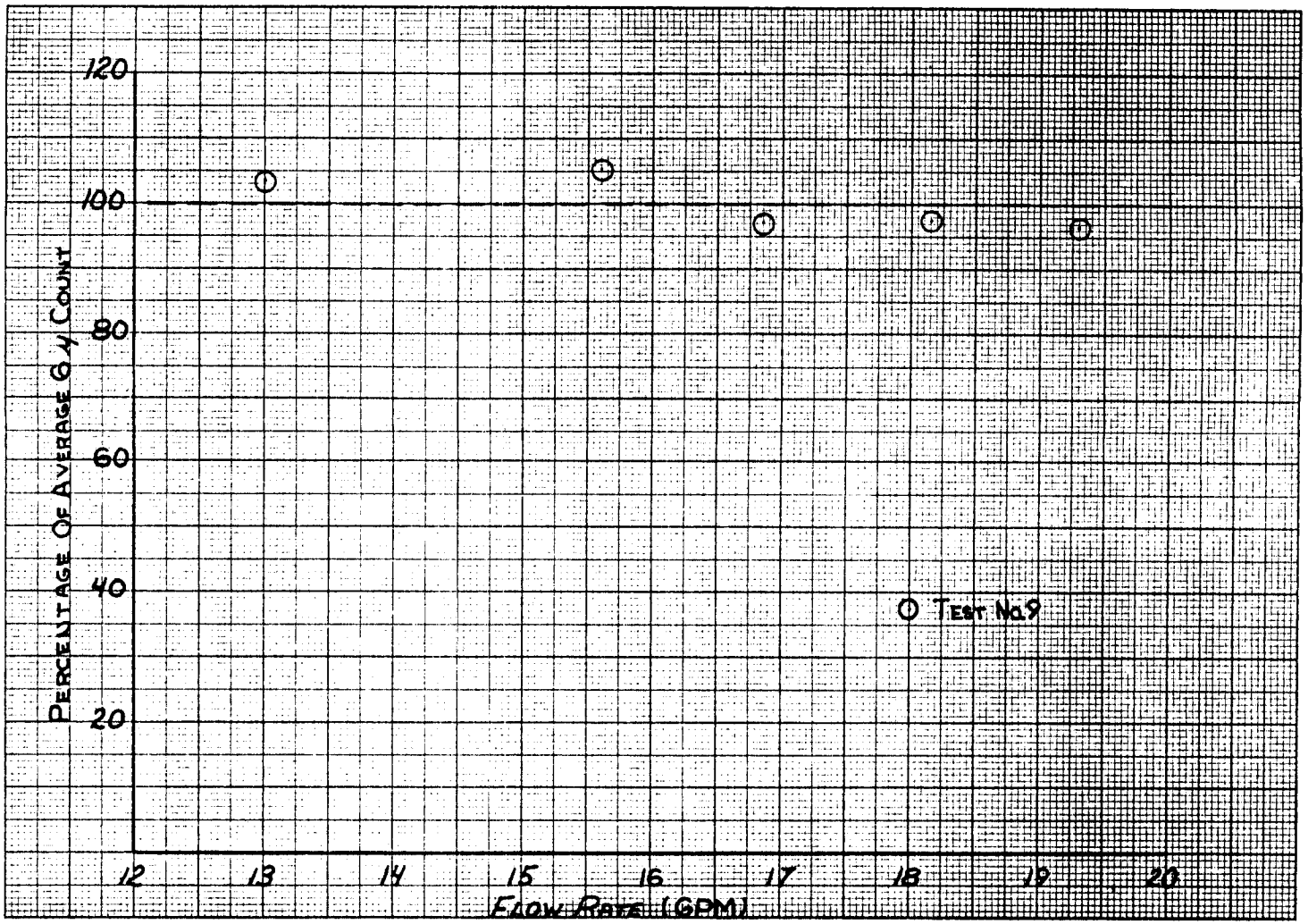

Fig. 39 Graph of Particle Count Percentages Vs Flow Rate (Test 9)

TABLE 12

ISOKINETIC SAMPLING VS. FLOWRATE, TEST NO. 9

	PARTICLE DIAMETER (MICRONS)			
AVERAGE NUMBER OF PARTICLES WITH DIAMETERS GREATER THAN OR EQUAL TO THE SPECIFIED	6	10	15	20
	2,568	341	99	17
FLOW RATE (GPM)	PERCENT DEVIATION FROM AVERAGE			
13.00	3.4	-13.5	-26.3	-53.0
15.60	5.3	7.3	16.2	29.4
16.85	-2.7	-7.0	-6.1	-5.9
18.15	-2.5	-2.3	-2.0	-5.9
19.30	-3.5	16.7	16.2	23.5

TABLE 13

EFFECTS OF ANISOKINETIC SAMPLING

SAMPLING CONDITION	PARTICLE DIAMETER (MICRONS)			
	6	10	15	20
Test No. 10 (V=0.1 V_i)	-10.5*	-12.9	-16.8	-31.1
Test No. 12 (V=0.1 V_i)	-6.1	-9.6	-18.8	-24.1
Test No. 11 (V=3.0 V_i)	5.5	3.3	1.6	15.9
Test No. 13 (V=3.6 V_i)	2.8	-0.6	0.1	2.9

V_i = Isokinetic Velocity

V = Sampling Velocity

*Tabular Values are Percent Deviation From The Respective Isokinetic Counts.

in cascade with such an isokinetic sampling section is removing a representative sample from the fluid system, then the particle count will be the same as the count for an isokinetic sample withdrawn simultaneously from the system. The value of such a comparison lies in the fact that the operating conditions for which a sampling device is applicable can be accurately determined.

CHAPTER X

SAMPLE VALVE EVALUATION

The analysis of the performance of a sample valve is of considerable importance to anyone using such a device in order to measure the contaminant level of a fluid system. The selection of sampling devices to determine the degree of system contamination is, in many instances, made on the basis of intuition or experience. Such a selection can often yield a sample which is not indicative of the actual state of the system. The use of the isokinetic sampling technique outlined in this report offers a means by which sample valves can be evaluated with regard to accuracy and also with regard to the sampling technique to be followed for the respective valves.

Two commercially available sampling valves were evaluated using the isokinetic sampling probe. The first of these was a commercially available "turbulent flow" sampling valve. The valve contains a flow path in which turbulence is induced in the liquid stream to provide a uniform mixing of the contaminant. A side port leads from the turbulent section to a ball valve through which the sample is removed for analysis.

The first test on the turbulent flow valve was conducted with the unit installed with its sample outlet pointing downward. With the valve mounted in this manner, the samples obtained deviated erratically from the isokinetic results, with the turbulent flow valve counts generally being the larger. In one particular test, the average from four sample

valve counts exceeded the average isokinetic count by 23 per cent; and one of the individual counts was in excess by 41 per cent.

The valve was then inverted so that the internal sampling port and the outlet were located on top of the assembly. The efflux from the valve was directed downward through a short piece of 1/4 inch stainless steel tubing. With the valve in this position, the results that were obtained compared satisfactorily with the isokinetic results. It is surmised that the cause of the deviation in comparison of the results is due in part to the dynamics of the particles of contaminant within the turbulent flow section of the valve. When the unit is operated with the valve pointed downward, the momentum of the particles tends to force them into the static volume of fluid in the internal port. Thus, an increased contaminant concentration builds up in this area. Also, during the time in which the system is not in operation, the sampling port acts as a sedimentation chamber for the contaminant entrained in the system. Locating the valve with the sample outlet directed upward eliminates this silting action in the sampling port, since the particles settle out of this area when the system is inoperative. All subsequent evaluations of the turbulent flow valve were made with the valve installed in the second position.

The valve was tested at flow rate of 13.00, 16.85, and 19.30 gpm by withdrawing two samples from each of the following:

1. The isokinetic probe
2. The turbulent flow valve (1/4 inch stainless steel tube attached to outlet)
3. The turbulent flow valve (Hypodermic Adapter attached to the stainless steel tube).

The effect of the hypodermic adapter downstream of the sample outlet was to reduce the sampling rate from the system. The results (Tables 14 and 15) show that the sample obtained from the turbulent flow valve contained the same contaminant distribution as that obtained from the isokinetic probe for each of the test flow rates. The fact that the valve demonstrated well both with and without the hypodermic adapter in place indicates that piping installed downstream of the sampling port has little or no effect on the sample insofar as the reduction in sampling rate is concerned.

The second type of valve which was tested was a commercially available "bleeder valve." The unit consists of a small needle valve which is opened with a screwdriver and a discharge port through which the sample is withdrawn. For the evaluation tests, the valve was installed in a turbulent flow section of the line immediately upstream of the laminar test section. The valve was screwed into a boss, constructed according to unit specifications, which had been soldered on the tube wall of the test section. Two samples were taken from the valve and were compared with two samples taken concurrently from the isokinetic probe. The results (Table 16) show excellent agreement with the isokinetic samples for each of the different test flow rates, which again were 13.00, 16.85, and 19.30 gpm, respectively.

It can be concluded from the results of the evaluation of the two commercial valves that both of them are capable of yielding representative fluid samples for the analysis of contamination in a system when properly installed and operated. Figure 40 shows the configuration of the sampling section with the turbulent flow and

TABLE 14

EVALUATION OF TURBULENT FLOW VALVE

Test No. 14 - (Samples taken through 1/4 inch stainless steel tube)

SYSTEM FLOW RATE (GPM)	PARTICLE DIAMETER (MICRONS)			
	6	10	15	20
13.00	2.4*	5.5	5.9	-4.5
16.85	3.8	3.7	5.0	16.0
19.30	2.9	1.5	0.4	-27.9

TABLE 15

Test No. 15 - (Samples taken through stainless tube with hypodermic adapter in place)

SYSTEM FLOW RATE (GPM)	PARTICLE DIAMETER (MICRONS)			
	6	10	15	20
13.00	-4.0	2.3	-5.5	-12.2
16.85	-1.3	-1.8	-1.0	8.7
19.30	5.3	4.3	3.8	-18.6

* Tabular values are percent deviations from the respective isokinetic counts.

TABLE 16

EVALUATION OF BLEEDER VALVE

Test No. 16

SYSTEM FLOW RATE (GPM)	PARTICLE DIAMETER (MICRONS)			
	6	10	15	20
13.00	1.0*	5.7	10.1	1.6
16.85	-0.7	5.6	5.9	13.0
19.30	-0.1	-2.0	-5.0	1.4

* Tabular values are percent deviations from the respective isokinetic counts.

bleeder valve installed. Since the flow rates covered in the evaluations were rather limited, their suitability at other flow rates can only be inferred; however, the operating limits of these sampling devices, as well as others, can be determined by extending the evaluation technique presented herein.

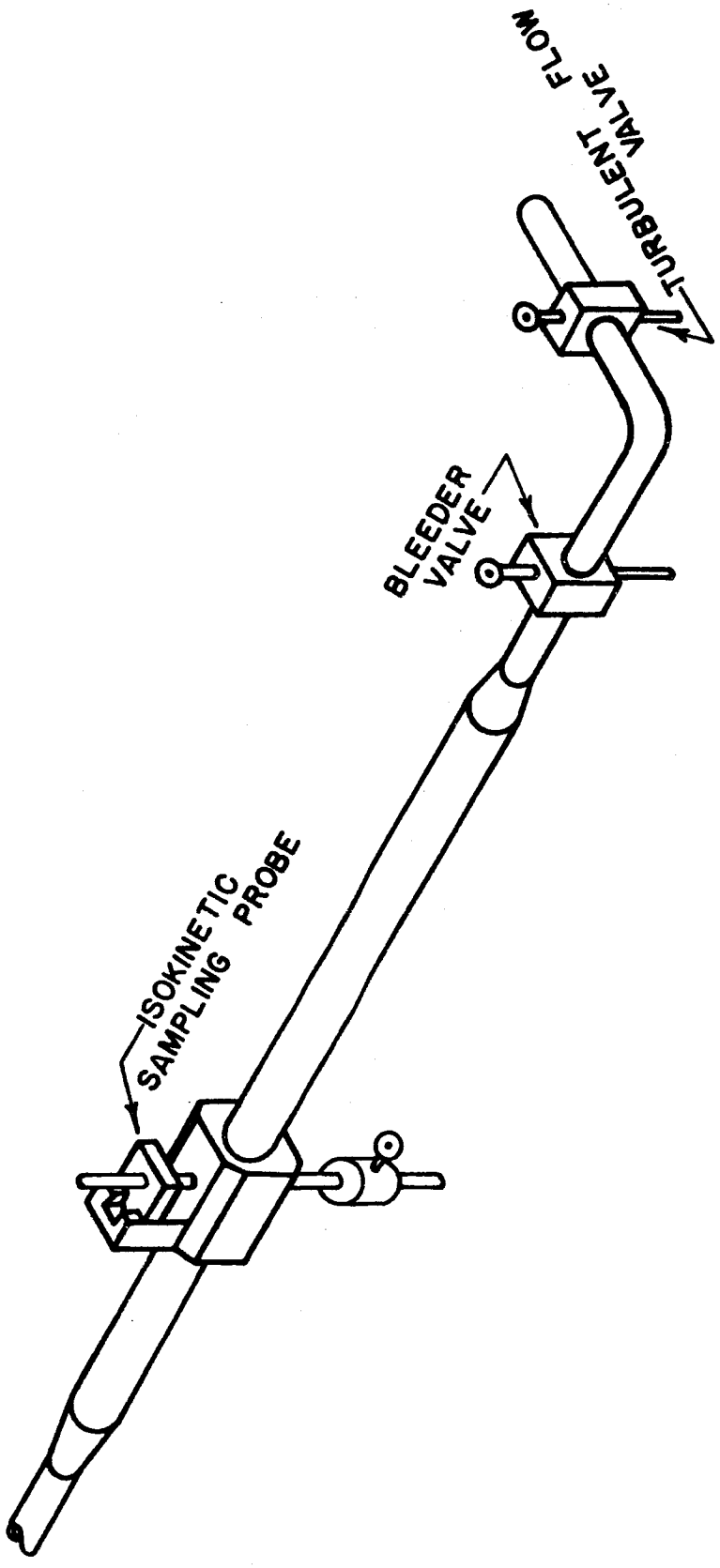

Fig. 40 Test Section for Evaluation of Sampling Valves

CHAPTER XI

CONCLUSIONS AND RECOMMENDATIONS FOR DYNAMIC SAMPLING

The assumption of a "nonsettling" mixture is valid for dynamic sampling of high-performance hydraulic systems. The particulate contaminant concentration of such systems is rarefied by filtration, and the mixture is considered to be a pseudo-homogeneous fluid.

Dynamic solid-liquid suspensions of the "nonsettling" classification can be sampled successfully with commercially available sampling valves whose limitations have been evaluated for the prevailing conditions. Turbulent mixing to maintain the pseudo-homogenuity of the fluid should be established upstream of the sample extraction location in the system being sampled. Configurations to induce turbulence can be effectively incorporated in a sampling valve proper (such as done in the turbulent flow valve). Under carefully controlled conditions in the laboratory, an isokinetic sampler can be used to evaluate capabilities of dynamic sampling devices. The carefully controlled conditions (impractical in field applications) that are required for isokinetic sampling with a pitot-type probe sampler are likely to be impractical in field applications.

Any handling of sampled fluid or counting of particles therein (such as required for analyses, etc.) must be governed with extreme rigor to circumvent errors due to contaminant particles which are acquired from sources extraneous to the system. The analysis phase

of sampling is equally important, in the final measurement of contamination level in a system, as the method used to get the sample from the system. In some instances, analysis errors are much greater than any other errors incurred in a sampling technique.

The experimentation and studies of the project in the area of dynamic sampling of hydraulic systems has lead to comprehensive observations and conclusions within the limits of the undertaking. Further study to expand the concepts is recommended. It is felt that valid sampling techniques and procedures can be developed for greater comprehension of results from dynamic sampling of systems in the field.

SELECTED BIBLIOGRAPHY

1. Grace, H. P., "Structure and Performance of Filter Media," American Institute of Chemical Engineering Journal, Vol. 2 (September, 1956), pp. 307-336.

2. Comer, A. G., Burchett, O. L., and Gilbert, J., Fluid Contamination Project Report No. 1, School of Mechanical Engineering, Oklahoma State University, 1959.

3. Fitch, E. C., "A Basic Science Program in Filtration Mechanics," Office of Engineering Research, Oklahoma State University, 1962.

4. Pall, D. B., "Development of Filters For 400° F. and 600° F. Aircraft Hydraulic Systems," Wright Air Development Center Technical Report No. 56-249, (May, 1956).

5. Ludvig, E., "Evaluation of Filter Media," Purolator Report No. 2633, (March, 1960).

6. Cranston, R. W., and Beynon, L. R., "Specification and Testing of Fine Particle Filters," Aircraft Engineering, Vol. 28 (September, 1956), pp. 318-321.

7. Govier, G. W., and Charles, M. E., "The Hydraulics of the Pipeline Flow of Solid-Liquid Mixtures," The Engineering Journal, August, 1961, Vol. 44, Part 2.

8. Starkey, T. V., "The Laminar Flow of Suspensions in Tubes," British Journal of Applied Physics, 1955, Vol. 6, pp. 34-37.

9. McNown J. S., "Particles in Slow Motion," La Houille Blance, Sept.-Oct., 1951, pp. 701-722.

10. Lapple, C. E., and Shepherd, C. B., "Calculation of Particle Trajectories," Industrial and Engineering Chemistry, Vol. 32, No. 5, pp. 605-617.

11. Rebert, C. J., "Particle Evaluation," Applied Hydraulics and Pneumatics, 1962, Vol. 15, Part 1, pp. 58-64.

12. Maude, A. D., and Whitmore, R. L., "The Turbulent Flow of Suspensions in Tubes," Trans. Instn. Chem. Engrs., 1958, Vol. 36, pp. 296-304.

Gayle, J. B., and Romine, J. O., "Evaluation of HIAC Products Corporation Model PC-101 Automatic Particle Counter," George C. Marshall Space Flight Center, Huntsville, Alabama, Report No. MTP-P&VE-M-63-3, 15 February 1963.

APPENDIX A

O.S.U. CLEAN ROOM

Ordinary room air is heavily laden with dust particles in the size range of the contaminant particles normally found in fluid samples. Hence, the need for a clean room to reduce analysis errors due to airborne dirt alone is apparent. Furthermore, the instrumentation required for comprehensive fluid contaminant analysis is sensitive to ambient conditions of temperature, humidity, and dirt. The cleanliness level of the supply air for the OSU Clean Room (Figure 41) is maintained by two filtering units. Return air from the clean room mixes with the filtered "make up" air, and the mixture is cleaned by electronic precipitation equipment. Positive pressure is maintained in the clean room and anterooms by weighted exhaust louvers. To minimize contaminant generation within this room, "lint free" clean room apparel is provided for personnel using the facility together with normal clean room precautions.

The gravimetric analysis equipment is maintained in the clean room since it is especially sensitive to environmental conditions. This equipment includes the Satorious Analytical Balance and the Millipore Filter Apparatus. A HIAC Particle Counter used in determining system contaminant levels is also located in the cleanroom. Samples taken from the filter media performance stand are carefully sealed until they are in the clean room where they are analyzed using the HIAC and/or microscopic techniques. All of the Filter Media Efficiency Tests are conducted in the clean room since

Fig. 41 O.S.U. Clean Room

they are especially susceptible to airborne contamination. Microscopic evaluations of the efficiency tests, which are conducted with the aid of the Cooke-A.E.I. image-splitting microscope eyepiece, are also conducted in the clean room.

APPENDIX B

ROLLER PARTICLE SIZE ANALYZER

The Roller Particle Size Analyzer (Figure 42), manufactured by the American Inst. Co., is a particle classifier which is used to separate finely divided materials into groupings of a desired size range. The particle classifier separates dry powdered materials, such as AC Test Dust, according to the particle size. By successive operations one can obtain classified particles of any desired size range within the instrument's overall limits of from 1 to 74 microns. In the determination of the filtration characteristics of a specific filter medium it is advantageous to use contaminants having a known particle size distribution. Classified contaminants are also invaluable in the measurement of the contaminant tolerance levels of various hydraulic systems.

The separation is accomplished by placing the contaminant in the sample tube at the base of a vertical settling chamber (Figure 42). The settling chamber consists of a diffuser section at the base, the actual settling region of constant cross section, followed by a diminishing cross section at the top. A steady stream of air is passed through the powdered sample where it picks up particles of the contaminant and carries them into the diffuser section. As the stream expands in the diffuser and enters the settling region it assumes a linear velocity. The force exerted by the air stream on the particles will be great enough to carry all particles of a given size, and those smaller, up through the settling chamber and out the top where they

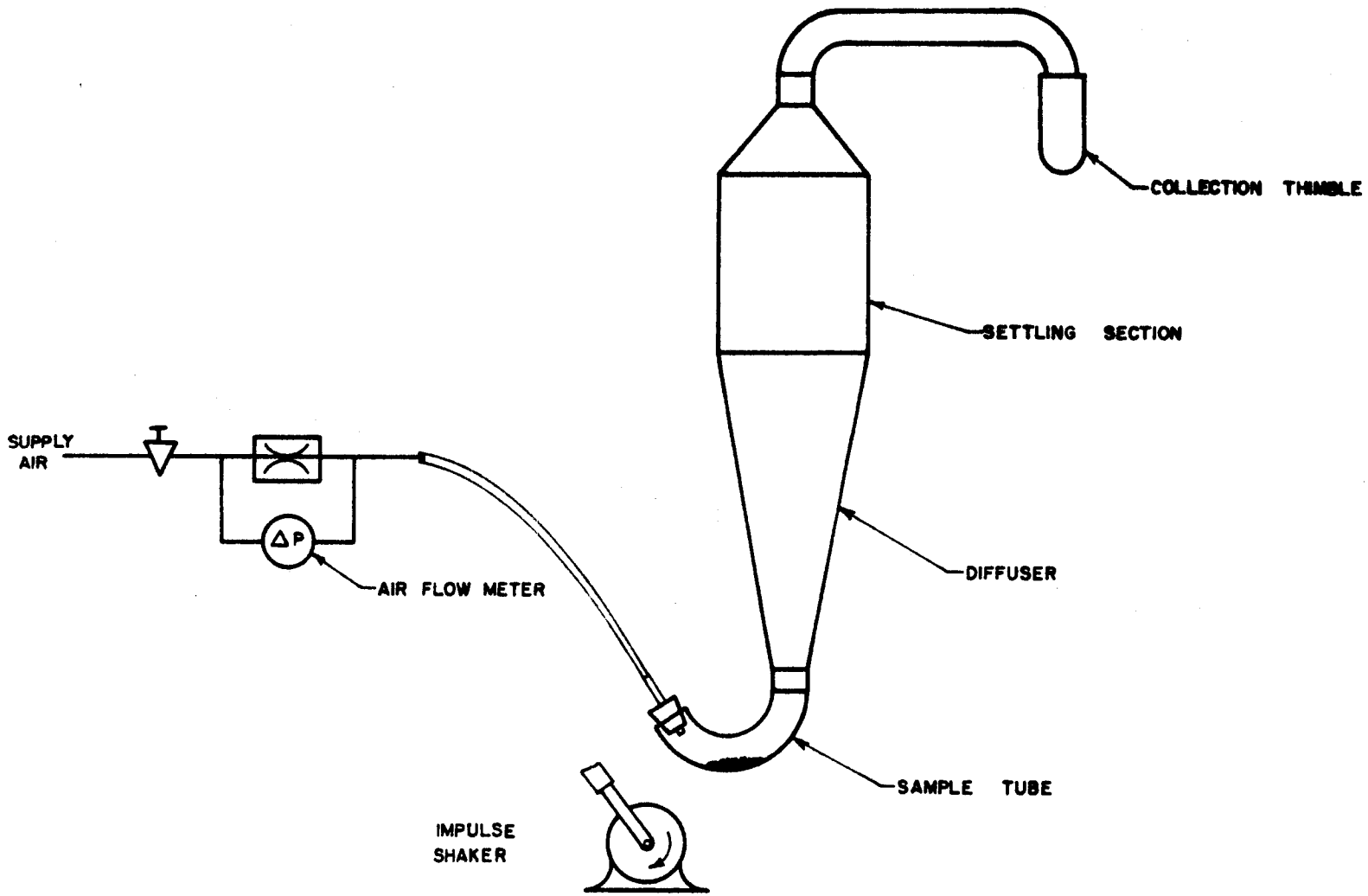

Fig. 42 Schematic of Roller Particle Size Analyzer

are collected in a porous filter thimble. All particles of a larger size will fall back into the diffuser section. By varying the velocity setting of the air stream the particle size of the sample collected can be controlled. From one operation, the sample is divided into two fractions; repeated fractionation at different air flow rates allows one to subdivide the contaminant into the desired size ranges.

APPENDIX C

LIST OF SYMBOLS

A_p	Cross Sectional Area of Individual Pore
A_s	Internal Surface Area of Capillary
A_t	Cross Sectional Area of Filter Medium
D	Capillary Diameter
d	Particle Diameter
D_h	Hydraulic Diameter of Flow Passage
F(D)	Pore Size Distribution Function
F_e	External Force on Capillary Fluid
F_i	Internal Force on Capillary Fluid
K	Permeability Constant
L	Capillary Length
L_p	Length of Wetted Perimeter of Pore
N	Number of Flow Passages in Medium
P	Pressure, Absolute
ΔP	Pressure, Differential
Q	Total Flow Rate
q	Flow Rate Through an Individual Capillary
R	Radius of Capillary
r	Radial Distance from Centerline of Capillary
t	Thickness of Medium
V	Pore Velocity in Capillary

V_A	Average Fluid Velocity Within Capillary
V_p	Pore Volume
V_s	Solid Volume of Medium
V_t	Total or Bulk Volume of Medium
Y	Distance Measured From Capillary Wall Perpendicular to Streamlines
γ	Mass Density of Solid Particle
θ	Wetting Angle of Liquid on Solid
μ	Dynamic Viscosity
ρ	Mass Density of Fluid
ρ_s	Specific Weight of Filter Material
σ	Surface Tension of Liquid
τ	Tortuosity of Medium
τ_w	Shearing Stress at Capillary Wall
Φ	Porosity of Medium